



State of the Art of Coupled Thermo–hydro–Mechanical–Chemical Modelling for Frozen Soils

Kai-Qi Li¹ · Zhen-Yu Yin¹

Received: 6 February 2024 / Accepted: 4 July 2024
© The Author(s) 2024

Abstract

Numerous studies have investigated the coupled multi-field processes in frozen soils, focusing on the variation in frozen soils and addressing the influences of climate change, hydrological processes, and ecosystems in cold regions. The investigation of coupled multi-physics field processes in frozen soils has emerged as a prominent research area, leading to significant advancements in coupling models and simulation solvers. However, substantial differences remain among various coupled models due to the insufficient observations and in-depth understanding of multi-field coupling processes. Therefore, this study comprehensively reviews the latest research process on multi-field models and numerical simulation methods, including thermo-hydraulic (TH) coupling, thermo-mechanical (TM) coupling, hydro-mechanical (HM) coupling, thermo–hydro-mechanical (THM) coupling, thermo–hydro-chemical (THC) coupling and thermo–hydro-mechanical–chemical (THMC) coupling. Furthermore, the primary simulation methods are summarised, including the continuum mechanics method, discrete or discontinuous mechanics method, and simulators specifically designed for heat and mass transfer modelling. Finally, this study outlines critical findings and proposes future research directions on multi-physical field modelling of frozen soils. This study provides the theoretical basis for in-depth mechanism analyses and practical engineering applications, contributing to the advancement of understanding and management of frozen soils.

1 Introduction

Permafrost and seasonally frozen soil cover approximately 50% of the exposed land surfaces in the Northern Hemisphere [59, 364]. In cold regions, these frozen soils are often subjected to complex multi-field coupling processes in varying temperatures, pressures, and intricate hydraulic–chemical environments. These multi-field coupling processes govern numerous phenomena observed in frozen soils, e.g., frost heave, thaw settlement, moisture migration, phase transition, and ice lens growth [40, 154, 188, 189]. For example, seasonally frozen regions experience frost heaving due to the volume expansion induced by water/ice phase changes, resulting in uneven deformation. These coupling interactions in frozen soils

are critical for construction safety in cold regions since the multi-field coupling process can cause significant deformation even without external loads. Therefore, developing robust and efficient multiphysics models is necessary to comprehensively understand the underlying mechanisms and obtain reliable simulation results for practical applications. Such coupled multi-physics models are theoretically superior to approaches that address individual processes in isolation.

The coupled multi-physics fields play significant roles in various engineering domains, such as railways and highway construction and management (e.g., [290, 347]), energy pipeline/water main projects in cold regions (e.g., [107, 108, 227, 269]), methane hydrates extraction under seabed (e.g., [72, 252]), and underground constructions involving artificial ground freezing (AGF, e.g., [162, 203, 213]). Furthermore, the intricate coupling processes exert a profound influence on the behaviour of frozen soils, giving rise to engineering and environmental challenges such as slope instability, climate change impacts, carbon emissions, subgrade settlements, and infrastructure damage [98, 255, 264, 268]. These coupled multi-physical modelling have direct relevance to numerous research fields, including

✉ Zhen-Yu Yin
zhenyu.yin@polyu.edu.hk

Kai-Qi Li
kqcee.li@polyu.edu.hk

¹ Department of Civil and Environmental Engineering, The Hong Kong Polytechnic University, Hung Hom, Kowloon, Hong Kong, China

hydrology and hydrogeology (e.g., [244, 270]), nuclear waste storage (e.g., [83, 101]), fluvial geomorphology (e.g., [136, 288]), Mars studies (e.g., [202]), climate modelling (e.g., [340]), and acid mine drainage in cold regions (e.g. [36]).

Various methods, including experimental and numerical methods, have been employed to investigate the fundamental behaviours of frozen soils. Some investigations focused on elucidating specific properties of frozen soils, such as strength and relationships between different parameters (e.g., soil freezing characteristic curve, SFCC describing the relationship between temperature and unfrozen water content) [174]. In addition, efforts have been made to explore the coupling mechanisms in frozen soils and develop governing equations for each field. The development of multi-physics modelling for frozen soils has benefited from the advancements in multiphysics investigations of other geomaterials and the development of simulation platforms. For insurance, multiple studies on the coupled model for rocks and soils have been conducted. However, these models have been derived from non-isothermal consolidation of deformable porous media or an extension of Biot's phenomenological model, which fails to consider the phase change in freezing soils. Furthermore, these models are often solved by numerical methods, such as the finite element method (FEM), finite volume method (FVM), and finite difference method (FDM), owing to the highly nonlinear governing equations and complex boundary conditions. On the other hand, field tests are challenging and expensive to perform, resulting in limited available data.

Therefore, it is necessary to establish reliable and efficient coupling models for simulating the multi-physical fields of frozen soils, which is crucial for evaluating the risks of engineering where conducting experiments are risky, such as the application of AGF for pollutant dispersion retardation.

The coupled thermo–hydro–mechanical–chemical (THMC) process involves the intricate interactions of thermal, hydraulic, mechanical, and chemical fields. Among these four fields, each pairing of two fields can be intricately interconnected through a coupling process, as illustrated in Fig. 1. The primary contents of each physical field are described as follows.

(1) The thermal (**T**) field is associated with temperature distribution and three heat transfer modes, i.e., conduction, convection, and radiation. The geothermal, solar energy, and local heat sink induced by human/engineering activity (e.g., thermal disturbances) and climate change (e.g., snow conduction and rainfall infiltration) can serve as heat sources. Besides, the temperature gradient acts as the driving force for water migration and phase transition. It is worth noting that the primary type of frozen soil contributing to disasters is warm frozen soil (-0.5 to 1.5°C).

(2) The hydraulic (**H**) field, referring to Darcy or non-Darcy flows in soils, is an unstable factor affecting frozen soil stability. Moisture migration and water/ice phase transition can exacerbate this deterioration effect. The water–ice phase change occurs when the soil freezes, increasing volume by 1.09 times and generating frost heave from 10 to thousands of kilopascals [39]. Furthermore, the directional growth of ice lenses during the freezing process can induce anisotropy

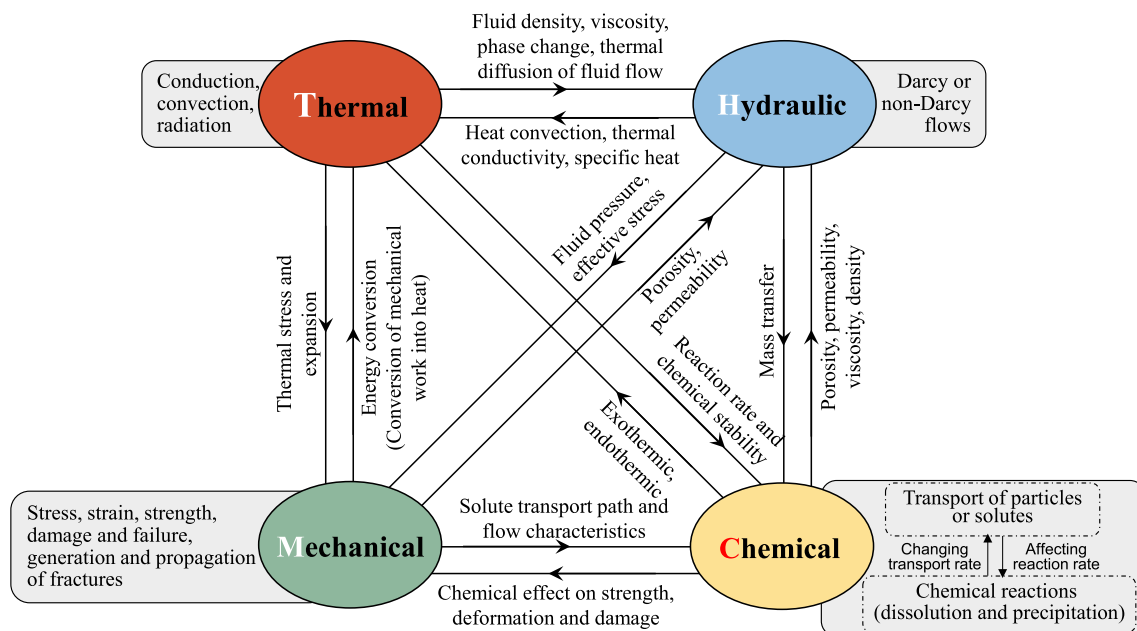


Fig. 1 Coupled THMC (thermo–hydro–mechanical–chemical) interactions in frozen soils

in hydraulic conductivities after thawing [340], thereby contributing to the inherent variability in the properties of frozen soils. During thawing, the increase in moisture can increase pore water pressure and reduce effective stress, consequently decreasing the shear strength of frozen soils.

(3) The mechanical (**M**) field mainly refers to stress, strain, strength, damage, failure, and generation and propagation of fractures. The variations of properties and internal structures can significantly influence frozen soils' stress state and mechanical behaviours. During freezing, the soil experiences physical changes induced by the interaction between water and heat, weakening and damaging microstructure in soils, and macroscopic deformation and failure.

(4) The chemical (**C**) field presents the transport of reactive or nonreactive particles or solutes and chemical reactions (dissolution and precipitation), which mainly determines the variation of material and chemical composition in soils, such as leakage and discharge of chemical waste liquids, minerals transformation, and salinisation.

Numerous studies have been conducted on multi-field coupling models for frozen soils, with significant attention given to the numerical implementations of these coupled models. However, these multi-physical field methods for frozen soils have not yet been adequately summarised. Accordingly, this study comprehensively reviews the current investigations on multi-filed coupling models for frozen soils, categorising them into six groups: thermo-hydraulic (TH) coupling, thermo-mechanical (TM) coupling, hydro-mechanical (HM) coupling, thermo–hydro-mechanical (THM) coupling, thermo–hydro-chemical (THC) coupling and thermo–hydro-mechanical–chemical (THMC) coupling. It is worth noting that although the studies on chemical coupling are relatively limited, models related to chemical fields coupled with THM fields (i.e., THMC model) are also considered. In addition to summarising the fruitful investigations on coupled multi-physical modelling, this review also provides a comprehensive overview of the numerical implementations of these coupled models and sheds light on the current research directions of coupled modelling for frozen soils. This comprehensive analysis can facilitate the development of new coupled models in closely related fields and drive advancements in the understanding and simulation of coupled multi-physical processes in frozen soils.

2 Multi-field Coupling Models

2.1 Thermo-hydraulic (TH) Coupling Approach

The heat transfer equation demonstrates that the rate of change of internal energy within a representative volume element (RVE) is contributed to heat flux resulting from thermal conduction, the release of latent heat due to phase

change, and the convective heat associated with liquid water seepage per unit time. The governing equation for thermal modelling based on energy conservation can be expressed as:

$$C_a \frac{\partial T}{\partial t} = \nabla(\lambda \nabla T) + L \frac{\partial}{\partial t}(\rho_i s_i n) - v_w \rho_w c_w \nabla T, \quad (1)$$

where C is volumetric heat capacity, T is temperature, λ is thermal conductivity. ρ_i and ρ_w are density of ice and water; s_i is ice saturation, n is porosity, v_w is velocity of liquid water; c_w is the specific heat of ice.

Based on the principle of mass conservation, the disparity between the inflow and outflow rates of water per unit time should be equal to the rate of change of total water mass within RVE. Therefore, the mathematical representation can be formulated as follows:

$$\frac{\partial}{\partial t}(\rho_w s_w n) + \frac{\partial}{\partial t}(\rho_i s_i n) = Q + \rho_w \nabla(k \nabla H), \quad (2)$$

where s_i is water saturation, k is hydraulic conductivity, H is water head, Q is internal sources or sinks. The left term represents the variation rate of liquid water mass and ice mass, and the right term are the flux of RVE and sources or sinks.

2.1.1 Coupled TH Models

The soils in the seasonal frozen zone experience freeze–thaw cycles annually. Previous soil freezing/thawing investigations primarily concentrate on heat transfer. Since the 1970s, it has been recognised that both thermal flow and mass transfer should be included in the analysis of soils' freezing and thawing process. Since the physical processes in frozen soils are complex, it is difficult to derive a solution to accurately predict the temperature and moisture variation in the freeze–thaw process. Accordingly, numerous numerical models have been developed to simulate the coupled thermo-hydraulic (TH) process within the freezing soils, which is significant for engineers to estimate the frost heave and for soil scientists to predict the temperature and moisture content profiles. Therefore, it is necessary to address the mechanisms of water and heat transfer processes in frozen soils, which is beneficial for revealing the interaction mechanisms of frozen soils and climate change and their influences on the environment and engineering.

Table 1 presents a summary of typical investigations on coupled TH models for frozen soils. The pioneering work by Harlan [89] established the first TH coupling model for partially frozen soils, providing a numerical finite difference solution to a one-dimensional (1D) coupled TH problem for a homogeneous porous medium under freezing/thawing conditions. Subsequently, numerous TH coupling models

Table 1 Summary of investigations on the coupled thermo-hydraulic (TH) modelling for frozen soils

References	Coupling mode	Theories	Phase change	Water migration	Heat convection	Validations	Soil types	Applications	Dimensions	Scales	Solvers
Harlan [89]	$[T \rightarrow H] k(T)$ $[H \rightarrow T] \lambda, C$	Steady or unsteady flow and conduction heat transfer	-	-	-	Quantitative comparison of freezing-affected soil-water redistribution and total head and total water head profiles during thawing	Unsaturated freezing soil	Quantitative comparison	1D	Macro	FDM
Taylor and Luthin [291]	$[T \rightarrow H] \theta_u(T), I(\theta_u), D(\theta_i)$ $[H \rightarrow T] \lambda, C$	Heat transfer and flow equation	-	-	-	T and ω in a horizontal soil column during freezing [114] ω in a soil column during freezing [58]	Freezing soil	Simulating heat and water flow and heaving	1D	Macro	FDM
Jame and Norum [115]	$[T \rightarrow H] \theta_u(T), I(\theta_u)$ $[H \rightarrow T] \lambda, C$	Modified Harlan [89] model*1	✓	-	-	T and ω from test by [114]	Unsaturated freezing soil	Simulating TH processes when ice lensing does not occur	1D	Macro	FDM
Giakoumakis [79]	$[T \rightarrow H] \theta_u(T), I(\theta_u)$ $[H \rightarrow T] \lambda, C$	Modified Harlan [89] model*2	✓	-	-	T and ω from vertical soil column	Unsaturated freezing soil	Predict T and ω profiles along the column	1D	Macro	FDM
Newman and Wilson [228]	$[T \rightarrow H] \kappa = K_f * \kappa_s$ $[H \rightarrow T] \lambda, C$	Modified Harlan [89] model by modifying k	✓	-	-	T and ω from tests by [114]	Unsaturated freezing soil	A model for unsaturated freezing soil	1D	Macro	FEM
Hansson et al. [87]	$[T \rightarrow H] k_f = k * 10^{-f/\theta}$, $k = K_f(S_f) * k_s$ $[H \rightarrow T] \lambda, C$	Modified Richard's equation and convection-convective heat flow equation	✓	-	√ (BC)	T and ω from short-term laboratory column freezing test	Frozen soil	Long-term freezing	1D	Macro	FDM (HYDRUS-ID)

Table 1 (continued)

References	Coupling mode	Theories	Phase change	Water migration	Heat convection	Validations	Soil types	Applications	Dimensions	Scales	Solvers
Zhao et al. [367]	$[T \rightarrow H] k_t = k * 10^{-T/\theta}$, $k = K_r(S_r) * k_s$ $[H \rightarrow T] \lambda, C$	Modified Richard's equation and conduction–convection heat flow equation	✓	–	✓	T and ω from in situ long-term test in Inner Mongolia grassland	Unfrozen and frozen soil	Simulation of soil freezing and thawing behaviour	1D	Macro	FDM (HYDRUS-1D)
Wang et al. [308]	$[T \rightarrow H] \theta_u(T)$, $D(\theta_u), K(\theta_u)$ $[H \rightarrow T] \lambda, C$	Richard's equation and heat transport equation	✓	–	–	T and ω in field test	Seasonal frozen soil	Simulation of water–heat coupled movements in seasonally frozen soil	1D	Macro	FDM
Zhou and Zhou [375]	$[T \rightarrow H] \theta_u(T)$, $k_t(\theta_w, k)$ $[H \rightarrow T] \lambda, C$	Gilpin's theory to describe the water in solid–liquid interface and heat transfer equation	✓	✓	–	The observed thickness of ice lenses in intermittent freezing test and continuous freezing test on Xuzhou silty clay	Freezing soil	Frost heave reduction	1D	Macro	FVM
Guo et al. [85]	$[T \rightarrow H] \theta_u(T)$, $D(\theta_w, T)$ $[H \rightarrow T] \lambda, C$	Mass conservation of pore water and enthalpy balance equation	✓	–	–	T and ω from freezing test on silica flour and Zhangye loam column	Freezing soil	Simulation of water–heat coupled movements	1D	Macro	FEM
Kelleners [132]	$[T \rightarrow H] k_t = k * 10^{-T/\theta}$, $k = K_r(S_r) * k_s$ $[H \rightarrow T] \lambda, C$	Modified Richard's equation ³ and heat transport equation	–	–	✓ (BC)	T from laboratory soil column freezing test [221], T and ω in rangeland soil field test	Seasonally frozen soil with snow accumulation	Beneficial for future studies on frozen soils with snow accumulation	1D	Macro	FDM
Li et al. [176]	$[T \rightarrow H] \theta_u(T)$ $[H \rightarrow T] \lambda, C$	Coupled heat transport and moisture flow model	✓	–	–	T from field test	Seasonally frozen soil	Frost heave prevention in canal linings in	2D	Macro	–

Table 1 (continued)

References	Coupling mode	Theories	Phase change	Water migration	Heat convection	Validations	Soil types	Applications	Dimensions	Scales	Solvers
Liu and Yu [201]	$[T \rightarrow H] k = K_f$ $* k_s$ $[H \rightarrow T] \lambda, C$	Energy and mass conservation ^{*4}	✓	✓	$\sqrt{(BC)}$	T and ω from field observations	Pavements in cold regions	Thermo-hydraulic behaviours of flexible and rigid pavements in cold regions	2D	Macro	FEM (COMSOL)
Zhao et al. [366]	$[T \rightarrow H] \theta_u(T)$ $[H \rightarrow T] \lambda, C$	Mass and momentum conservations	✓	✓	-	-	Thawing frozen soil	Buried oil pipeline in cold region	2D	Macro	FVM
Chen et al. [38]	$[T \rightarrow H] \theta_u(T)$ $[H \rightarrow T] \lambda, C$	Mixed-form modified Richards' equation for mass transfer (i.e., mass equation) and heat transport equation for heat transient flow	✓	-	-	-	Variably saturated frozen soil	Slope	2D	Macro	FEM (FSoil)
Vitel et al. [300]	$[T \rightarrow H] \kappa = K_f$ $* \kappa_s, \mu(T)$ $[H \rightarrow T] \lambda, C$	Energy and mass conservations	✓	-	-	T from field test	Fractured sandstone	AGF	3D	Macro	FEM (COMSOL)
Dong and Yu [63]	$[T \rightarrow H] \theta_u(T)$ $[H \rightarrow T] \lambda, C$	Mass and momentum conservations	-	-	-	-	Unsaturated frozen clay	Describing the thermo-hydro-mechanical behaviours of unsaturated frozen soil subjected to the freezing/thawing process	2D	Micro	FEM (COMSOL)
Huang et al. [104]	$[T \rightarrow H] \theta_u(T), \mu(T)$ $\kappa_f = K_f(\theta_u) * \kappa$ $[H \rightarrow T] \lambda, C$	Energy and mass conservations	✓	✓	-	T from laboratory test by [243]	Saturated frozen sand	AGF optimization	2D	Macro	FEM (COMSOL)

Table 1 (continued)

References	Coupling mode	Theories	Phase change	Water migration	Heat convection	Validations	Soil types	Applications	Dimensions	Scales	Solvers
Li et al. [168]	$[T \rightarrow H] \theta_u(T)$ $[H \rightarrow T] \lambda, C$	Energy and mass conservation	✓	✓	✓ (BC)	T in one-sided freezing test for silty clay columns in an open system [151]	Saturated frozen sand	TH behaviour around a buried pipeline in cold regions	2D	Macro	FEM (COMSOL)
Heinze [96]	$[T \rightarrow H] \theta_u(T)$, $\kappa = K_r(S_r) * \kappa_s, I = 10^{-7*0.61}$ $[H \rightarrow T] \lambda, C$	Local thermal nonequilibrium model	✓	–	–	T and ω in FT test with water infiltration into homogeneous soil by [322]; ω in a common freezing test by [87]	Saturated and unsaturated silt loam and sandy loam soil	Water infiltration into frozen soil	2D	Macro	FDM
Kjelstrup et al. [139]	$[T \rightarrow H] \kappa(T)$ $[H \rightarrow T]$ thermodynamic frost heave coefficient, $\lambda(T)$	Energy and mass conservation involving hydraulic conductivity, thermal conductivity and thermodynamic frost heave coefficient	✓	–	–	T and p profiles in frost heave tests by [142]	Partially frozen soil matrix (frozen fringe)	Frost heave simulations	1D	Macro	–
Tang et al. [289]	$[T \rightarrow H]$ $k = K_r(S_r) * k_{s^*}$, $I = 10^{-10*0.61}$, $D(\theta_u) = f(k, D)$ $[H \rightarrow T] \lambda, C$	Energy and mass conservation	✓	✓	–	θ_u and s from horizontal freezing test	Unsaturated silt	Simulate coupled water–heat movement during the horizontal freezing process	3D	Macro	FEM (COMSOL)
Wang and Ma [312]	$[T \rightarrow H]$ $\kappa = K_r(S_r) * \kappa_s$, $I = 10^{-10*0.61}$, $D(\theta_u) = f(\kappa, D)$ $[H \rightarrow T] \lambda, C$	Energy and mass conservation	✓	✓	–	T and ω from field test	Freezing soil	Subgrade of unsaturated soil in the seasonal freezing zone	2D	Macro	FEM (COMSOL)

Table 1 (continued)

References	Coupling mode	Theories	Phase change	Water migration	Heat convection	Validations	Soil types	Applications	Dimensions	Scales	Solvers
Zhang et al. [357]	[T → H] $k_f(\kappa, T)$ [H → T] λ, C	Energy and mass conservations	✓	✓	✓	T and ω from in situ data	Freezing soil	Maximum frozen depth prediction and water and heat simulation in the seasonally frozen saline soil ground	2D	Macro	–
Chen et al. [41]	[T → H] $k_f = k * 10^{-T/\theta_0}$, $k = K_r(S_r) * k_s$ [H → T] λ, C	Two equations, i.e., hydraulic and heat transfer equation and SFCC	✓	✓	✓ (BC)	T and ω from vertical and horizontal unidirectional freezing tests of soil columns from [115, 377]	Unsaturated freezing soils-non heaving frozen soils	Unidirectional freezing tests of unsaturated soils	2D	Macro	FEM
Hu et al. [102]	[T → H] $k_f = k * 10^{-T/\theta_0}$, $k = K_r(S_r) * k_s$ [H → T] λ, C	Cryo-hydrogeological model including mass, momentum, and energy conservation laws	✓	–	–	T and ω from field test	Frozen soil	Slope in a small valley in the Heihe River Basin (Qilian Mountain on the Qinghai-Tibetan Plateau)	2D	Macro	CFD (OpenFOAM)
Liu et al. [198]	[T → H] $k = K_r(S_r) * k_s, \mu(T)$ [H → T] λ, C	Heat balance equation based on heat transfer and energy conservation	✓	–	–	Field measurements (T and deformation) in a ground-freezing case in Beijing Metro Line 19	Frozen soil	AGF	3D	Macro	FEM (COMSOL)
Liu et al. [196]	[T → H] $k = K_r(S_r) * k_s, \mu(T), \theta_u(T), S_r(T)$ [H → T] λ, C	Energy and mass equilibrium conservation	✓	–	–	T in laboratory test by [243]	Frozen soil	AGF	3D	Macro	FEM (COMSOL)

Table 1 (continued)

References	Coupling mode	Theories	Phase change	Water migration	Heat convection	Validations	Soil types	Applications	Dimensions	Scales	Solvers
Nikolaev et al. [229]	[T → H] $K_r(S_r)$ [H → T] λ, C	Mass and energy conservation, Darcy's and Fourier's laws	✓	–	✓	Analytical solutions for 1D problems and finite element transient solutions for 2D problems	Freezing and thawing soil	Simulating TH processes	1D and 2D	Macro–micro	Bond-based peridynamics
Jiao et al. [121]	[T → H] $K_r(\theta)$, $\theta_u(T)$ [H → T] λ, C	Continuity equation and general advective–dispersive heat transport equation	✓	✓	–	T, ω and q from in situ data	–	Retrgressive thaw slump on soil freeze–thaw erosion	2D	Macro	Heatflow
Lan et al. [157]	[T → H] $\theta_u(T)$ [H → T] λ, C	Heat transfer and water migration equation	✓	✓	✓	T in an experimental Qinghai–Tibet Expressway engineering [36], ω in a unidirectional test conducted by [221]	Unsaturated soil	Embankment in the permafrost regions of the Qinghai–Tibet Plateau (QTP)	2D	Macro	FEM (COMSOL)
Wang et al. [316]	[T → H] $\theta_u(T)$ [H → T]	Pseudo-potential model Relation of thermal diffusivity and kinematic viscosity is described by Prandtl number	✓	–	–	T and ω in FT test	Thawing soil	–	2D	Meso	LBM

Table 1 (continued)

References	Coupling mode	Theories	Phase change	Water migration	Heat convection	Validations	Soil types	Applications	Dimensions	Scales	Solvers
Zhan et al. [349]	[T → H] $\theta_u(T), k_r = k * 10^{-10^{*\theta_i}}$, $k = K_r(S_i) * k_s$ [H → T] λ, C	Richards' equation (water migration) Fick's law (vapour migration) Heat conservation equation (heat transfer)	$\sqrt{\quad}$	-	-	T and ω in FT test	Unsaturated frozen soil	Unsaturated seasonal frozen soil slope	2D	Macro	FEM (COMSOL)

AGF artificial ground freezing, BC boundary condition, C heat capacity, D diffusivity coefficient, $f()$ function, FT freeze-thaw, I impedance factor, κ permeability, k hydraulic conductivity of unfrozen soils, k_s saturated hydraulic conductivity of frozen soils, k_u hydraulic conductivity of frozen soils, K_r relative permeability/hydraulic conductivity, p pressure, q heat flux, s matrix suction, T temperature, θ_u unfrozen water content, θ_i ice content, ω water content, μ viscosity, θ_u unfrozen water content, λ thermal conductivity, CFD computational fluid dynamic, LBM lattice Boltzmann method, CoupModel coupled heat and mass transfer, RFEM random finite element model

*1 Represents Harlan [89] model that was modified by adding water diffusivity with impedance factor; *2 represents the modified Harlan [89] model by considering liquid moisture flux in the unsaturated zone induced by thermal gradient; *3 represent the effect of dissolved ions on soil water freezing point depression was included by combining an expression for the osmotic head with Clapeyron equation and van Genuchten soil water retention function); *4 represents that energy transport in porous materials was described by a modified Fourier's equation with both conduction and convection terms; fluid migration in the variably unsaturated porous media was described by the mix-type Richards equation

were developed to simulate frozen soils' water and heat transfer processes, employing various governing equations and model parameterisations. Some critical conclusions from Table 1 are as follows:

(1) The majority of models account for the variations of unfrozen water content with temperature, especially when the temperature drops below subzero temperature. However, only a few studies consider the migration of unfrozen water. Besides, the water and vapour transfer within frozen soils can affect the water infiltration process and thermal properties during the freezing and thawing, as well as heat transfer by releasing/absorbing a large amount of latent heat [253, 307].

(2) Most models used the soil temperature as a prognostic parameter (i.e., a threshold freezing point) to determine the phase change of water, which might lead to numerical instability in simulations [51, 87].

(3) The freezing and thawing of frozen soils are accompanied by heat exchanges involving three processes: (i) conductive and convective heat transfer induced by temperature gradient and water migration, (ii) heat release/sink due to the freezing of liquid water and thaw of ice, and (iii) heat exchange between the soil and external environment [248]. The heat transfer resulting from the latent heat during the phase change of permafrost near 0 °C is considerably larger than that caused by heat conduction or convection resulting from water and vapour flow during freeze-thaw processes. However, as for unsaturated freezing soils, vaporisation is not considered, which would induce errors since the phase change between liquid water and vapour is 7.4 times more energy than that between ice and liquid water [251].

(4) Many TH coupling models have been validated by comparing field observations, such as variations in temperature and water content within frozen soils at the soil surface or around freezing pipes in AGF and buried oil pipelines. However, it is crucial for TH models to incorporate a sufficiently deep soil profile to enable realistic simulations of temperature profiles over time, particularly for permafrost regions [254]. For example, to accurately simulate century-long permafrost changes, it is advisable to consider a steady geothermal heat flow as the lower boundary condition, particularly at depths exceeding 30 m [283]. Besides, numerous studies have shown the significance of enhancing the simulated ground depth and incorporating a greater number of ground layers to capture the diminishing impact of multi-decadal variability with increasing depth more precisely [3, 6].

Therefore, it is imperative to investigate the energy distribution state at different depths and transfer features within deeper frozen soils. Given the potential extension of calculation memories with deeper soil configurations, it is crucial to meticulously determine the appropriate soil depth

and geothermal flux for surface modelling in cold regions. It is essential to consider the soil properties, commonly derived from lookup tables using available soil maps, as they exhibit variations across diverse areas and subsoil layers [217].

(5) The majority of TH models commonly fail to address the snow process and surface features that are crucial inputs for accurate TH modelling. Nevertheless, Kelleners [132] and Lan et al. [157] have made notable contributions in this regard. Kelleners [132] developed a numerical coupled TH model for seasonally frozen soils with snow cover, aiming to explore mass and energy exchange among soil, plant, and atmosphere. Snow cover plays a significant role in the land surface, influencing the outcomes of TH model simulations and the energy exchange between the soil and atmosphere. Its impact is primarily attributed to factors such as low thermal conductivity, high surface albedo, and energy absorption resulting from latent heat during snowmelt [69, 90]. However, the blowing snow and snow melt are not considered, which causes the underestimation of snow height prediction and overestimation of water content in shallow soils. Accurately simulating the snow process is essential to comprehend frozen soils' thermal and energy balance and better understand coupled TH processes.

In a related study, Lan et al. [157] established a coupled TH model to analyse the reciprocal relationship between desertification and permafrost degradation, highlighting the crucial role of permafrost in maintaining environmental stability on the Qinghai–Tibet Plateau. Surface parameters, such as surface albedo, emissivity, roughness, sand accumulation, and vegetation coverage, also serve as significant inputs for TH models [337]. Besides, some researchers [42, 362] have emphasised the importance of considering the impacts of freeze–thaw processes on surface parameters to avoid significant errors in simulating water and heat processes in permafrost regions of the Qinghai–Tibetan Plateau. Thus, when exploring coupled TH processes in cold areas, it is crucial to incorporate surface parameters that account for freeze–thaw impacts.

(6) These existing TH models are fully coupled to simulate the interaction between the thermal and hydraulic fields of frozen soils. The thermal transfer within the soil can significantly impact the hydraulic field through phase change phenomena. As freezing progresses, the ice content increases, leading to changes in the hydraulic properties of the soil. To account for this, many studies have incorporated empirical functions to represent the effect of temperature on unfrozen water content. Additionally, some researchers have assumed that the fluid's viscosity coefficient or the frozen soil's hydraulic properties, such as permeability and saturation, depend on temperature. Besides, the impedance impact of ice lenses was also involved in some coupled TH models, and its detailed discussion is depicted in Sect. 2.2.2. Regarding the influence of the hydraulic field

on heat transfer, it is crucial to consider the movement of moisture within the frozen soil, which is strongly influenced by temperature gradients. The variation in ice and water content within the soil also affects the effective heat capacity and thermal conductivity values. By accounting for these influences, the coupled TH models can accurately represent the impact of the hydraulic field on heat transfer processes within the frozen soil.

(7) Existing TH models were developed from one-dimensional to two- and three-dimensional configurations, with most models adopting a macroscopic perspective. However, several studies have also been conducted from meso/micro perspectives (e.g., [63, 316]). Dong and Yu [63] specifically developed a microstructure-based four-phase model for clay, employing finite element software (i.e., COMSOL Multiphysics, hereafter referred to as COMSOL) to simulate the coupling TH process. Moreover, Wang et al. [316] established a multiphase pseudo-potential model with an enthalpy-based model, and employed the lattice Boltzmann method (LBM) to predict the spatial distributions of temperature and water content during the thawing process of frozen soil.

(8) Various solvers have simulated the complex heat and mass transfer processes within frozen soils. Notable examples of coupled TH models include Coupled Heat and Mass Transfer (CoupModel) [117, 169], Hydrus-1D model [87, 367], and Heatflow model [121]. These models provide a comprehensive understanding of the combined effects of water flow and heat transfer in frozen soils. Additionally, advanced methods, such as the lattice Boltzmann method, LBM [316] and bond-based peridynamics [229], have been employed to analyse the coupled TH process. Numerical methods, including the finite volume method (FVM), finite difference method (FDM), and finite element method (FEM), are alternative approaches for simulating the TH coupling process. These methods are often implemented using popular software packages such as COMSOL and OpenFOAM. A comprehensive discussion of the different solvers will be presented in Sect. 3.

2.1.2 Parameterisation of TH Model

2.1.2.1 Phase Change

Phase change significantly impacts not only the thermal characteristics of soils but also the heat and mass transfer processes within frozen soils. During phase change, a significant release or absorption of latent heat occurs, which impedes rapid cooling or warming of the soil and causes temperature disparities between the air and ground [15, 65].

In general, two methods can be employed to account for phase change [28]. The commonly used method for phase-change porous media problems is apparent heat capacity that

adds the latent energy associated with the phase change to the heat conduction equation, which could be defined as [27]

$$C_a = \frac{C_i + C_w}{2} + \frac{L}{2(T_w - T_i)}, \quad (3)$$

where C_a is apparent heat capacity, C is heat capacity, T is temperature, and L is latent heat during water/ice phase change. The subscripts w and i correspond to the water and ice phases, respectively. However, a notable feature of heat transfer in frozen soils that is different from the conventional process is the presence of unfrozen water, which is not accounted for in the apparent heat capacity method. Another approach to consider the phase change is the excess energy method [206]. The temperature of soil undergoing phase change remains constant at the freezing point until the heat gain or loss equals the latent heat of the soil. The excess energy method offers a practical approximation of modelling phase change phenomena and enables the coexistence of multiple phases of water within the soil [231]. Nonetheless, this method does not allow for supercooled water (i.e., liquid water coexists with ice over a range of temperatures below the freezing point), which can be compensated by the relationship between temperature (T) and unfrozen water content [48, 170]. By comparing the two methods with analytical solutions from Jumikis [124] and Lunardini [206], Bonan [28] indicated that frost penetration depths from the two methods align with the analytical solution, while results from excess energy produce some fluctuations. Furthermore, incorporating phase change improves the accuracy of the simulation.

2.1.2.2 Thermal Conductivity As a multi-phase medium, the thermal conductivity (λ) of soils can be influenced by the content and properties of each component [172, 180, 181]. Moreover, soils with smaller particle sizes, possessing smaller unfrozen water content and lower saturation, tend to have a higher thermal conductivity value in the warm season than that in the cold season [173]. Many scholars have proposed prediction models for thermal conductivity where λ is a function of soil mineral composition (e.g., [46, 123, 160, 171]). He et al. [95] evaluated 39 models for λ and suggested the need for further research to develop a more accurate and generalised model for λ . Besides, some researchers have proposed data-driven models to aid the development of a theory that can better estimate soil thermal conductivity [166, 167, 177, 183].

2.1.2.3 Hydraulic Conductivity Hydraulic conductivity (k) is another important factor affecting water and heat transfer. Previous studies assume that the soil water content is zero and hydraulic conductivity is directly set to 0 when the temperature is subzero [28, 50]. Considering fluid flow in

porous soils, two methods have been developed to address the variation of k as water freezes into ice, i.e., k is a function of T , and k is a function of ice and water content.

Previous numerical studies have indicated the accumulation of a significant amount of ice behind the frost front. Jame and Norum [115] introduced an impedance factor (I) to illustrate the resistance imposed by ice on the porous medium's water flow to elucidate the disruption of the presence of ice on frozen soils.

$$k_f = k_u \times I, \quad (4a)$$

$$I = 10^{-a\theta_i}, \quad (4b)$$

where k_f and k_u are the hydraulic conductivity of frozen soils and unfrozen soils; a is an empirical constant depending on soil type, which can be obtained by fitting a diffusivity versus water content function in the laboratory experiments; and θ_i is the volumetric ice content. I is the impedance factor, which indicates that a larger value of I can promote a lower value in the conductivity of liquid as the ice content increases. However, there is no consensus regarding the specific value of the impedance factor (I) in existing studies. For example, Jame and Norum [115] reported that the impedance factor increases exponentially from 1 for ice-free conditions to 1000 when ice contents exceed 20%. Gosink et al. [81] suggested values of 8 for fine sand and silts and 20–30 for coarse gravel soils. In contrast, Black and Hardenberg [23] considered the impedance factor method as a “potent and wholly arbitrary correction function” for determining hydraulic conductivity. Generally, the determination of I relies on calibration using measurements, which restricts its application and integration within numerical models. Besides, the numerical results from Newman and Wilson [228] demonstrated that the application of impedance factors remarkably affects the prediction accuracy of ice content and suggested that the adoption of I becomes unnecessary if soil water characteristic curve data is available.

Another approach employed to quantify the hydraulic conductivity (k) of soils under freezing conditions is incorporating a scalar parameter, i.e., relative permeability (K_r) ranging from 0 to 1 [196]. The most commonly used equation for K_r is relevant to saturation degree as follows.

$$K_r = \sqrt{S_r} \left[1 - (1 - S_r^{1/b})^b \right]^2, \quad (5)$$

where b is material constant, and S_r is saturation. In addition, the saturation degree is considered to be a function of temperature. Two widely used formulas of S_r are presented in Eqs. (6)–(7) (Nishimura et al. [230], Marwan et al. [213], Li et al. [184], Lunardini [206]; McKenzie et al. [216]).

$$S_r = \left[1 + \left(\frac{T_0 - T}{\chi} \right)^{\frac{1}{1-\eta}} \right]^\eta, \quad (6) \quad \frac{\partial}{\partial t} \left(\frac{\partial u}{\partial x} + \frac{\partial v}{\partial y} + \frac{\partial w}{\partial z} \right) = \frac{k}{\gamma_w} \nabla^2 p, \quad (12)$$

$$S_r = (1 - S_{r,\text{res}}) \left(\frac{T_0 - T}{\chi} \right)^2 + S_{r,\text{res}}, \quad (7)$$

where T_f is the freezing point; T is temperature; χ and η are material constants; $S_{r,\text{res}}$ is residual saturation that equals the minimum value of S_r . It is worth noting that the process history can affect K_r , i.e., K_r during the thawing process differs from K_r during the freezing process. As reported by Kaviani [130], the hysteresis phenomenon can lead to various values of S_r at the same saturation. Previous studies have achieved reasonable results using the concept of K_r , such as in studies on AGF [184, 196]. However, it remains challenging to obtain accurate values of hydraulic conductivity over a wide range of T [323]. Therefore, further research should be dedicated to addressing the effect of ice blocking on the hydraulic properties of soils.

2.2 Hydro-mechanical (HM) Coupling Approach

The hydro-mechanical (HM) coupling models explore the interactions of hydraulic and mechanical fields. Terzaghi [292] initially proposed the concept of effective stress (σ') and linked the pore pressure and medium deformation through the stress balance equation. The specific consolidation equation was derived by Tarzaghi [292] as follows.

$$\frac{\partial u_w}{\partial t} = C_{vx} \frac{\partial u_w^2}{\partial x^2} + C_{vy} \frac{\partial u_w^2}{\partial y^2} + C_{vz} \frac{\partial u_w^2}{\partial z^2}, \quad (8)$$

where u_w is excess pore pressure, which reflects the variation of pore pressure due to stress; C_{vx} , C_{vy} , and C_{vz} are consolidation coefficients in x -, y -, and z -direction, respectively. Different from the one-dimensional (1D) consolidation model proposed by Tarzaghi [292], Biot [20, 21] extended the consolidation mechanism to a three-dimensional (3D) condition with consideration of the interaction between solids and fluids [see Eqs. (9)–(12)], whose model describes the relations between pore pressure dissipation and medium skeleton deformation.

$$G \nabla^2 u + \frac{G}{1 - 2\nu} \frac{\partial}{\partial x} \left(\frac{\partial u}{\partial x} + \frac{\partial v}{\partial y} + \frac{\partial w}{\partial z} \right) - \frac{\partial u_w}{\partial x} = 0, \quad (9)$$

$$G \nabla^2 v + \frac{G}{1 - 2\nu} \frac{\partial}{\partial y} \left(\frac{\partial u}{\partial x} + \frac{\partial v}{\partial y} + \frac{\partial w}{\partial z} \right) - \frac{\partial u_w}{\partial y} = 0, \quad (10)$$

$$G \nabla^2 w + \frac{G}{1 - 2\nu} \frac{\partial}{\partial z} \left(\frac{\partial u}{\partial x} + \frac{\partial v}{\partial y} + \frac{\partial w}{\partial z} \right) - \frac{\partial u_w}{\partial z} + \gamma = 0, \quad (11)$$

where p is pore pressure; u , v and w are displacements along x -, y -, and z -direction, respectively. G is shear modulus; ν is Poisson ratio; γ is solid density; k is hydraulic conductivity of soils.

Based on Terzaghi and Biot models, various coupled HM models have been developed. After the introduction of the mixture theory concept [297], the macro homogenization and superposition assumptions have been applied to multi-phase media materials. Bowen [29, 30] further advanced the coupling HM mechanics equations based on the mixture theory and proposed a comprehensive elastic stress–hydraulic mixture constitutive theory. Subsequently, Borja and his co-authors [351, 365] used coupled HM finite element models to calculate the stress and deformation fields in steep hillsides impacted by rainfall infiltration. They have derived the analytical expression for the Biot tensor, effective tensor, and total Cauchy stress tensor:

$$\sigma' = \sigma + pb, \quad (13)$$

where σ and σ' are total Cauchy stress tensor and effective stress tensor, respectively; b is Biot tensor.

It is worth noting that since the freezing and thawing processes are significantly related to temperature, it seems impossible to simulate solely the coupled HM process in frozen soils without considering the thermal aspect.

2.3 Thermo-mechanical (TM) Coupling Approach

The phenomena of frost heave and thaw settlement in cold regions are closely related to the THM process within frozen soils, which can be attributed to the movements of soils affected by strength enhancing during freezing and strength weakening during the thawing process. To gain insights into the underlying mechanisms of frost heave and thaw settlement, a reliable computational coupled THM model is required to be developed based on TM or TH models. However, early studies primarily focused on studying the thermo-mechanical (TM) coupling models due to the greater complexity and challenges associated with solving THM models. Table 2 provides a summary of notable investigations on TM models for frozen soils. It is evident from Table 2 that various TM models have been proposed to simulate the TM process of frozen soils and address engineering issues such as frost heave, thawing settlements, crack formation, and pipeline settlements. These models have been validated by test results or numerical simulations. The majority of TM models predominantly focus on 3D macro-scale analyses employing FEM, in addition to the work of Sun et al. [281],

where the TM behaviours of frozen soils were modelled by the discrete element method (DEM).

As shown in Table 2, these TM models for frozen soils are typically derived from energy conservation and linear momentum equations without directly considering cryogenic suction and water migration into the frozen zone (e.g., neglecting the heat convection due to water migration). In addition, they simplified the coupling TM process by considering a partially unidirectional coupling relationship, i.e., only considering heat transfer's influence on mechanical aspects, such as assuming mechanical properties (e.g., elastic modulus, Poisson ratio, friction angle and cohesion) are functions of temperature, involving thermal strain/damage. In terms of the mechanical aspects, most models employed relatively simple representations of the mechanical behaviours of frozen soils, such as the linear elastic model [311], Mohr–Coulomb failure criterion [54, 60, 259], modified Cam Clay model [205] and so on.

Regarding the thermal aspect of the coupled TM model, TM models typically employ heat conduction and energy conservation to describe the thermal behaviours of frozen soils, allowing the models to account for the heat transfer and energy exchange processes within the frozen soil [37, 60, 205, 290, 311, 373]. Furthermore, some TM models incorporate specific mechanisms to account for water migration within the frozen soil as the temperature varies. For instance, Dayarathne et al. [54] utilised the Konrad–Morgenstern segregation potential model [144] to determine the velocity of water migration towards the ice lens. Shan et al. [259] proposed a novel coupled TM model incorporating a damage mechanism. Based on the strain equivalent theory of damage mechanisms, their study adopted the initial elastic modulus as a temperature damage parameter and introduced a composite damage factor to reflect the interdependence between mechanical and thermal damage.

Therefore, advancements in TM models for frozen soils deserve to be explored, including the development of constitutive models capable of capturing complex mechanical behaviours (e.g., anisotropic and rheological behaviour of ice lenses, nonlinearity of strength envelope, and potential pressure melting phenomena) and establishment of fully coupled models. Furthermore, the parameterisation of TM models should be refined to allow for more accurate representations of the TM processes in frozen soils. These advancements offer opportunities to improve the parameterisation process and enhance the reliability of TM models in capturing the complex TM response of frozen soils.

2.4 Thermo–hydro-mechanical (THM) Coupling Approach

The THM coupling phenomena during freezing and thawing processes play a pivotal role in soil frost heave and thaw settlement. Figure 2 illustrates the THM interactions in frozen soils involving governing equations and auxiliary relationships. To solve these models effectively, numerical methods such as the finite difference method (FDM), finite element method (FEM), or finite volume method (FVM) are commonly employed, which are validated independently through comparisons with experimental data, i.e., in situ monitoring data and laboratory measurements. Accurate simulations of this intricate THM process within frozen soils are imperative for comprehending the fundamental mechanisms underlying frost heave and thaw settlements in cold regions. Consequently, this section offers a comprehensive synthesis and classification of the technical underpinnings of various THM models, aiming to identify apparent disparities and commonalities by integrating contributions from diverse disciplines.

2.4.1 Coupled THM Models

Table 3 presents a compilation of typical investigations on THM models for frozen soils, including the governing equations for each field and detailed model information (i.e., suitable soil types, validations, applications, dimensions, and corresponding solvers).

2.4.1.1 Partially or Fully Coupled Model As depicted in Table 3, one of the earliest studies on the coupled THM model for frozen soils was proposed by Mu and Ladanyi [225], who derived a simplified model for solving the frost heave issues in practice based on some simplifying assumptions, such as a constant volume of soil skeleton during the freezing process, neglecting the effect of consolidation and stress on heat transport, considering elastic unfrozen soils, and assuming that the elastic modulus and yield points are independent of strain rate and confining pressure. Specifically, the frozen soils were treated as isotropic Mises materials, and creep was assumed to follow the Prandtl–Reuss law. However, these oversimplifying assumptions limited its application.

Selvadurai et al. [257] derived a numerical model for the heave of soil–pipeline interaction, calibrating the model with unidirectional freezing of saturated soil [242]. Besides, Selvadurai et al. [258] extended their 3D model to simulate the interaction between the buried pipeline and soil region. Lai et al. [152, 153] conducted numerical investigations on the behaviour of existing tunnels and retaining walls in cold regions by proposing a THM model according to thermal transfer theory, seepage theory, and frozen soil mechanics. However, their coupling THM analyses did not account for

Table 2 Summary of investigations on the coupled thermo-mechanical (TM) modelling for frozen soils

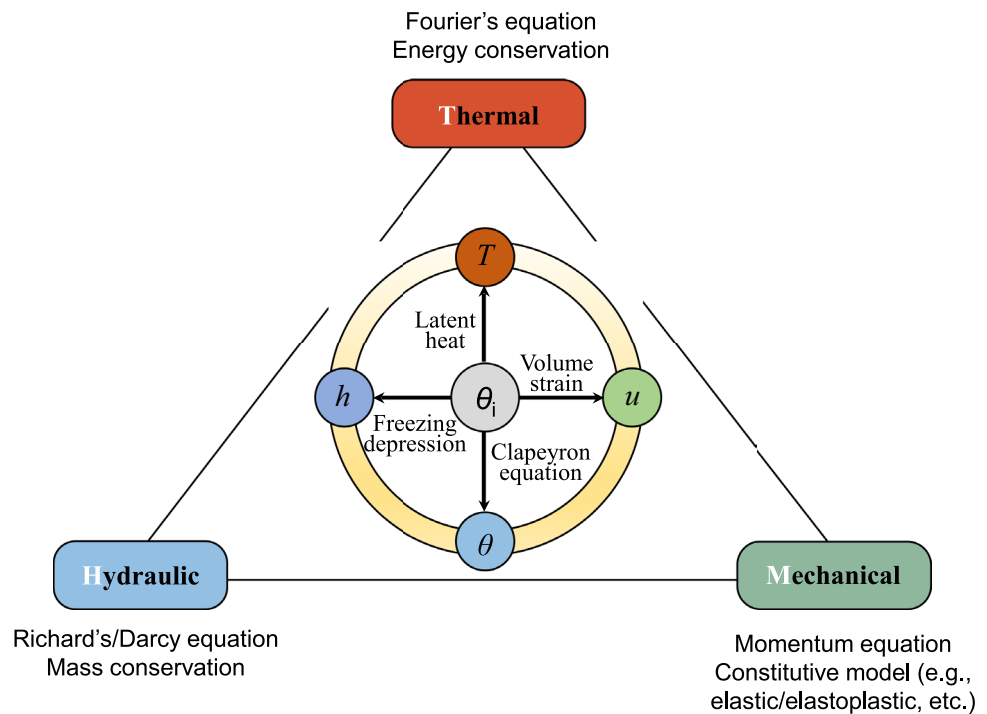
References	Coupling modes	Mechanical aspect	Thermal aspect	Heat convection	Validations	Applications	Dimensions	Scales	Solvers
Wang et al. [311]	[T→M] Thermal strain, $E(T), \nu(T), \varphi(T)$	Linear elastic model	Energy conservation	–	Frost depth from laboratory tests	Simulating the frost-jacking behaviour of screw piles subjected to frost heave	3D	Macro	FEM (ABAQUS)
Loli et al. [205]	[T→M] Compression index is related to pore ice ratio	Modified Cam Clay model	Energy conservation	–	Laboratory element tests*	Simulating the thawing of frozen soil	3D	Macro	FEM (ABAQUS)
Dong et al. [60]	[T→M] thermal expansion	Mohr–Coulomb	Heat conduction with phase change	–	–	Stability of thawing slope in cold region	2D	Macro	RFEM (COMSOL)
Tang et al. [290]	[T→M] creep strain rate= $f(T)$	Large-strain consolidation	Heat conduction	–	T from filed test	Thaw consolidation of embankments	3D	Macro	–
Cai et al. [33]	[T→M] Thermal strain	Orthotropic deformation with Hooke theorem	Heat transfer	$\sqrt{(BC)}$	Displacement from field test	Freeze sealing pipe-roof method used in Gongbei Tunnel	2D	Macro	FEM (ABAQUS)
Shan et al. [259]	[T→M] temperature damage, $E(T), \nu(T), \varphi(T)$	Mohr–Coulomb (nominal stress represents stress damage)	Temperature damage	–	Stress–strain curve of temperature-controlled triaxial compression test of frozen sand	Coupled TM damage model	3D	Macro	–
Zhou et al. [373]	[T→M] thermal strain	Thermal strain	Heat conduction	–	Thaw depth from numerical simulation*2	Modelling of settlement of oil pipeline	3D	Macro	FEM (PYTHON-ABAQUS secondary development)
Dayarathne et al. [54]	[T→M] $E(T), \nu(T), c(T)$	Mohr–Coulomb	Segregation potential model to calculate the velocity of water migration	–	T, ω , and frost heave from the Calgary full-scale test results	Modelling of long-term frost heave beneath chilled gas pipelines	2D	Macro	FEM (ABAQUS)
Sun et al. [281]	[T→M] Normal and tangential bond strength and modulus of particle= $f(T)$	3D contact model for cemented granular	Effects of T on bond strength and elastic modulus of ice cementation	–	Analytical solutions and triaxial test data of clayey sand	Modelling TM behaviour of frozen soil	3D	Micro	DEM (PFC3D)

c Cohesion, E elastic modulus, $f(T)$ function, T temperature, ν Poisson ratio, ω water content, φ friction angle, FEM finite element model, DEM discrete element method

*1Represents the test conducted by Yao et al. [341]

*2Depicts results from Zhang et al. [355]

Fig. 2 Schematic diagram of coupled THM model of frozen soils (h total water head, T temperature, u displacement, θ volumetric water content, θ_i volumetric ice content)



water migration. Subsequently, Lai et al. [155] developed a novel THM model that incorporated the water migration theory and explored the frost-heaving process of land bridges in the Qinghai–Tibetan railway. Yang et al. [338] analysed the frost heave in AGF via semi-coupled THM models with consideration of the effect of water migration on the temperature field and the impacts of stresses and temperature on the frost heave strain by introducing some empirical equation to simply the hydraulic aspect.

In contrast, fully coupled THM models are more reasonable and capable of accurately reproducing the deformation and coupled heat and mass transfer in frozen soils. To achieve a comprehensive integration, the mechanical constitutive model of frozen soils should maintain consistency with the effective-stress constitutive models of unfrozen soils. Most boundary value problems include both states and transient moving boundaries among them. However, the framework for such models does not seem to be well-established. Accordingly, given the similarity between behaviours of unsaturated soil and frozen soil, Nishimura et al. [230] developed a fully coupled THM framework (i.e., critical state elastoplastic model) for freezing and thawing soils by involving two sets of stress variables, i.e., net stress and suction-equivalent stress. This model possesses a similar form to the Barcelona Basic Model (BBM) for unfrozen, unsaturated soils [4] and was validated by in situ tests with buried large chilled gas pipelines [269]. However, some essential behaviours of frozen soils, such as strain-rate-dependent features and cumulative response to the freeze–thaw cycles,

are excluded from their model. Besides, Shastri and Sanchez [262] employed the THM model of Nishimura et al. [4] and validated it by comparing numerical results calculated by the finite element program CODE_BRIGHT and results from unconfined and triaxial tests from Parameswaran [237] and Parameswaran and Jones [238]. The comparison demonstrated that the coupled model behaves well in confined tests, but the differences increase with increasing confining pressure, which might be attributed to the fact that the model of Nishimura et al. [230] ignored the ice melting caused by higher confining stress. Subsequently, some scholars also employed the THM model of Nishimura et al. [230] to analyse other geotechnical issues, such as slope stability and AGF in underground construction [35, 148]. Some scholars also employed the concept of effective stress and developed various expressions to calculate effective stress for modelling the THM process within frozen soils. Furthermore, Qi et al. (2024) have comprehensively examined the expressions of effective stress for frozen soils and classified them into two categories. Based on extensive analysis, they concluded that developing a mechanism-based principle of effective stress for geotechnical engineering in cold regions is highly challenging, which arises from the presence of new substances in ice and the dynamic occurrence of phase change. A more detailed discussion on the effective stress applied in cold regions geotechnical engineering can be found in Qi et al. [245].

Table 3 Summary of investigations on the coupled thermo–hydro–mechanical (THM) modelling for frozen soils

No	Reference	Coupling modes	Mechanical aspect	Thermal aspect	Hydraulic aspect	Validation	U/S	F/T	Application	Dimension	Solver
1	Mu and Ladanyi [225]	$\begin{matrix} T \\ \swarrow \searrow \\ H \leftrightarrow M \end{matrix}$ [T → H] $\theta_0(T)$, $k_f(T)$, phase change with Clapeyron eq [T → M] initial tangent modulus = $f(T)$, volumetric expansion caused by ice [H → T] λ , C	Elastic material for unfrozen soil; elastoplastic model with Prandtl–Reuss law for frozen soil	Heat conduction eq	Moisture transport eq	Heave from unidirectional freezing of saturated soil [242]	S	F	Frost heave	1D	FEM (M), FDM (TH)
2	Lai et al. [152, 153]	$\begin{matrix} T \\ \swarrow \searrow \\ H \leftrightarrow M \end{matrix}$ [T → H] $k_f(T)$, phase change with Clapeyron eq [H → M] volumetric expansion caused by ice [H → T] heat convection [M → H] k_u (stress)	Elastic model (Taylor and Luthin criterion to define the frost heave)	Heat transfer theory ($\lambda(T)$, $C(T)$)	Seepage theory	–	S	F & T	Tunnel and retaining wall	2D	FEM
3	Selvadurai et al. [257]	$\begin{matrix} T \\ \swarrow \searrow \\ H \leftrightarrow M \end{matrix}$ [T → H] $k(T)$, $\theta_{ic}(T)$, phase change with Clapeyron eq. [H → M] volumetric expansion caused by ice [H → T] λ , C	Elastic model	Heat conduction eq	Moisture transport eq	Heave from unidirectional freezing of saturated soil [242]	S	F	Frost heave induced by soil–pipeline interaction	1, 2, 3D	FEM
4	Selvadurai et al. [258]	$\begin{matrix} T \\ \swarrow \searrow \\ H \leftrightarrow M \end{matrix}$ [T → H] $k(T)$, $\theta_{ic}(T)$, phase change with Clapeyron eq [H → M] volumetric expansion caused by ice [H → T] λ , C	Mohr–Coulomb criterion for unfrozen soil, linear elastic model for frozen soil	Heat conduction eq	Moisture transport eq	large-scale test [52, 53]	S	F	Frost heave of soil–pipeline	3D	FEM
5	Li et al. [161]	$\begin{matrix} T \\ \swarrow \searrow \\ H \leftrightarrow M \end{matrix}$ [T → H] water migration due to temperature gradient [T → M] thermal expansion [H → T] λ , C [H → M] volumetric expansion caused by ice [M → T] deformation energy [M → H] water compression	Bishop type's effective stress theory (thermo-elasticticity model) Effective stress eq, related to thermal stress, pore pressure, water compressive	Energy conservation	Mass conservation and Darcy's law	Settlement from thermo-elastic consolidation of 1D sand column [1]	S	F & T	THM modelling	2D	FEM
6	Lai et al. [155]	$\begin{matrix} T \\ \swarrow \searrow \\ H \leftrightarrow M \end{matrix}$ [T → H] $\theta_{ic}(T)$, phase change with Clapeyron eq [H → M] volumetric expansion caused by ice	Hooke's law	Heat transfer theory ($\lambda(T)$, $C(T)$)	Seepage theory	–	S	F & T	Land bridge in the cold region	3D	FEM

Table 3 (continued)

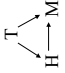
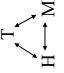
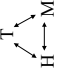
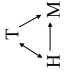
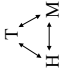
No	Reference	Coupling modes	Mechanical aspect	Thermal aspect	Hydraulic aspect	Validation	U/S	F/T	Application	Dimension	Solver
7	Yang et al. [338]	 <p>[T → H] $\theta_i(T)$ [T → M] thermal expansion [H → M] volumetric expansion caused by ice</p>	Hooke's law	Energy conservation ($\lambda(T)$, $C(T)$)	Mass conservation and Darcy's law	Frost heave from in situ observations	S	F	AGF	2D	FEM (MARC)
8	Nishimura et al. [230]	 <p>[T → H] $\theta_i(T)$, $\mu(T)$, $K(S_i)$, phase change with Clapeyron eq [T → M] shear strength = $f(T, n)$ [H → T] λ, heat convection caused by water migration [H → M] change of σ [M → T] λ [M → H] change of n</p>	Elastoplastic hardening constitutive model based on BBM	Energy conservation	Mass conservation and Darcy's law	Heave and ω from in situ frost heave tests conducted by [269]	S	F & T	THM modelling	2D	FEM (CODE_BRIGHT)
9	Thomas et al. [293]	 <p>[T → H] $k = f(T)$, $S_i = f(T)$; phase change with Clapeyron eq [T → M] thermal expansion [H → T] λ, C, heat convection caused by water migration [H → M] change of σ [M → T] λ, C [M → H] water flow driven by pore pressure gradients</p>	Terzaghi's effective stress principle	Energy conservation	Mass conservation and Darcy's law	Frost heave and T from small-scale laboratory freezing and thawing tests [133]	S	T	Thaw-related slow mass movement (solifluction)	1D	FEM (COMPASS)
10	Liu and Yu [200]	 <p>[T → H] hydraulic conductivity due to thermal gradient, phase change with Clapeyron eq [T → M] thermal expansion [H → T] λ, C, heat convection caused by water migration [H → M] volumetric expansion caused by ice; strain due to matric potential</p>	Navier's eq. (sum of elastic, thermal, phase change of water, change of matric potential and initial strains)	Modified Fourier's law for conduction and convection	Richards' eq. with modification for ice term to describe fluid motion	T and ω from in situ observations	U	F	THM modelling	2D	FEM (COMSOL)
11	Zhou and Meschke [378]	 <p>[T → H] $S_i(T)$, phase change with liquid-crystal equilibrium [T → M] thermal expansion [H → M] Biot coefficient [H → T] entropy balance [M → H] change of n [M → T] density of entropy</p>	Poroelastic constitutive relations	Entropy conservation for mixture	Mass conservation and Darcy's law	T and $S_{,i}$ from phase-change model of Lackner et al. [150]; P_L and displacement of analytical solution from 1D consolidation test; volume dilatation of analytical solution for hardened cement paste during freezing [16]	S	F	AGF	1D	FEM (KRATOS)

Table 3 (continued)

No	Reference	Coupling modes	Mechanical aspect	Thermal aspect	Hydraulic aspect	Validation	U/S	F/T	Application	Dimension	Solver
12	Shastri and Sanchez [262]	<p>[T → H] $\theta_i(T), \mu(T), K_i(S_i)$, phase change with Clapeyron eq [T → M] shear strength = $f(T, n)$ [H → T] λ, energy change caused by convection [H → M] change of σ' [M → H] change of n [M → T] λ</p>	Elastoplastic hardening constitutive model based on BBM	Energy conservation	Mass conservation and Darcy's law	Stress from unconfined and confined tests on Ottawa sand [237, 238]	S	F	THM modelling	3D	FEM (CODE_BRIGHT)
13	Zhou and Li [372]	<p>[T → H] $S_r(T), k(T)$, water migration due to temperature gradient, phase change with Clapeyron eq [H → T] λ, C [H → M] change of pore pressure [M → T] λ, C [M → H] change of e</p>	Effective stress	Energy conservation	Mass conservation and Darcy's law	–	S	F	THM modelling	1D	FEM (COMSOL)
14	Zhou and Meschke [374]	<p>[T → H] $S_r(T), \mu(T)$, phase change with liquid–crystal equilibrium [T → M] thermal expansion [H → M] Biot coefficient, mechanical dissipation [H → T] λ [M → T] density of entropy [M → H] change of n</p>	Momentum balance, linear thermo-poro-elasticity	Entropy conservation, Fourier's law	Mass conservation and Darcy's law	Same as [378]	S	F	AGF	1D, 3D	FEM (KRATOS)
15	Zhang and Michalowski [363]	<p>[T → H] pore ice ratio = $f(T), \theta_u(T)$ [T → M] change of slope of NCL, URL [H → M] tensile yield strength and pre-consolidation pressure is related to pore ice ratio [H → T] λ, C [M → H] change of n</p>	Effective stress and elastoplastic model	Energy conservation	Mass conservation and Darcy's law	–	S	F & T	Frost heave and thaw settlement	2D	FEM (ABAQUS)

Table 3 (continued)

No	Reference	Coupling modes	Mechanical aspect	Thermal aspect	Hydraulic aspect	Validation	U/S	F/T	Application	Dimension	Solver
16	Lai et al. [151]	<p>[T → H] $\theta_i(T)$, $k_t = f(k_w, n, \theta_w)$, phase change with Clapeyron eq [T → M] compression modulus = $f(T)$, thermal strain = $f(T)$ [H → M] pore water pressure change [H → T] thermal diffusivity under hydraulic gradient, λ, C [M → H] change of n [M → T] heat caused by soil deformation, λ, C</p>	Terzaghi effective stress	Energy conservation, Fourier's law	Mass conservation and Darcy's law Fourier's law	Frost heave and freezing front position from one-side freezing experiments of saturated silty clay	S	F	Frost heave	ID	FEM (COM-SOL)
17	Zhang and Michalowski [353]	<p>[T → H] pore ice ratio = $f(T)$, porosity change, $\theta_w(T)$ [T → M] change of slope of NCL, URL [H → M] tensile yield strength and pre-consolidation pressure is related to pore ice ratio [H → T] λ, C [M → H] change of n</p>	Effective stress and elastoplastic model	Energy conservation	Mass conservation and Darcy's law	Frost heave from step freezing process [74]	S	F & T	Frost heave and thaw settlement	2D	FEM (ABAQUS)
18	Zheng and Kanie [370]	<p>[T → H] $k_t(T)$ [T → M] Young's modulus [H → T] heat convection caused by water migration, $C = f(\theta_w)$ [M → H] change of σ' [M → T] $k_t = f(\text{pore pressure head})$, $\theta_w = f(\text{pore pressure head})$ [M → T] $C = f(\text{pore pressure head})$</p>	Takashi's eq	Energy conservation, Fourier's law	Mass conservation and Darcy's law	Frost heave comparison of different water tables	S & U	F	Frost heave	2D	FEM
19	Zhang et al. [361]	<p>[T → H] $\theta_w(T)$; $k_t = f(T)$ [H → M] pore pressure changes, Biot coefficient [H → T] $C = f(\theta_w)$ [M → H] $k_t(\epsilon_v)$, water migration</p>	Effective stress with Burger's viscoelasticity model	Energy conservation $(\lambda(T), C(T))$	Biot's consolidation	T and settlement from in situ long-term plate loading test	S	T	Settlement	2D	FEM (COM-SOL)

Table 3 (continued)

No	Reference	Coupling modes	Mechanical aspect	Thermal aspect	Hydraulic aspect	Validation	U/S	F/T	Application	Dimension	Solver
20	Bekele et al. [17]	<p>[T → H] $S_r(T)$, $K_r(S_r)$, phase change with Clapeyron eq [T → M] thermal strain [H → T] λ, C, water convection [H → M] E, $\nu = f(S_{r,i})$, volumetric strain = $f(n, S_{r,i})$ [M → H] $S_r(p_w)$</p>	Bishop-type effective stress (nonlinear elastic relation with T)	Energy conservation, Fourier's law	Mass conservation, Darcy's law	0°C isotherm from field-scale observations [271]	S	F & T	Ground freezing and thawing	1D, 2D	FEM
21	Luo et al. [207]	<p>[T → H] $K_r(S_r)$, $k = f(K_r)$ [T → M] thermal expansion and contraction strain [H → M] volumetric strain [H → T] C [M → H] $k = f(\text{effective stress})$</p>	Bishop's effective stress	Energy conservation	Mass conservation, Darcy's law	Axial strain from frost heave test, T from in situ observations	U	F & T	Pavement Structure	2D	FEM
22	Na and Sun [226]	<p>[T → H] $K_r(S_r)$, $\mu(T)$, $S_r(T)$, phase change with Clapeyron eq [T → M] cryosuction pressure = $f(T)$ [H → M] change of pore pressure [H → T] λ, C [M → H] K_r is sensitive to pore pressure [M → T] dissipation energy due to pure mechanical load</p>	Linear momentum balance eq. (Bishop's effective stress with critical state elastoplastic model)	Energy conservation, Fourier's law	Mass conservation, Darcy's law	Settlement from thawing consolidation [342]	S	F & T	THM modelling	2D and 3D	FEM
23	Zhang et al. [354]	<p>[T → H] $\theta_{i0}(T)$, $I = 10^{10\%}$, $k(\theta_{i0})$, $D(\theta_{i0}, I)$ [T → M] E, ν, c, $\varphi = f(T)$ [H → T] $\lambda(\theta_{i0})$, $C(\theta_{i0})$ [H → M] volumetric strain</p>	Equilibrium eq. with DP criterion considering frost rate	Energy conservation ($\lambda(T)$, $C(T)$)	Mass conservation	T from in situ observations	S	F & T	Embankment	2D	FEM (COM-SOL)
24	Arzanfudi and Al-Khoury [9]	<p>[T → H] $\theta_{i0}(T)$, $K_r(\theta_{i0})$, phase change with Clapeyron eq [T → M] thermal expansion, $E(T)$ [H → M] Biot coefficient [H → T] λ [M → H] $n = f(p_w)$, cryosuction, solid displacement [M → T] $\lambda(\theta_{i0})$, melting point depression due to cryosuction</p>	Linear momentum balance eq	Energy conservation, Fourier's law	Mass conservation, Darcy's law	Numerical solution of 2D thawing benchmark [82]	S	F & T	Energy pile application	2D	XFEM

Table 3 (continued)

No	Reference	Coupling modes	Mechanical aspect	Thermal aspect	Hydraulic aspect	Validation	U/S	F/T	Application	Dimension	Solver
25	He et al. [194]	<p>[T → H] $\theta_w(T)$, $k(T)$, water migration due to heat gradient, phase change with Clapeyron eq [H → M] $E(T)$ [H → M] change of pore pressure [H → T] λ, C, heat convection caused by water migration [M → H] water migration due to stress [M → T] deformation energy</p>	Momentum equilibrium eq. (nonlinear elastic model)	Energy conservation, Fourier's law	Continuity eq	Numerical solution of heave test [43, 225]	S	F	Frost heave	2D	FEM
26	Ji et al. [120]	<p>[T → H] $w_v(T)$, $k_w(\theta_w)$ [T → M] tensile strength = $f(T)$ [H → M] change of pore pressure [H → T] λ, C, [M → H] $\theta_w(p_w)$, water velocity, change of n [M → T] λ, C</p>	Effective stress	Energy conservation	Mass conservation, Darcy's law	Frost heave-induced pressure from in situ observations	S	F	Frost heave	2D	FVM
27	Li et al. [189]	<p>[T → H] $\theta_w(T)$, $\mu(T)$, $k_s(\theta_w)$, $D(\theta_w)$ [H → M] volumetric strain [H → T] E, ν, c, φ, $H = f(T)$</p>	Bingham model with DP criterion	Energy conservation ($\lambda(T)$, $C(T)$)	Mass conservation	T and freezing front from one-side freezing experiment for soil column	S	F	Frost heave	2D	FEM (MHMIP-2D)
28	Yin et al. [344]	<p>[T → H] $k(T)$, latent heat and density of vapour condensation = $f(T)$, phase change with Clapeyron eq [H → M] change of pore pressure [H → T] λ, C, heat convection due to water migration [M → H] change of n</p>	Bishop's effective stress theory	Energy conservation	Mass conservation, Darcy's law	Frost heave from numerical results of saturated freezing soil [372]	U	F	Frost heave	1D	FEM (COM-SOL)
29	Zhan et al. [348]	<p>[T → H] $\theta_w(T)$, $I = 10^{10\%}$, $k(\theta_w, I)$ [H → M] volumetric strain</p>	Thermoelastic model	Heat conduction eq	Richards' eq	T and ω from in situ observations	U	F & T	Slope	2D	FEM (COM-SOL)
30	Deng et al. [56]	<p>[T → H] $\rho(T)$ [H → M] Biot coefficient [H → T] λ, C, heat convection due to water migration [M → H] change of n</p>	Navier eq	Heat conduction eq	Darcy's law, continuity eq	T from in situ observations (10-year FT period of a silty rock layer); surface settlement from in situ observations	S	T	Thawing subsidence	2D	FEM (COM-SOL)
31	Tian et al. [294]	<p>[T → H] $\theta_w(T)$, $I = 10^{10\%}$, $k(S)$, $D(k(\theta_w), I)$, $S_s(\theta_w)$ [T → M] E, ν, c, $\varphi = f(T)$ [H → M] volumetric strain</p>	Elastoplastic model with Mohr-Coulomb criterion	Heat conduction eq	Richards' eq	-	U	F & T	Railway embankment	2D	FEM (COM-SOL)

Table 3 (continued)

No	Reference	Coupling modes	Mechanical aspect	Thermal aspect	Hydraulic aspect	Validation	U/S	F/T	Application	Dimension	Solver
32	Bai et al. [12]	<p>[T → H] $\theta_s(T)$, $I = 10^{10} \text{ kg}$, $k(\theta_w)$, $D(\theta_w)$ [T → M] E, ν, c, $\varphi = f(T)$, frost heave strain and shrinkage strain are related to T [H → M] volumetric strain and shrinkage strain due to water migration</p>	Momentum equilibrium (Drucker–Prager yield criterion with Mohr–Coulomb criterion)	Heat conduction eq	Mass conservation	T and freezing front from the stepwise freezing test [320]	S	F	Frost heave	2D	FEM
33	Dong and Yu [62]	<p>[T → M] thermal expansion, E, ν, c, $\varphi = f(T)$ [H → M] strain caused by suction</p>	Navier’s eq	Energy conservation	Mass conservation, Darcy’s law	T from freezing and thawing test	S	F	Frost heave in retaining wall	2D	RFEM
34	Lei et al. [158]	<p>[T → H] $\xi_s(T)$, $k(T)$, phase change with Clapeyron eq [T → M] cryosuction pressure = $f(T)$ [H → T] λ, C [M → M] Biot coefficient, change of pore pressure [M → T] λ, C [M → H] change of n</p>	Biot’s effective stress	Heat conduction eq	Mass conservation	T and frost heave from one-side freezing experiments for silty clay columns [151]	S	F	THM modelling	ID	FEM (COM-SOL)
35	Na et al. [227]	<p>[T → H] $K_s(\xi_s)$, phase change with Clapeyron eq [T → M] change of yield surface [H → T] λ, C [H → M] change of pore pressure [M → T] λ, C [M → H] change of n</p>	Linear momentum balance eq. (effective stress elastoplastic model)	Energy conservation	Mass conservation, Darcy’s law	–	U	F	Frost heave with chilled gas pipelines	ID and 2D	FEM
36	Weng et al. [324]	<p>[T → H] $k_{sp}(T)$ [T → M] thermal strain [H → M] change of pore pressure [H → T] λ, C, heat convection caused by water migration [M → T] viscoplastic dissipation potential [M → H] change of n</p>	Elastic-viscoplastic model (viscoplasticity is modelled by linear Norton Hoff’s law)	Energy conservation	Mass conservation, Darcy’s law	Frost heave and flux rate from 1D saturated soil column	S	F	THM modelling	ID	FEM (COM-SOL)

Table 3 (continued)

No	Reference	Coupling modes	Mechanical aspect	Thermal aspect	Hydraulic aspect	Validation	U/S	F/T	Application	Dimension	Solver
37	Sweidan et al. [286]	<p>Phase field method by using phase-field variable (pressure, seepage velocity, displacement) temperature and fraction of each phase to indicate state of pore-fluid</p>	Momentum balance (effective stress)	Energy conservation	Mass conservation	Solid-liquid interface evolution from experimental results for freezing of water in a copper foam [68]; T from simulation results of water freezing in soils [374]; S_{ii} from a TPM-based model considering mass production terms to account for the phase change [24]	S	F	Frost heave	2D	FEM (Flexible PDE)
38	Yu et al. [341]	<p>[T → H] $S_s(T)$ [T → M] compression index = $f(T)$ [H → T] λ, C, heat convection due to pore water [H → M] deformation due to water migration [M → T] water flow due to thermal gradient [M → H] $\kappa(e)$, water flow due to pressure gradient</p>	Momentum equilibrium	Heat transfer eq	Mass conservation, Darcy's law	Surface settlement and thaw depth, e , u_w , and T from small- and large-strain thaw consolidation theories [64, 223]	S	F & T	Frost heave, thaw consolidation	ID	FEM
39	Zhang et al. [345]	<p>[T → H] $\theta_v(T)$, $k(\theta_v)$, $D(\theta_v)$, phase change with Clapeyron eq [T → M] thermal strain [H → M] volumetric strain due to phase change [H → T] energy change caused by water migration</p>	Elastic model	Energy conservation	Mass conservation, Darcy's law	Frost depth from in situ observations	U	F & T	High-Speed Railway Roadbeds	2D	FEM (COM-SOL)
40	Huang and Rudolph [105]	<p>[T → H] $S_{ii}(T)$, $k_s(T)$, $\theta_v(T)$, $K_s(S_p)$, phase change with Clapeyron eq [T → M] change of pore pressure [H → M] compression modulus = $f(S_p)$ [H → T] λ, C [M → H] change of e, $k_s(e)$ [M → T] λ, C</p>	Terzaghi's effective stress principle	Energy conservation	Mass conservation eq. and Darcy's law	T from laboratory top-down freezing test [219]	U	F	THM modelling	ID	FEM (COM-SOL)
41	Ji et al. [119]	<p>[T → H] $\theta_v(T)$, phase change with Clapeyron eq [H → M] change of pore pressure, solid consolidation [H → T] λ, C [M → H] $\theta_v(p_w)$</p>	Effective stress principle [260]	Energy conservation	Mass conservation	Heave from freezing test on freezing saturated clay [103] and other models [375, 376]	S	F	Frost heave	ID	FVM

Table 3 (continued)

No	Reference	Coupling modes	Mechanical aspect	Thermal aspect	Hydraulic aspect	Validation	U/S	F/T	Application	Dimension	Solver
42	Li et al. [178]	<p>[T → H]$\theta_v = f(T)$, $k(\theta_v)$, $D(\theta_v, T)$, $I = 10^{-10\theta_v}$ [T → M] thermal expansion, frost heave force = $f(T)$ [H → M] frost heave force = $f(\omega)$</p>	Linear elastic model (thermal expansion)	Fourier's law	Richards eq	–	S	F	Frost heave on tunnel	2D	FEM (COM-SOL)
43	Li et al. [164]	<p>[T → H]$\theta_v(T)$, $K_r(S_p)$, relative humidity and $\rho_v = f(T)$, soil water potential, $D_v = f(T)$, latent heat of vapour condensation, diffusion coefficient = $f(T)$, phase change with Clapeyron eq [T → M] pore ice pressure = $f(T)$ [H → M] consolidation due to water, frost heave due to ice formation [H → T] heat convection due to water and moist air, λ, C [M → H] change of e, S_r [M → T] λ, C</p>	Elastic model	Energy conservation	Mass conservation eq. with Darcy's law	T from unidirectional freezing soil-column test; ω from simulations from Hansson et al. [87]	U	F	Frost heave	ID	FEM (COM-SOL)
44	Qin et al. [246]	<p>[T → H]$K_r(S_p)$, $\theta_v(T)$ [H → T] heat convection due to water migration [TH → M] c, $\rho = f(\text{number of freeze–thaw cycles})$</p>	Modified Mohr–Coulomb criterion based on double-stress variables	Energy conservation	Mass conservation eq. and Darcy's law	T from in situ observations	U	F & T	Slope stability	2D	FEM (GEO-STUDIO)
45	Shastri et al. [261]	<p>[T → H]$K_r(S_p)$, $S_r(T)$ phase change with Clapeyron eq [T → M] cryogenic suction is related to T, strength is related to T, size of yield surface [H → M] cryosuction [H → T] heat convection due to water migration, λ [M → H] change of e [M → T] λ</p>	HISS sub-loading model	Energy conservation, Fourier's law	Mass conservation eq. and Darcy's law	q and ϵ_v from hydrostatic, uniaxial and deviatoric compression	S	F	Thawing behaviour of frozen soil under the building foundation	2D	FEM (CODE-BRIGHT)
46	Sweidan et al. [286]	<p>Phase field method by using phase-field variable (pressure, seepage velocity, displacement) temperature and fraction of each phase to indicate the state of the pore-fluid</p>	Momentum balance	Energy conservation eq	Mass conservation eq. With Darcy's law	0°C isotherm position, frost heave, and final ice lens position from the test	S	F	THM modelling	ID	FEM (Flex-PDE)

Table 3 (continued)

No	Reference	Coupling modes	Mechanical aspect	Thermal aspect	Hydraulic aspect	Validation	U/S	F/T	Application	Dimension	Solver
47	Wu et al. [331]	<p>[T → H] $\theta_{i1}, k = f(T)$, phase change with Clapeyron eq [T → M] compression modulus = $f(T)$ [H → M] volumetric strain [H → T] heat convection due to water migration, λ, C [M → H] change of e [M → T] λ, C</p>	Effective stress principle	Energy conservation eq	Mass conservation law with Darcy's law	T from soil columns experiencing FT cycles	S	F & T	Deformation under FT condition	ID	FEM (COM-SOL)
48	Xiao et al. [334]	<p>[T → H] $S_{ij}(T), k_i(T)$, phase change with Clapeyron eq [T → M] compression modulus = $f(T)$ [H → M] change of pore pressure [H → T] heat convection due to water migration, λ, C [M → H] change of e [M → T] λ, C</p>	Effective stress	Energy conservation eq	Mass conservation, Darcy's law	Axial strain and thaw depth from the test [343]	S	T	Thaw settlement	ID	FEM (COM-SOL)
49	Yu et al. [346]	<p>[T → H] $K_i(S_p), S_i(T), \theta_{i1}(T), k$ affected by T [T → M] $E = f(T)$ [H → T] λ, C [H → M] volumetric expansion [M → H] change of n [M → T] λ, C</p>	Elastic model	Heat transfer eq	Mass conservation, Darcy's law	T , normal pressure, axial force from model testing; internal force from simulation [333]	S	F	Frost heave in a shallow tunnel	3D	FEM (ABAQUS)
50	Zhelinin et al. [2021]	<p>[T → H] $S_i(T), \theta_{i1}(T), k_i(T)$, phase change with Clapeyron eq [T → M] thermal strain [H → T] heat convection due to water migration [H → M] volumetric expansion [M → H] change of n</p>	Coussy poromechanics	Energy conservation eq	Mass conservation, Darcy's law	–	S	F	AGF	3D	FEM (COM-SOL)

Table 3 (continued)

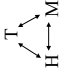
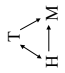
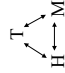
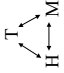
No	Reference	Coupling modes	Mechanical aspect	Thermal aspect	Hydraulic aspect	Validation	U/S	F/T	Application	Dimension	Solver
51	Gao et al. [76]	 <p>[T → H] $k_f(T)$, $k(K_r(S_r))$, water flow caused by temperature gradient, phase change with Clapeyron eq [T → M] thermal strain [H → M] shear modulus, bulk modulus and density are related to component content [H → T] C, heat convection due to water migration [M → H] water flow caused by pressure gradient [M → T] energy change due to solid deformation</p>	Linear momentum balance	Energy conservation	Mass conservation	Heave depth from frost heave tests on Devon silt [145]	S	F	Ice lens formation and growth modelling	2D	FEM and XFEM
52	Huang et al. [107]	 <p>[T → H] $K_r(S_r)$, $I = 10^{-6\theta}$, k affected by temperature, phase change with Clapeyron eq [T → M] thermal expansion [H → M] volumetric expansion [H → T] heat convection due to water migration, λ, C [M → H] Biot–Willis coefficient</p>	Linear thermo-poroelastic model	Energy conservation	Modified Richards eq	Unidirectional freezing of non-heaving unsaturated soil [116]; frost heave and penetration from the test [242]; heave depth from simulation [163, 225]	S	F	Water main failure caused by roadbed frost	2D	FEM (COM-SOL)
53	Ji et al. [118]	 <p>[T → H] ice lens growth rate = $f(T)$, phase change with Clapeyron eq [H → T] λ, C [T → M] deformation due to pressure [H → M] change of pore pressure [M → T] phase transition rate change due to overburden pressure [M → H] pore blocking due to overburden pressure</p>	Effective stress	Energy conservation	Darcy's law	Frost heave from experimental observations and model of [376]	S	F	Ice lens growth modelling	1D	FDM
54	Kebria et al. [131]	 <p>[T → H] $\theta_s(T)$, phase change with Clapeyron eq [T → M] λ, C [H → T] heat convection [H → M] Biot coefficient, change of σ' [M → H] change of n</p>	Plastic model with deviatoric hardening and Mohr–Coulomb criterion	Heat transfer eq	Mass balance eq	T and ω from the test [377]	U	F	THM modelling	2D	FEM

Table 3 (continued)

No	Reference	Coupling modes	Mechanical aspect	Thermal aspect	Hydraulic aspect	Validation	U/S	F/T	Application	Dimension	Solver
55	Li et al. [179]	$\begin{matrix} T \\ \swarrow \searrow \\ H \leftrightarrow M \end{matrix}$ <p>[T → H] $S_{v,i}(T)$, thermally induced pore volume change [T → M] thermal volumetric dilation [H → M] volumetric expansion, change of pore pressure [H → T] λ, C, [M → H] change of n [M → T] λ, C,</p>	Momentum balance (poroelasticity model, Coussy 2005)	Energy conservation and Fourier's law	Mass conservation and Darcy's law	Analytical solution	S	F	THM modeling with different hydraulic boundary conditions	ID	FEM (COM-SOL)
56	Ling et al. [191]	$\begin{matrix} T \\ \swarrow \searrow \\ H \leftrightarrow M \end{matrix}$ <p>[T → H] $\theta_v(T), K_r(S_r, D)$, $J = 10^{-30} \theta_v^n$, k affected by temperature, phase change with Clapeyron eq [T → M] surface tension = $f(T)$ [H → M] volumetric expansion [H → T] λ, C, change of p_w [M → H] change of n [M → T] λ, C</p>	Effective stress	Heat transfer eq	Darcy's law	Internal force from in situ observations [333]	S	F	Tunnel	2D	FEM (ABAQUS)
57	Suh and Sun [280]	$\begin{matrix} T \\ \swarrow \searrow \\ H \leftrightarrow M \end{matrix}$ <p>Multi-phase-field poromechanics model where the governing equations are coupled with balance law</p>	Extending Miller's model (neutral stress) into the phase-field framework with damage	Energy conservation	Mass balance eq	T from other models [150, 286], pore pressure from Terzaghi's 1D consolidation problem, T from the test [68]	S	F	Freezing-induced fracture modeling	2D	FEM
58	Wang et al. [306]	$\begin{matrix} T \\ \swarrow \searrow \\ H \leftrightarrow M \end{matrix}$ <p>[T → H] $\theta_v, \theta_v^n(T), D(\theta_v, D)$, $J = 10^{-10} \theta_v^n$ [T → M] $E, \nu, c, \phi = f(T)$ [H → M] volumetric strain, frost heave rate = $f(\text{ice content})$ [H → T] λ, C</p>	Elastic model	Energy conservation and Fourier's law	Richards eq	–	U	F	Frost heave and frost jacking response	2D	FEM (COM-SOL)
59	Wu and Ishikawa [326]	$\begin{matrix} T \\ \swarrow \searrow \\ H \leftrightarrow M \end{matrix}$ <p>[T → H] $k(K_r, I, S_r, T), K_r(S_r)$, phase change with Clapeyron eq [T → M] thermal expansion [H → M] volumetric expansion [H → T] λ, C</p>	Linear elastic model (Navier's eq.)	Energy conservation	Richard's eq	Frost heave and water migration from frost heave tests of Toyuro soil [112] and Fujinomori soil [295]	U	F	Frost heave and water migration	2D	FEM (COM-SOL)

Table 3 (continued)

No	Reference	Coupling modes	Mechanical aspect	Thermal aspect	Hydraulic aspect	Validation	U/S	F/T	Application	Dimension	Solver
60	Yang et al. [339]	$\begin{matrix} T \\ \swarrow \searrow \\ H \leftrightarrow M \end{matrix}$ $[T \rightarrow H] S_{v,i}(T), \mu(T), \text{moisture migration due to temperature gradient}$ $[T \rightarrow M] E(S_{v,i}(T))$ $[H \rightarrow M] E(S_{v,i})$ $[H \rightarrow T] \text{heat convection due to water migration, } \lambda, C$ $[M \rightarrow H] \text{moisture migration due to pore pressure and gravity, change of } n$ $[M \rightarrow T] \lambda, C$	Elastic theory	Energy conservation	Mass conservation and cubic law for fracture seepage	T from the model test [243]; T and frost heave from in situ observations [305]	S	F	THM modelling	2D	–
61	Zhelmin et al. [369]	$\begin{matrix} T \\ \swarrow \searrow \\ H \leftrightarrow M \end{matrix}$ $[T \rightarrow H] S_{v,i}(T), k(T), \text{phase change with Clapeyron eq}$ $[T \rightarrow M] \text{thermal strain}$ $[H \rightarrow M] \text{Biot coefficient, change of } p_w$ $[H \rightarrow T] \lambda, C$ $[M \rightarrow H] \text{change of } n$ $[M \rightarrow T] \lambda, C$	Poromechanics theory of Coussy [47]	Energy conservation	Mass conservation, Darcy's law	T from one-sided freezing of saturated silty clay columns [15]; T and radial strain in radial freezing of sand	S	F	Frost heave and water migration	3D	FEM (COM-SOL)
62	Zheng et al. [371]	$\begin{matrix} T \\ \swarrow \searrow \\ H \leftrightarrow M \end{matrix}$ $\text{Theory of porous media (TPM) by using the entropy inequality with Coleman–Noll procedure}$	Momentum balance	Energy conservation	Mass conservation eq	Analytical solutions (freezing front position for freezing wall by [34]) and T for point heat source consolidation by [140])	S	F	THM modelling	2D	FEM
63	Ma et al. [208]	$\begin{matrix} T \\ \swarrow \searrow \\ H \leftrightarrow M \end{matrix}$ $[T \rightarrow H] \theta_v(T), k(\theta_v, D), D(\theta_v, D), I = 10^{10} \theta_v^h$ $[T \rightarrow M] E, \nu, c, \varphi = f(T)$ $[H \rightarrow T] \text{heat convection due to water migration}$	DP yield rule	Heat conduction eq	Water transport eq	T from field monitoring	S	FT	Canals with berms in cold regions	2D	FEM
64	Park et al. [239]	$\begin{matrix} T \\ \swarrow \searrow \\ H \leftrightarrow M \end{matrix}$ $[T \rightarrow H] \text{pore ice ratio} = f(T), \text{porosity change, } \theta_v(T), \text{tensile strength is related to freeze–thaw cycles}$ $[H \rightarrow M] \text{change of NCL, URL}$ $[H \rightarrow M] \text{pre-consolidation is related to pore ice ratio}$ $[H \rightarrow T] \lambda, C$ $[M \rightarrow H] \text{change of } n$ $[M \rightarrow T] \lambda, C$	Elasto-viscoplastic model (Bingham model)	Heat transfer eq	Moisture transport eq	T from field monitoring	S	F & T	Embankment	2D	FEM (COM-SOL)
65	Shi et al. [265]	$\begin{matrix} T \\ \swarrow \searrow \\ H \leftrightarrow M \end{matrix}$ $[T \rightarrow H] \theta_v(T), k(\theta_v, D), D(\theta_v, D), I = 10^{10} \theta_v^h$ $[T \rightarrow M] E, \nu, c, \varphi, H = f(T)$ $[H \rightarrow M] \text{volumetric expansion}$	MCC model	Energy conservation	Porosity rate function	σ – ϵ relations from triaxial compression soils [33, 49]	U	T	Slope stability	2D	FEM (ABAQUS)

Table 3 (continued)

No	Reference	Coupling modes	Mechanical aspect	Thermal aspect	Hydraulic aspect	Validation	U/S	F/T	Application	Dimension	Solver
66	Soltanpour and Fortiero [273]	$\begin{matrix} T \\ \swarrow \\ H \rightarrow M \end{matrix}$	Linear momentum balance	Energy conservation, Fourier's law	Darcy's law with continuity eq	T and heave from full-scale freeze-thaw tests conducted at CRREL (shallow water table and deep-water table) [18]	U	F	Frost heave	3D	FEM (COM-SOL)
67	Liu et al. [192]	$\begin{matrix} T \\ \swarrow \\ H \leftrightarrow M \end{matrix}$	Elastoplastic model based on MCC with associated flow law	Heat transfer eq	Richard's eq	T and thawing displacement from thaw-consolidation tests [342]; T , ω and deformation from one-sided freezing tests [310]	U	F & T	Frost heave and thaw settlement	2D	FEM

F and T freezing and thawing soils, respectively, U and S unsaturated soil and saturated soils, respectively, AGF Artificial ground freezing, BBM Barcelona Basic model is proposed by Alonso et al. [4] for unsaturated soils, c cohesion, CI compression index, s_c cryogenic suction, ρ density of fluid, ρ_v density of vapour, q deviatoric stress, D diffusivity coefficient, DP Drucker-Prager, σ' effective stress, E elastic modulus, eq. equation, e void ratio, u_w excess pore water pressure, FEM finite element model, FT freeze-thaw, η freezing ratio, ϕ friction angle, ϵ_r frost expansion strain, $f(\cdot)$ function, H hardening parameter, K_r relative permeability/hydraulic conductivity, k hydraulic conductivity, k_f hydraulic conductivity of frozen soil, NCL normal compression line, URL unloading-reloading line, θ_u unfrozen water content, w_u gravimetric unfrozen water content, θ_i ice content, P_w water pressure, P_i ice pressure, $S_{r,i}$ ice saturation, IF impedance factor (reflecting the ice effect on water migration), P_L liquid pressure, s matric suction, MCC modified Cam Clay model, ID one-dimensional, PIR pore ice ratio (= ratio of volume of ice in pores to the soil skeleton volume), PSD pore size distribution, n porosity, PRF porosity rate function, P pressure, k_r relative hydraulic conductivity, k_s saturated hydraulic conductivity, S_r saturation, SFCC soil freezing characteristic curves, SWCC soil water characteristic curve, SLR solid-liquid ratio (ratio of volumetric content of ice to water content), ϵ strain, TH thermo-hydraulic, ϵ_v volumetric strain, ϵ_t thaw contraction strain, λ thermal conductivity, θ_u unfrozen water content, D_v vapour diffusion coefficient, VG model SWCC of van Genuchten (1980), μ viscosity, e void ratio, ω water content

2.4.1.2 Coupling Modes As shown in Table 3, the interactions between thermal, hydraulic, and mechanical fields in frozen soil can be simulated by multiple governing and complementary equations. The specific manifestations can be summarised as follows:

(i) *Thermal aspect* heat conduction and heat convection (due to water migration) are generally considered in THM models accompanied by the phase change phenomena. The thermal properties (i.e., thermal conductivity, heat capacity) of soil mixtures are calculated by the fraction of each phase, which can reflect the effect of the hydraulic field on the temperature field. Similarly, the impact of porosity or void ratio variations on soil mixtures' thermal properties (i.e., thermal conductivity, heat capacity) is also considered to describe the TM interactions. Moreover, deformation energy is often included in the energy conservation equation as a strategy to capture the influence of the mechanical field on the thermal field.

(ii) *Hydraulic aspect* water movement can be caused by temperature gradients, hydraulic gradients and pressure variations; therefore, the corresponding items are involved in the mass conservation equation. Darcy's law for saturated flow or Richards' equation for unsaturated flow are used to model water flow. The permeability of frozen soil is typically temperature/pore pressure-dependent, as freezing and thawing affect pore structure and water flow paths.

(iii) *Mechanical aspect* the stress caused by thermal expansion and volumetric expansion due to ice are taken into account to reflect the influences of the thermal and hydraulic fields on the mechanical field. In addition, elastic parameters are often assumed to be related to temperature, saturation and porosity, with their relationships capturing the effects of the thermal and hydraulic processes on the mechanical field. A more detailed discussion of the Coupling modes for the THM process can be found in Sect. 2.4.2.

2.4.1.3 Freezing and Thawing Soils It can be noted from Table 3 that various models have been proposed to predict the frost heave in frozen soils. Because of the complexity of these problems, many studies independently developed the coupled THM model of frozen soils subject to freezing conditions, which merely focused on the investigations of frost heave of frozen soils while often neglecting the thawing issue caused by temperature rise and seasonal changes (e.g., [56, 197, 265, 334, 342, 361]). Existing investigations have demonstrated that the thawing soils suffer from strength reduction and settle deformation, negatively affecting construction safety [93, 357]. A general method for simultaneously simulating the frost heave and thaw settlements is to establish a unified constitutive model for both frozen soils and unfrozen soils [195, 226, 374]. Therefore, some scholars have devoted themselves to developing more unified THM models for both freezing and

thawing soils (e.g., [9, 17, 192, 207, 208, 226, 239, 246, 331, 345, 348, 350, 353, 354, 363]).

One notable work is proposed by Zhou and Meschke [374] who presented a three-phase model considering solid particles, liquid water, and ice crystals as separate phases and regulated temperature, fluid pressure, and solid displacement as primary field variables. Their model was developed within the framework of Coussy's linear poro-elasticity [47] and premelting dynamics of Wettlaufer and Worster [325], essentially derived using the entropy concept. Being validated by an in-situ frost test, the THM model of Zhou and Meschke [374] demonstrated its ability to capture the volume expansion caused by change changes, water migration, and mechanical deformation. Na and Sun [226] introduced a novel generalised theory that incorporates all critical aspects of THM mechanisms into balance equations within the finite deformation range to simulate the complex responses of freezing and thawing soils. Unlike the single-physics solid mechanics problem, the generalised hardening rule proposed by Na and Sun [226], explicitly incorporating thermal and cryo-suction effects, enables the evolution of the yield surface with the variation of pore ice content and temperature.

2.4.1.4 Saturated and Unsaturated Frozen Soils It can be noted from Table 3 that the number of THM models under saturated conditions exceeds those for partially saturated conditions. The frost heave can occur when the saturation exceeds 80–90% rather than reaching 100% [58]. Furthermore, most in situ frozen soils are unsaturated, and vapour plays a significant role in the water and energy balance, especially when the temperature gradient is large and the initial water content is low. Accordingly, some scholars have emphasised the influence of vapour on THM modelling of frozen soils (e.g., [105, 131, 164, 178, 192, 200, 207, 227, 246, 265, 273, 294, 306, 326, 344, 348, 370]). For example, Liu and Yu [200] combined Fourier's law, generalised Richards' equation, and mechanical relation (i.e., Navier's equation) to model the THM process in unsaturated frozen soils. Considering the condensation and congelation of vapour in unsaturated freezing soil, a novel THM model was proposed by Yin et al. [344] by involving three variables (i.e., temperature, overburden pressure, and saturation), but their simulated results were not validated by laboratory or field tests. Huang et al. [109] developed a fully coupled THM model for unsaturated freezing soils and conducted a numerical simulation to replicate one-side freezing tests. Wang et al. [306] proposed a THM model of a single pile in frozen soil to simulate the ground heave and pile uplift under one-dimensional freezing conditions. Soltanpour and Foriero [273] derived a THM model for predicting the frost heave in unsaturated freezing fine sands compared with full-scale freeze–thaw tests at CRREL. Based

on the modified Cam Clay model, Li et al. [192] developed a thermo–elastoplastic model for unsaturated freezing soils to address the soil hardening caused by temperature and compression during thawing, whose model was applied to assess the long-term freezing and thawing behaviours of Railway subgrade.

2.4.1.5 Impact of Ice Lens In addition, some studies proposed novel THM models that consider the formation and evolution of ice lenses to reproduce frozen soil behaviours more accurately. Table 4 summarises the criterion of ice lens formation, indicating that ice lens generation is influenced not only by temperature and overburden pressure but also by the separation strength. The ice lenses can induce volume expansion, alter the yield condition and strength variations, and block water migration within freezing soils. The growth of ice lenses tends to be anisotropic due to the directional formation of ice lenses perpendicular to the heat transfer direction. Therefore, accurately determining the occurrence moment and position of ice lenses is crucial for capturing the THM process in frozen soils.

2.4.2 Coupling Modes for THM Fields

It can be noted from Table 3 that the coupling interactions among THM fields can be achieved in three manners. The first is directly incorporating the relevant actions into the governing partial differential equations (PDEs), i.e., the impact of water on the temperature field can be addressed by including corresponding terms in Fourier's equation [200]. The second is establishing explicit relations, i.e., connections among the state variables can be regarded as independent variables within the governing equations. The last method is to develop the implicit relationships, referring to the dependence of material properties on the state variables and other parameters.

2.4.2.1 Basic Mechanisms For the first coupling mode, the fundamental governing equations of THM models (i.e., mass conservation, energy conservation, and momentum conservation equations) describe the basic mechanisms and serve as critical components of the THM models. The basic framework of THM models is to define the governing balance equations based on different assumptions and to propose a mechanical constitutive model. Three primary governing laws form the foundation for describing the THM process, which are: (i) mass conservation for the hydraulic field. The mass conservation can be formulated in two ways, i.e., considering the bulk mixture body as a whole or accounting for the mass balance for each component while applying the superposition of mass balance. (ii) Momentum conservation for the mechanical field. The momentum conservation indicates that the time derivation of momentum equals the

summation of external forces. (iii) Energy conservation for the thermal field. Energy conservation refers to the first law of thermodynamics, which represents that the sum of time derivatives of internal and kinetic energies is equal to the rates of mechanical work rate and heat. Generally, phenomenological thermodynamics, energy conservation, and Fourier's law serve as the fundamental theories for temperature fields, while mass conservation, Darcy's law, and Richards' equation form the basis of moisture fields. However, the approaches to mechanical constitutive models vary considerably in the literature. Therefore, a comprehensive review of the mechanical constitutive models for frozen soils was summarised by the authors [185] who categorised the constitutive models into different groups based on their underlying theories.

It can be noted from Table 3 that existing THM models primarily rely on stress fields governed by Navier's equation, effective stress theory, poromechanics theory, and elastic/ elastoplasticity theory. It is worth noting that treating the frozen soils as temperature-dependent elastic materials during freezing is generally reasonable, but the responses of thawing soils under freeze–thaw cycles exhibit non-linear elastoplastic behaviours. Therefore, more advanced mechanical constitutive models capable of describing multiple mechanical responses of frozen soils should be incorporated into the THM models to provide a more precise understanding of the complex coupling process related to frozen soils.

2.4.2.2 Explicit Relations Among these explicit relations, the state variables (i.e., T , ω and displacement) are independent variables and do not directly influence the coupling process, but the PDEs' solutions are sensitive to these explicit relationships. The soil water characteristic curve (SWCC) and the Clapeyron equation are two typical explicit relations.

The SWCC depicts the relationship between water content and suction, which depends on the soil type and is employed to model drying and wetting processes in soils [186]. Due to the similarity between the drying–wetting process and freezing–thawing process, the relationship described by SWCC is extensively utilised for freezing processes in frozen soils. Various empirical equations are proposed for SWCC (e.g., [31, 73, 298, 301]), and van Genuchten's [298] model and Fredlund and Xing [73] model are widely employed in existing THM models (van Genuchten [298], Fredlund and Xing [73]).

$$\frac{\theta - \theta_r}{\theta_s - \theta_r} = \frac{1}{1 + [(as)^n]^m}, \quad (14)$$

$$\theta = \frac{\theta_s}{\ln\left(\exp(1) + \left(\frac{s}{a}\right)^n\right)^m} \left(1 - \frac{\ln\left(1 + \frac{s}{s_r}\right)}{\ln\left(1 + \frac{10^6}{s_r}\right)}\right), \quad (15)$$

where s is suction (kPa); θ is the volumetric water content and θ_s and θ_r are the saturated and residual volumetric water contents, respectively. a , m and n are fitting parameters. s_r is suction corresponding to the residual water content. However, directly applying the SWCC equation to frozen soils remains questionable [22, 147], as it is only suitable when the suction in frozen soils exceeds 50 kPa [275, 276]. Besides, the SWCC displays noticeable hysteresis, whereas these commonly used SWCC equations do not account for hysteresis effects.

The Clapeyron equation depicts the relationships between pressure and temperature, which can be expressed in various ways and notations. Based on equilibrium assumptions of the Clapeyron equation, the soil water potential is influenced by ice and water pressures [149]. Table 5 lists the typical Clapeyron equation for frozen soils. The original derivation of the Clapeyron equation was formulated by combining the thermodynamic concept of Gibbs free energy and the Gibbs–Duhem relationship for each phase [84]. Equation (2) in Table 5 is often used in THM models due to its convenience in implementation. It accurately describes the behaviour of an ice crystal using ice pressure once the temperature and water pressure values are available. However, it is essential to note that the strict validity of its application in frozen soils is questionable since the equation assumes a closed system, whereas a porous medium represents an open system. Besides, equilibrium in the quasi-static sense can only be confidently ensured near interfaces. Thus, caution is necessary when applying the Clapeyron equation across the entire region, especially for rapid transient transport processes.

It is worth noting that the primary state variables in existing THM models include displacement, pore pressure, and temperature, which are suitable for slow freezing rate scenarios. However, in cases of high freezing rates, such as AGF, the selection of state variables should be carefully selected to avoid the occurrence of spurious oscillations unless they are appropriately treated. For example, Suh and Sun [280] alleviated this issue by implementing a stabilization procedure in the weighted residuals of the heat and mass balance equation. Arzanfudi and Al-Khoury [9] also treated cryogenic suction as a primary state variable to address this problem.

2.4.2.3 Implicit Relations The implicit relations refer to the variations of soil properties (e.g., thermal conductivity, hydraulic conductivity/permeability, heat capacity) with the change of state variables (e.g., T , ω and displacement).

In addition, other soil properties are also functions of state variables, such as the hydraulic conductivity of the vapour phase, coefficient of convective/conduction, and various moduli. These implicit relations can remarkably influence the coupled THM process and introduce high nonlinearity into PDEs governing frozen soils. When unknown parameters exceed the number of PDEs, supplementary equations should be added. Typically, empirical equations and the concept of ice–water ratio are utilised to solve the PDEs. The coefficients in these supplementary equations are derived from experimental measurements, which are highly influenced by testing conditions and the type and location of soil samples.

Solving the PDEs requires the incorporation of explicit relations, such as the soil water characteristic curve (SWCC) and the Clapeyron equation, as well as implicit relations. However, the inclusion of these relations can lead to computational challenges. Implementing numerical calculations becomes difficult due to the PDEs' highly nonlinear and interdependent nature. Existing THM models have primarily focused on the coupling interactions between the mechanical field and the other two fields, as these couplings typically exert weaker effects, particularly the coupling from the mechanical field to the thermal or hydraulic fields. In most THM models, simplified methods based on mixture theories, poromechanics, or direct coupling using experimental relationships are employed, which can capture the complicated THM interactions while reducing computational complexity. However, they may overlook critical behaviours of frozen soils under freezing/thawing conditions, such as pressure melting phenomena, freezing point depression, and time-dependent behaviours. Therefore, further research and development are necessary to enhance the understanding and modelling of the interdependencies among the mechanical, thermal, and hydraulic fields within frozen soils.

2.5 Thermo–hydro–chemical (THC) Coupling Approach

As outlined in Sect. 2.1, numerous modelling studies have focused on the coupled mechanisms of heat and water transport in frozen soils, which often neglects the freezing point depression. The freezing point of pure water occurs at 0°C, but in a soil–water system, it appears below 0°C. The depression of the freezing point can be neglected in coarse soils with a small specific surface area (SSA). However, fine-grained soils, such as silts and clays, with a high SSA and the ability to retain unfrozen water content, experience a temperature depression of up to 5°C [8]. Water content, overburden pressures, and the presence of solutes could induce lower values of freezing/melting point [11]. Therefore, it is necessary to consider the influence of freezing

point depression in subsequent research and extension of THM models. In other words, the chemical aspect should be incorporated into the coupled modelling of frozen soils.

Existing studies demonstrate that neglecting the effect of salt in the simulation of frozen soils can introduce significant uncertainties in modelling the freezing and thawing processes [232, 327]. Generally, salt exists in two phases within frozen soils: dissolved salt and salt crystals. Recent findings reveal that dissolved salt tends to be expelled into the unfrozen water during the freezing process. Furthermore, diffusion and migration of salt lead to the formation of a zone with a higher concentration of salt crystals near the freezing fringe [13, 92]. The effect of salt on frozen soils is complicated, the concrete manifestation of which can be concluded into two aspects: one is the freezing point depression of soils due to the existence of salt; another is the salt dynamics of soils under freezing/thawing is influenced by the processes of diffusion and repulsion [315, 329].

Accordingly, some scholars have attempted to explore the influences of salt on the frozen soils during freezing/thawing, as well as the interactions between freezing/thawing and salination in cold regions. Considering the heat flux during salt crystallization, Koniorczyk [141] developed a fully coupled THC model using the kinetics of salt phase change but without accounting for the influence of crystallization pressure on the stress field. Wu et al. [330] analysed the salt dynamics and soil freezing/thawing over three winter periods based on CoupModel, and their model was verified by comparing simulated results and observed data (i.e., temperature, water content, and groundwater table depth). Their model mainly focused on the coupled water and heat transfer by considering the effect of temperature on hydraulic conductivity, freezing on thermal properties and heat convection due to water flux, and the freezing point depression caused by salt. Wan et al. [303] also employed the CoupModel as a coupled THC model to investigate the effect of climate change on water, heat, and salt migration of unsaturated frozen soils, and their model was validated by the comparison between the meteorological data (i.e., temperature, precipitation, evaporation) from filed observations and simulated data. In their model, temperature gradient served as the driving force for water migration and salt transport, while salt dispersion or diffusion was not considered. Liu et al. [194] modified the simultaneous heat and water (SHAW) model by considering soil deformation and its impact on hydrothermal properties during the freeze and thaw process. When simulating water, heat and salt transport processes, the heat convection due to water flux, blocking impact of ice and solute absorption (i.e., diffusion, convection and dispersion processes) are involved in this coupled model. Besides, their model was compared with in situ water content and temperature observations, demonstrating its ability to capture water–heat–salt

dynamics in frozen soils. However, since neglecting the lateral groundwater exchange, ground surface albedo, and salt expulsion, their model yielded underestimations of water content in deep soil layers and mispredicted the temperature during the thawing period. Hence, THC models can be further improved by considering these essential factors.

Furthermore, the presence of salinity can alter the evolution of the freezing front and freezing points, which, in turn, affects the formation of frozen walls in artificial ground freezing (AGF) and poses safety concerns for AGF construction [175, 199]. Therefore, investigations on coupled THC models are relatively scarce, and more effort should be dedicated to analysing the complex interactions among the fluid field, thermal field, and chemical field in frozen soils, which is crucial for understanding the mechanisms of THC processes in frozen soils and to identify the salinisation for better water management and construction safety in cold regions.

2.6 Thermo–hydro–Mechanical–Chemical (THMC) Coupling Approach

The coupled thermo–hydro–mechanical–chemical (THMC) process is a widely researched topic that significantly impacts frozen soils' mechanical behaviour and failure mechanisms. Investigating the mechanical behaviour of frozen soils under multi-physics coupled processes is crucial for ensuring construction safety in cold regions, such as railway construction on the Qinghai–Tibet Plateau and tunnel constructions related to AGF. Salinity significantly alters the freezing behaviour of frozen soils, leading to freezing point depression [19, 263]. However, the effect of salt in the fluid on the performance of frozen soils has been rarely investigated, despite its relevance to construction safety and potential harm to adjacent structures and infrastructure foundations caused by frost heave in sulfate saline soils [141, 328]. It is worth noting that methane hydrates are ice-like materials comprising methane gas and water, wherein the methane gas is confined within cage-like structures in solid form due to high-pressure and low-temperature conditions [247, 317]. The methane hydrates occur naturally in permafrost regions and beneath the deep marine bed. Table 6 presents an overview of existing investigations on coupled THMC models for frozen soils, revealing that most studies have explored the effect of salt on the THM process in frozen soils, while some investigations have focused on the THMC process during natural gas hydrates.

As for the THMC models for frozen soils, Zhang et al. [356] established a coupled THM model for freezing saturated saline soils and explored the effect of salt by involving mass conservation, Darcy's law, and energy conservation. However, their models did not account

for salt expansion. Tounsi et al. [296] derived a fully coupled THM model considering salinity influence to explore the THM behaviours of AGF, but they neglected salt crystallisation and its impact on ground deformation. Accordingly, Zhang et al. [352] proposed a coupled THMC model to simulate the one-side freezing process of saturated frozen sulfate saline soil by employing the crystallisation kinetics theory to elaborate the ice and salt crystallisation mechanism. However, many studies assumed soil saturation and neglected the vapour phase in freezing soils. To enhance the modelling of dynamic processes within frozen soils, including heat transfer, vapour flow, water migration, deformation, and solute transport, Zhang et al. [359] enhanced the THMC model, while their model neglected the salt effect on the mechanical aspect. Additionally, Huang and Rudolph [106] developed a 2D THMC model for variably saturated soils under freezing/thawing conditions, considering the influence of freeze–thaw cycles. However, their models' configuration (i.e., shallow model and short simulation duration) and assumptions (i.e., ignoring subsurface lateral flow, surface runoff, rainfalls, snow, irrigation, and other mass sinks) may introduce errors when modelling the coupled processes in the subsurface during freeze–thaw cycles. Furthermore, they neglected the interaction between the mechanical field and chemical field, the hysteresis of freeze–thaw cycles and the occurrence of ice lenses.

In recent years, some THMC models have been developed to simulate the dissociation of methane hydrates and the mechanical responses of reservoirs using numerical simulations. Kimoto et al. [137, 138] established 1D and 2D THMC models for simulating the hydrate dissociation and indicated that the ground deformation is remarkably influenced by water and gas generation and dissipation, as well as soil strength reduction due to hydrate loss. However, their model ignored the mechanical–chemical interaction, and its effectiveness was limited by the lack of validation through experimental data. Based on thermodynamics theory and critical state concept, Sun et al. [282] also developed novel THMC models for analysing the mechanical responses of methane hydrate-bearing sediment and showed that decoupling the mechanical and hydraulic fields (i.e., keeping porosity and volume strain constant) would result in an overestimation of the depressurization rate. Furthermore, Wan et al. [304] developed a THMC model to simulate fluid flow within hydrate sediments, dividing it into fluid and solid subsystems and solving it using a hybrid control volume finite element method (CVFEM)–finite element method (FEM). They validated the model with two classical experimental cases, demonstrating its capability to capture coupled THMC behaviours.

Therefore, it can be concluded that most existing THMC models for frozen soils are formulated based on a set of assumptions aimed at simplifying the governing equations that govern the complex coupling processes. Although these assumptions are physically reasonable, they have the potential to introduce inaccuracies in the numerical results. Table 6 demonstrates how these models simplify the coupling of THMC processes by tailoring them to specific problem characteristics, typically focusing on partial bidirectional coupling relationships. For example, the interactions between the mechanical field and chemical field (e.g., salt expansion and crystallisation) were rarely taken into account. Neglecting these critical factors or phenomena can lead to incomplete or inaccurate representations of the actual behaviour of frozen soils. Furthermore, loading/unloading actions often occur on the ground surface in cold regions. Therefore, enhancements should be made to incorporate a more comprehensive understanding of the underlying processes and phenomena to simulate the non-elastic deformation and develop complete coupled models to fully reflect the coupling relationship between multiple physical fields.

3 Numerical Simulation Methods

The coupling of multi-physical fields (i.e., thermal, hydraulic, mechanical, and chemical fields) can be realised by variables that interactively transfer information. Although the effective stress principle and consolidation model of the HM coupling model were proposed in the early 1920s, along with the establishment of the corresponding differential equations, their solutions required modifications due to the limitations in computational power. Besides, analytical solutions were derived for some simple cases, such as axisymmetric and plane strain issues [156, 240, 319]. However, obtaining analytical or exact solutions for more general cases with slightly complex boundary conditions is not feasible. To address this issue, computational techniques, specifically advancements in numerical methods for discretely solving the coupled model's differential equations, become necessary.

This section mainly summarises the typical numerical methods that can solve the coupled multi-physical models according to their underlying principles, which include two types of methods, i.e., continuum mechanics method (CMM) and discrete or discontinuous mechanics method (DMM). The continuum mechanics methods include the finite element method (FEM) and its modified versions (XFEM), finite volume method (FVM), finite difference method (FDM), and phase-field modelling (PFM). The discrete element method (DEM), lattice Boltzmann model (LBM), and peridynamics (PD) are the typical discrete or discontinuous mechanics methods. Section 3.3 presents the

primary advantages and disadvantages of each numerical method for reference on the choice of suitable numerical solvers for coupled models of frozen soils. As summarised in Sect. 2.1, the coupled TH models are different from other models related to the mechanical field. Therefore, some typical models that are tailored for TH coupling issues are introduced in Sect. 3.4.

3.1 Continuum Mechanics Method (CMM)

The continuum mechanics method treats frozen soils as a continuous medium, where they are considered to be occupied by fluid or solid substances that can be modelled as a continuous medium composed of particles without pores. The macroscopic physical quantities of these particles adhere to fundamental physical laws, including mass, energy and momentum conservation, thermal dynamics, diffusion, and heat conduction [10, 91, 165, 190]. The governing differential equations representing these physical laws can be solved using various numerical methods, i.e., FEM and modified FEM (e.g., XFEM, RFEM), FVM, FDM, and PFM methods.

3.1.1 Finite Element Method (FEM)

The finite element method (FEM) is one of the most popular numerical techniques used to solve differential equations that arise in engineering and mathematical modelling. The foundational works of Zienkiewicz [380] and Strang and Fix [279] have laid the groundwork for future advancements in FEM. FEM discretises a continuous object into finite elements, each possessing a set of nodes, thereby representing the continuum as a series of interconnected elements [44, 67, 122, 165]. The value of each node in the field function serves as primary unknowns, and an approximate interpolation function is assumed in each element. Accordingly, the simple equations of these finite elements can be subsequently assembled into a more extensive system of equations modelling the entire problem.

Based on the review of coupled models in Sect. 2, it can be noted that FEM has been extensively employed to simulate complex multi-physical processes in frozen soils, especially for coupled models involving mechanical aspects. When combined with phenomenological constitutive models, this continuum-based numerical method (i.e., FEM) has demonstrated robustness and efficiency in multi-physical modelling. Various commercial software packages, such as COMSOL, ABAQUS, and ANSYS, have been widely adopted for finite element analysis in coupled modelling. COMSOL offers a user-friendly graphical user interface (GUI), enabling researchers to build and modify governing equations through secondary development, which is helpful for improving modelling efficiency and different hypothesis

testing. COMSOL has proven to be an effective tool for simulating complex multi-physical coupled issues [105].

FEM is capable of addressing nonlinear and heterogeneous issues and complex boundary conditions. However, the applications of FEM in modelling coupled processes in frozen soils are limited when dealing with specific issues such as severe discontinuity problems and regional scale systems. These limitations can be attributed to several factors. (i) Internal flaws (e.g., fractures) introduce discontinuities in the research object, necessitating the refinement of local meshes surrounding these flaws, which increases the computational burden. (ii) Large deformations can distort the mesh, leading to calculation deviations and computational challenges. Additionally, the remeshing process at each step introduces a significant workload. (iii) The generation and propagation of ice lenses are difficult to solve since the ice lenses should be attached to nodes so that the formation of ice lenses becomes a dynamic internal boundary, which also introduces additional complications due to remeshing. The classical FEM discretization for such issues often results in unstable solutions and requires extremely small-time steps; (iv) when solving large-scale problems, FEM requires multiple parameters and involves a vast number of elements and nodes that demand substantial computational resources and time. Hence, approximate upscaling schemes should be employed to improve computational efficiency [160].

Accordingly, modified versions of FEM have been developed to remedy the weakness of FEM in solving special issues, such as extended finite element model (XFEM) and random finite element model (RFEM). The classic FEM is limited in its ability to handle discontinuities within an element due to the continuity requirements of the shape functions. As for coupled models of frozen soils, FEM struggles to accurately capture the sharp interface between ice and water, which involves a weak discontinuity in the temperature field and then induces a discontinuity in its gradient field. To overcome this limitation, the XFEM method has been effectively developed to model such discontinuities and high gradient fields [134], which introduces an additional field to the standard interpolation field. Recently, some scholars have employed XFEM to reproduce frozen soils' freezing and thawing behaviours. For example, Amiri et al. [5] proposed a TH model via XFEM to model the temperature discontinuity of the ice/water interface. Arzanfudi and Al-Khoury [9] focused on issues involving relatively high freezing–thawing rates, such as AGF, and employed the partition of unity within the framework of XFEM to discrete cryo-suction.

Another modified version of FEM is RFEM, which accounts for the randomness in materials components and properties. Dong and Yu [61] employed XFEM to explore slope stability based on a coupled TM model. In addition,

Dong and Yu [62] developed a microstructure-based THM model using RFEM to model frost heave in frozen soils, which was validated by laboratory-scale experiments.

3.1.2 Finite Difference Method (FDM) and Finite Volume Method (FVM)

The finite difference method (FDM) was one of the earliest discretization schemes, primarily favoured for its simplicity and ease of implementation on structured grids. However, the limitations of FDM become apparent when dealing with complex geometries, particularly in multiple dimensions. This drawback has motivated the development of more advanced integral-based discretization techniques, such as the FVM and FEM [241], which offer greater flexibility and accuracy in handling complex geometries.

The finite volume method (FVM) is well-suited for handling geometrically complex regions without the need for variable transformations due to the flexible utilization of grids (e.g., unstructured grids). In FVM, the computational domain is divided into a collection of control volumes, and the PDEs are integrated over the control volume and solved [66, 159]. FVM has been extensively utilised as a numerical technique for modelling fluid flow and heat transfer. Its popularity arises from its inherent conservation properties, ensuring that the discretised equations preserve physical quantities and clear physical interpretations of coefficients in the FVM equations. Recently, FVM has been extended into solid mechanics analysis [360, 379] and proved to be a promising method for THM coupling issues [55, 272]. However, numerical diffusion in FVM is likely to induce the smoothing of sharp gradients and loss of fine-scale details, which might limit its accuracy in capturing the transport process. Besides, FVM might encounter difficulties when handling complex equations involving non-linearities or coupling different physical processes.

The choice of the appropriate numerical discretization method is critical for multi-physics modelling for frozen soils, such as FEM, FDM, and FVM. FEM was initially developed for static stress analysis and then extended to various fields, which has been the most widely utilised method in computational mechanics and solving material and geometric nonlinearities due to its ability to handle complex, highly heterogeneous domains with irregular boundaries [215, 277]. However, when it comes to flow modelling, FVM is considered a superior choice compared to FEM due to its maintenance of local conservation properties at the discrete level and accurate representation of flow behaviour [111]. FVM combines the advantages of FDM in terms of simplicity of implementation and the flexibility of FEM in handling complex geometries.

3.1.3 Phase-Field Modelling (PFM)

Phase-field modelling (PFM) has recently emerged as a robust computational tool for simulating and modelling the mesoscale development of morphological and microstructure in materials [126, 182, 187, 278], which introduces phase-field variables to track the dynamic evolution of interfaces. The temporal evolution of the phase field variables is governed by a system of PDEs, which is typically solved using numerical methods. PFM possesses two key characteristics: (i) a continuous phase field used to distinguish different microstructure domains; (ii) a diffuse interface where physical properties smoothly transition between phases [299]. Depending on the problem being addressed, the phase field can serve as an auxiliary variable or a physical parameter [32, 45]. In both scenarios, the diffuse interface is characterised by excess free energy, typically expressed as a function of the spatial gradient of the phase field. For a comprehensive understanding and further information on PFM, relevant details and references can be found in some publications (e.g., [100, 127, 278]).

Recently, researchers have formulated the framework of PFM coupled with the continuum theory of porous media (TPM) to address coupled issues and developed interface models to describe the ice–water interface. Sweidan et al. [286] derived a unified model to simulate frost action in saturated frozen soils, extending TPM with PFM to describe the macroscopic phase-change process in saturated frozen soils. Sweidan et al. [287] combined TPM and PFM to develop a unified kinematics approach for modelling the coupled thermal, hydraulic, and mechanical (THM) processes in freezing soils with different frost penetration directions. Suh and Sun [280] formulated a THM model to simulate freezing-induced fracture caused by the growth of ice lenses, introducing two-phase field variables.

The PFM method lays a solid foundation for future research in the coupled modelling of frozen soils. However, some improvements can be addressed in future work to provide a more realistic description of soil freezing/thawing processes. This can be achieved by extending the framework for unsaturated soils and considering the hysteresis effect in freeze–thaw cycles. Furthermore, the initiation and formation of ice lenses will be modelled with the aid of fracture-based PFM.

3.2 Discrete or Discontinuous Mechanics Method (DMM)

3.2.1 Discrete Element Method (DEM)

The discrete element method (DEM) is a well-known micromechanics-based approach that captures the inherent discrete characteristics of particles. Specifically, heat

Table 4 Summary of criteria for the formation of ice lenses

Criteria		References	Equations	Remarks
Pressure	Pore water pressure	Miller [218]	$p_w \geq p_{sep}$	Pore water pressure (p_w) \geq separating stress of soil particles (p_{sep})
	Pore ice pressure	Gilpin [80]	$p_i \geq \sigma + p_{sep}$	Pore ice pressure (p_i) \geq sum of total stress (σ) and separation strength (p_{sep})
		Koop et al. [146]	$p_i \geq p_{ex}$	Pore ice pressure (p_i) \geq total external pressure (p_{ex})
	Pore total stress	O'Neill and Miller [233]	$\sigma \geq p_{over}$	Total stress (σ) \geq overburden pressure (P_{over})
	Liquid pressure at the ice–water interface	Ji et al. [119, 120]	$p_{LH} \geq p_{ex} + \sigma_t$	Liquid pressure at the ice-water interface (p_{LH}) \geq sum of external pressure (p_{ex}) and tensile strength (σ_t)
	Vertical stress	Thomas et al. [293]	$\sigma_v \leq -p_{sep}$	Vertical stress (σ_v) $\leq -p_{sep}$ (tension)
	Normal stress	Gao et al. [76]	$\sigma_{nT} \leq -\sigma_t$	Normal stress on the plane perpendicular to the temperature gradient (σ_{nT}) \leq tensile strength (σ_t)
	Average stress (microscopic)	Liu et al. [195]	$\sigma_{av} \leq -\sigma_t$	Average stress (σ_v) \leq tensile strength (σ_t)
Strain		Konard and Duquennoi [142]	$\varepsilon \geq \varepsilon_f$	Strain in frozen fringe (ε) \geq tensile failure strain (ε_f)
Volumetric water content (for saturated conditions)		Bai et al. [12]	$\theta \geq \theta_{sep}$	Volumetric content of water (θ) \geq separating water content (θ_{sep})
Temperature		Konrad and Morgenstern [143]	$\theta_{sm} \leq T \leq \theta_{sf}$	Ice lens formation when temperature ranges from θ_{sm} to θ_{sf}
Void ratio		Zhou and Li [372]	$e \geq e_{sep}$	Void ratio $>$ separating void ratio; used by Yin et al., Sweidan et al. Suh and Sun [280, 287, 344]
Porosity		Lai et al. [151]	$n \geq n_{sep}$	Porosity (n) $>$ separating porosity (n_{sep}), n_{sep} is related to initial porosity, compression, temperature gradient, and overburden pressure

transfer in frozen soils can be regarded as heat flows at the grain scale, where the thermally-induced inter-particle force can be described by the contact force model in DEM [14, 75, 309]. Furthermore, combining DEM with computational fluid dynamics (CFD) has been developed to account for heat convection through granular materials [309, 318, 335]. However, conducting large-scale DEM simulations (involving billions of particles) is computationally expensive when solving actual engineering problems, particularly when coupled with CFD, although speed-up techniques (e.g., parallelization with multi-core CPUs and distinguishing GPU acceleration techniques) can be conducted [274].

3.2.2 Lattice Boltzmann Method (LBM)

The lattice Boltzmann method (LBM) was initially proposed by Hardy et al. [88] as a micromechanics-based approach. In LBM, variables are typically obtained from particle interactions [125, 220], which have higher parallel

computation efficiencies than traditional macroscopic methods due to the improved functional form and quantities [110]. Another advantage of LBM is that the equations used are dimensionless, expanding its applicability to various scenarios. With these advantages, LBM has been widely used in several fields, including multi-component flow (e.g., multiphase and thermal flow), chemical reaction, mass transfer in fuel cells, and flow in porous media, and so on [77, 224, 332, 336].

Overall, investigations on coupled models of frozen soils via LBM are relatively scarce since the studies on frozen soils initially focused on macroscopic relations. Wang et al. [316] established a multiphase model based on LBM to simulate heat and mass transfer in frozen soils and evaluate the intricate temperature and water content distribution during the thawing process. However, one limitation of LBM is the relatively small model dimension, which poses challenges when dealing with macroscopic issues that involve enormous calculation quantities. Additionally,

obtaining parameters for small particles is relatively difficult. It remains challenging to transform the parameters obtained from in situ observations into the micro/mesoscale parameters required in LBM [162].

3.2.3 Peridynamics (PD)

Peridynamics (PD) was initially developed to describe the mechanical behaviours of solids [266, 267] and subsequently extended to address various diffusion phenomena [26, 212]. Unlike classical local theories that employ partial differential equations (PDEs), such as those used in FEM, PD utilises a set of integral–differential equations. This approach ensures a mathematically consistent formulation that remains valid despite significant non-linearities and discontinuities.

Initially introduced as a bond-based approach, PD has evolved into a state-based PD, presenting two variants: ordinary and non-ordinary [2]. Recent developments have introduced an element-based PD formulation [193]. The connection between PD and continuum formulations is established using the concept of peridynamics differential operator [210]. Previous studies have demonstrated the successful applications of PD in solving problems such as heat conduction [25, 38, 78], phase change [211] and water flow in porous media [113, 129], which shows the simplicity and universality of this theory in addressing coupled issues. Nikolaev et al. [229] developed a non-local approach based on bond-based PD to analyse the heat and water transfer with phase change in saturated frozen soils under freezing and thawing conditions. To validate the accuracy of their model, they compared the calculated temperature distribution from PD with the analytical solutions and FEM

results. More importantly, their model was successfully applied for convention-dominated heat transfer simulations in frozen soils with high-pressure gradients, which poses a challenge for other methods such as FEM. Therefore, the PD-based method can be extended further for THM and THMC models, which is beneficial for modelling the hydrological behaviours of permafrost soils and frost heave that remarkably influences construction safety and increases the risk of geological disasters.

3.3 Comparison Between CMM and DMM

The selection of an appropriate numerical method is of utmost importance when addressing various coupling problems associated with frozen soils. Different numerical methods possess distinct characteristics and application domains. Table 7 summarises the advantages and disadvantages of relevant numerical methods. Based on Table 7, researchers and practitioners can adopt the most suitable approach for solving their specific coupling problems in frozen soil applications.

3.4 Heat and Mass Transfer Simulators

Various coupled water and heat process models for frozen soils, without considering the mechanical aspect, are depicted in this section, such as simultaneous heat and water (SHAW), coupled heat and mass transfer (CoupModel), and Hydrus-1D models. Table 8 presents a compilation of typical simulators for modelling water and mass transfer processes related to frozen soils, providing a brief overview of their distinct characteristics.

Table 5 Summary of Clapeyron equations for frozen soils

No	References	Equations	Remarks
1	Groenevelt and Kay, [84]	$\frac{1}{\rho_w} \left(\frac{dP_w}{dT} \right) - \frac{1}{\rho_i} \left(\frac{dP_i}{dT} \right) = \frac{L}{T+T_f}$	considering Gibbs–Duhem relationship for each phase and thermodynamic of Gibbs free energy
2	Loch [204], Henry [97]	$\frac{P_w}{\rho_w} - \frac{P_i}{\rho_i} = L \ln \left(\frac{T}{T_f} \right)$	Assuming that liquid water coexists with ice, and ice pressure is a function of P_w , T , ρ_w and ρ_i
3	Schofield [256]	$\frac{dP_w}{dT} = \frac{L\rho_w}{T+T_f}$	Assuming that liquid water coexists with ice at constant pressure and density
4	Liu and Yu [191]	$\frac{dh}{dT} = \frac{L}{gT}$	A generalised Clapeyron equation to describe the coexistence of water–ice condition
5	Watanabe et al. [321]	$P_w = L\rho_w \ln \left(\frac{T+T_f}{T_f} \right)$	Assuming that water density is temperature-independent
6	Ma et al. [209]	$\left(\frac{1}{\rho_w} - \frac{1}{\rho_i} \right) P = L \frac{T-T_f}{T_f}$, $P = P_w = P_i$	Assuming that water pressure and ice pressure are not equal
7	Padilla and Villeneuve [236]	$\frac{P_w}{\rho_w} - \frac{P_i}{\rho_i} = L \frac{T}{T_f} + \frac{P_0}{\rho_w}$	A general thermodynamic relation and has been verified by experimental data

P_w and P_i equilibrium gauge pressures for the liquid water and ice, P gauge pressure of water and ice, P_0 osmotic pressure, ρ_w and ρ_i density of water and ice, T and T_f equilibrium temperature and freezing point temperature, L latent heat, h water head, g gravitational acceleration

Table 6 Summary of investigations on the thermo-hydro-mechanical-chemical (THMC) modelling for frozen soils

Objects	References	Coupling modes	Mechanical aspect	Thermal aspect	Hydraulic aspect	Chemical aspect	Validations	Applications	Dimensions	Scales	Solvers
Frozen soil	Zhang et al. [356]	$T \leftrightarrow H$ $T \leftrightarrow M$ $H \leftrightarrow C$ $M \leftrightarrow C$	Elastic mechanics	Energy conservation	Mass conservation	Solute conservation	ω and salt transport from soil column freezing test	Simulating soil salinisation and frost heave behaviour	1D	Macro	FEM (COM-SOL)
			<p>[T → H] $\theta_s(T), k_f(T)$, Temperature potential, phase change with Clapeyron eq</p> <p>[T → M] compression modulus = $f(T)$</p> <p>[H → M] pore pressure causes change of σ'</p> <p>[H → T] heat convection due to water flux, $\lambda(\theta_s), C(\theta_s)$</p> <p>[H → C] effect of velocity on advective flux, hydrodynamic dispersion of solute is related to θ_u and velocity</p> <p>[M → H] $k_f(e)$, pressure potential, gravity potential</p> <p>[M → T] $\lambda(e), C(e)$</p> <p>[C → H] change of θ_u due to phase change of solutes</p>								
	Tounsi et al. [296]	$T \leftrightarrow H$ $T \leftrightarrow M$ $H \leftrightarrow C$ $M \leftrightarrow C$	Nonlinear elastic mechanics	Energy conservation	Water chemical equilibrium (NaCl)	Solute conservation	T and ε from laboratory freezing test	Simulating THMC process	2D	Macro	FEM (COM-SOL)
			<p>[T → H] $S_i(T), \rho_i(T), v_i(T)$, diffusivity of salt = $f(T), \kappa_0(T)$</p> <p>[T → M] thermal expansion</p> <p>[T → C] $c_s(T)$</p> <p>[H → M] Biot coefficient, $E(S_{ci}), \nu(S_{ci})$</p> <p>[H → T] heat convection due to water flux, $C(p), \lambda(S)$</p> <p>[H → C] $D_s(\rho)$</p> <p>[M → H] S_i(capillary pressure)</p> <p>[M → T] $C(n), \lambda(n)$</p> <p>[M → C] effect of deformation on solute transport</p> <p>[C → T] $L_0(c), C_i(c), C_i(c), \lambda(c)$</p> <p>[C → H] $v_i(c), \kappa_0(c), \eta(c), S_i^*(c)$</p> <p>[C → M] change of pore pressure (pore pressure is the function of capillary pressure, and capillary pressure is related to c)</p>								

Table 6 (continued)

Objects	References	Coupling modes	Mechanical aspect	Thermal aspect	Hydraulic aspect	Chemical aspect	Validations	Applications	Dimensions	Scales	Solvers
Zhang et al. [352]	<p> $T \leftrightarrow H$ $T \leftrightarrow M$ $M \leftrightarrow C$ $H \leftrightarrow C$ </p>	<p> $[T \rightarrow H] \theta_d(T), \mu(T)$, temperature gradient potential, phase change with Clapeyron eq $[T \rightarrow M]$ thermal strain, $E(T)$ [T → C] supersaturation of solution is related to T $[H \rightarrow M] P_w, P_i$, tensile stress results from p_i and P_s $[H \rightarrow T] C(\theta_w), \lambda(\theta_w)$ $[H \rightarrow C]$ salt migration (advection and dispersion), supersaturation of solution is related to water activity $[M \rightarrow H]$ gravity potential $[M \rightarrow T] C(n), \lambda(n)$ $[M \rightarrow C]$ change of n affects the growth rate of salt crystals $[C \rightarrow T] C(\theta_s), \lambda(\theta_s), T_f$ (solute content), latent heat released by salt crystallisation $[C \rightarrow H] \mu(C), \theta_w(\theta_s)$, change of n and κ, osmotic potential, ice crystallisation and crystal formation $[C \rightarrow M]$ tensile stress results from P_s </p>	Elastic mechanics	Energy conservation	Mass conservation	Solute conservation (sulfate, Na_2SO_4)	T from one-side freezing test	Predict the deformation with the effects of frost heave and salt expansion	2D	Macro	FEM (COM-SOL)
Zhang et al. [359]	<p> $T \leftrightarrow H$ $T \leftrightarrow M$ $M \leftrightarrow C$ </p>	<p> $[T \rightarrow H] \theta_d(T), \kappa(T, K_i), K_r(S_i)$, phase change with Clapeyron eq $[T \rightarrow M] E(T)$ $[H \rightarrow M] \sigma^* = f(e, \theta_w, S_i)$ $[H \rightarrow T] C(\theta_w), \lambda(\theta_w)$, heat convection of water flow, phase change due to vapour condensation $[M \rightarrow H]$ change of e $[M \rightarrow T] C(e), \lambda(e)$ $[H \rightarrow C]$ advective flux and hydrodynamic dispersion of solute $[C \rightarrow H]$ change of θ_w due to salt crystallisation </p>	Terzaghi theory	Energy conservation	Mass conservation	Hydrodynamic dispersion with Fick's law	T from soil column freezing test	Simulating THMC process	1D	Macro	FEM (COM-SOL)

Table 6 (continued)

Objects	References	Coupling modes	Mechanical aspect	Thermal aspect	Hydraulic aspect	Chemical aspect	Validations	Applications	Dimensions	Scales	Solvers
		$ \begin{array}{c} T \leftrightarrow H \\ \uparrow \quad \downarrow \\ \uparrow \quad \downarrow \\ M \quad C \end{array} $	<p>Poroelectric model (Hooke–Duhamel’s law)</p>	<p>Energy conservation and Fourier’s law</p>	<p>Mass conservation</p>	<p>Advective–dispersive transport</p>	<p>T from soil column freezing test⁴⁸</p>	<p>Simulating THMC process</p>	<p>2D</p>	<p>Macro</p>	<p>FEM (COM-SOL)</p>
	Huang and Rudolph [106]	<p>[T→H] $\theta_s(T)$, $k_f = K_f(S_f) * k_s * 10^{-7\theta_s}$, saturated vapour density = $f(T)$, diffusivity of water vapour = $f(T)$, water–ice phase change with Clapeyron eq., latent heat of vaporisation of liquid water, $L_v = f(T)$</p> <p>[T→M] thermal expansion</p> <p>[H→M] volumetric expansion, Biot–Willis coefficient</p> <p>[H→T] heat convection due to water flux, $C(\theta_w)$, $\lambda(\theta_w)$</p> <p>[M→H] water and vapour migration driven by gravity, change of e</p> <p>[M→T] $C(e)$, $\lambda(e)$</p> <p>[H→C] advective–dispersive transport of solute</p> <p>[C→T] $T_c(e)$</p>									
Natural gas hydrate	Kimoto et al. [138]	$ \begin{array}{c} T \leftrightarrow H \\ \uparrow \quad \downarrow \\ \uparrow \quad \downarrow \\ M \quad C \end{array} $	<p>Elasto-viscoplastic model</p>	<p>Energy conservation</p>	<p>Mass conservation</p>	<p>Mass and energy conservation with dissociation heat ratio</p>	<p>–</p>	<p>Predicting ground deformation by the generation of water and gas</p>	<p>1D</p>	<p>Macro</p>	<p>FEM</p>
	Kimoto et al. [137]	<p>[T→H] gas density = $f(T)$, viscoplastic properties depend on T</p> <p>[T→C] T changes hydrate stability and affects dissociation ratio</p> <p>[H→M] hydrate saturation on strength</p> <p>[H→T] $C(f)$, $\lambda(f)$</p> <p>[H→C] dissociation ratio = f (pore pressure)</p> <p>[M→T] heat from viscoplastic stretching</p> <p>[C→T] $C(f)$, $\lambda(f)$, dissociation heat energy</p> <p>[C→H] hydrate dissociation induces change in water and gas fraction</p> <p>Similar to Kimoto et al. (2007), it considers the effect of saturation of hydrate on the permeability of gas and water (C→H)</p>									

Table 6 (continued)

Objects	References	Coupling modes	Mechanical aspect	Thermal aspect	Hydraulic aspect	Chemical aspect	Validations	Applications	Dimensions	Scales	Solvers
		$ \begin{array}{c} T \leftrightarrow H \\ \downarrow \quad \uparrow \\ \text{gas} = f(T) \\ \uparrow \quad \downarrow \\ M \leftrightarrow C \\ \text{[T} \rightarrow \text{M] hardening parameters} = f(T) \end{array} $	Biot's effective stress principle	Energy conservation	Mass and momentum conservation	Kim–Bishnoi equation [135]	T and cumulative gas production from test*2	Simulating the gas hydrate production	2D	Macro	FEM (COM-SOL)
Sun et al. [282]		$ \begin{array}{c} \text{[T} \rightarrow \text{H]} \text{ density of water and gas} = f(T) \\ \text{[T} \rightarrow \text{M]} \text{ hardening parameters} = f(T) \\ \text{[T} \rightarrow \text{C]} \text{ hydrate dissociation constant} = f(T), \text{ phase equilibrium pressure} = f(T) \\ \text{[H} \rightarrow \text{M]} \text{ Biot coefficient} \\ \text{[H} \rightarrow \text{T]} C(f), \lambda(f) \\ \text{[H} \rightarrow \text{C]} \text{ change of pore pressure} \\ \text{[C} \rightarrow \text{T]} C(f), \lambda(f), \text{ endothermic process during hydrate dissociation} \\ \text{[C} \rightarrow \text{H]} \text{ hydrate dissociation increases permeability} \\ \text{[C} \rightarrow \text{M]} \text{ elastic/shear modulus} = f(\text{saturation of hydrate}), \text{ effective stress is related to saturation of hydrate} \end{array} $									
Wan et al. [304]		$ \begin{array}{c} T \leftrightarrow H \\ \downarrow \quad \uparrow \\ \text{[T} \rightarrow \text{C]} \text{ thermal expansion dynamics constant} = f(T), \text{ phase equilibrium pressure} = f(T) \\ \text{[H} \rightarrow \text{T]} C(f), \lambda(f) \\ \text{[H} \rightarrow \text{M]} \text{ Biot coefficient} \\ \text{[H} \rightarrow \text{C]} \text{ change of pore pressure} \\ \text{[C} \rightarrow \text{T]} \text{ endothermic process during hydrate dissociation, } C(f), \lambda(f) \\ \text{[C} \rightarrow \text{H]} \text{ permeability is related to saturation of hydrate} \\ \text{[C} \rightarrow \text{M]} \text{ cohesion} = f(\text{elastic matrix of hydrate saturation}) \end{array} $	Terzaghi effective stress principle	Energy conservation	Mass and momentum conservation	Kim–Bishnoi equation [135]	T, V_g , far-field pressure from test*2, p , V_g and volume strain from triaxial compression*3, p , T , hydrate saturation, gas/water production rate from a large-scale example*4	Simulating the gas hydrate production	2D	Macro	CVFEM-FEM

C heat capacity, C_l heat capacity of liquid, C_s heat capacity of ice, c salt concentration at saturation state, D_s diffusivity of salt, E elastic modulus, n porosity, e void ratio, f_j volume fraction of each phase, f_c fraction of chemical phase, k_f hydraulic conductivity, L_0 latent heat of phase change at reference state, L_v latent heat of vaporisation, p_w pore water pressure, p_l pressure of liquid, p_i ice pressure, p_s salt crystal pressure, S_T saturation, $S_{T,ice}$ ice saturation, T temperature, T_f freezing temperature, T_0 reference temperature, θ_u unfrozen water content, θ_c volume of salt, λ heat conductivity, ρ_i ice density, ρ_s specific volume of ice, κ permeability, κ_0 intrinsic permeability, K_r relative hydraulic conductivity, k_s saturated hydraulic conductivity, ν Poisson ratio, v_l specific volume of liquid, V_g gas volume, σ' effective stress, η dynamic viscosity of liquid, FEM finite element model, CVFEM control volume finite element method

*1 Represents the test conducted by Wu [328] and Wang et al. [314]; *2 represents the test by Masuda [214]; *3 Represents the test from Gupta et al. [86]; *4 represents a large-scale example of case 2 of benchmark problem 4 (BP4-case2) in the second international gas hydrate code comparison study (IGHCCS2). CVFEM–FEM is hybrid control volume finite element method and finite element method

Table 7 Comparison of different numerical methods for coupled modelling of frozen soils

Types of solvers	Numerical methods	Coupling conditions	Modelling platforms for solving coupled issues	Advantages	Disadvantages
Continuum mechanics method (CMM)	FEM	TH, THM, THMC	ABAQUS, CODE_BRIGHT, COMPASS, COMSOL, FlexPDE, GEOSTUDIO, KRATOS, MARC	<ol style="list-style-type: none"> (1) It can handle complex geometries, irregular boundaries, and heterogeneous materials (2) Highly accuracy (3) Adaptive refinement (4) Effective treatment of boundary conditions (5) Well-established methodology and software packages 	<ol style="list-style-type: none"> (1) Complexity in implementation (requiring a deeper understanding of underlying theory and formulation) (2) Computationally expensive, particularly for large-scale problems (3) Difficulty in handling singularities and highly localised problems (4) Sensitivity to mesh quality and material parameters
	FVM	THM	OpenFOAM	<ol style="list-style-type: none"> (1) Being suitable for handling geometrically complex regions with unstructured grids without the need for variable transformations (2) Easily handle non-uniform and unstructured grids (3) Its inherent conservation properties ensure that the discretised equations preserve physical quantities and clear physical interpretations of coefficients (4) Local accuracy (as the discretization is performed on control volumes or cells) (5) Offers stability and convergence properties (6) Being easier to implement and troubleshoot due to the numerous available software packages 	<ol style="list-style-type: none"> (1) Numerical diffusion limits its accuracy in transport problems (2) Difficulty in handling complex non-linear equations related to different physical processes (3) Grid dependence (4) Limited flexibility in handling moving boundaries
	FDM	TH, THM	-	<ol style="list-style-type: none"> (1) Simple implementation with structured grids (2) Straightforward discretization (3) Local accuracy (as the discretization is performed on control volumes or cells) (4) Well-suited for problems on regular grids 	<ol style="list-style-type: none"> (1) Difficulty with complex geometries (2) Limitations in capturing sharp gradients (3) Requiring careful treatment and specialised techniques for non-standard boundary conditions (4) Grid dependence

Table 7 (continued)

Types of solvers	Numerical methods	Coupling conditions	Modelling platforms for solving coupled issues	Advantages	Disadvantages
Continuum mechanics method (CMIM)	PFM	THM		<ol style="list-style-type: none"> (1) It eliminates the need for explicit tracking or re-meshing of interfaces, as the interface is implicitly captured within the diffuse interface region (2) Ability to model multiple phases and complex phenomena (3) It provides a continuum-level representation of phase transitions and interfaces, allowing for studying macroscopic behaviour and capturing mesoscale phenomena 	<ol style="list-style-type: none"> (1) Computationally expensive, particularly for 3D simulations or problems with a large number of phases and interfaces (2) The choice and calibration of material parameters can influence the accuracy and reliability of the results (3) PFM introduces a diffuse interface region that leads to smoothed representations of sharp interfaces, which limits the accuracy, particularly for problems with fine-scale interface behaviour or sharp gradients
Discrete or discontinuous mechanics method (DMM)	DEM	TH	PFC3D	<ol style="list-style-type: none"> (1) An efficient tool for explicitly simulating the interaction between ice and soil particles (2) It provides detailed insights into the micro-scale behaviours and replicates the macroscopic behaviours of frozen soils rather than using a constitutive model based on a continuum approach 	<ol style="list-style-type: none"> (1) Heavy calculation burden (2) Intricate particle descriptions (3) It requires careful calibration of parameters based on experimental or empirical data
	LBM	TH	–	<ol style="list-style-type: none"> (1) High parallel computing efficiency (2) Equations of state in LBM are typically dimensionless, which are feasible to apply in diverse scenarios (3) It sheds light on the flow mechanism in porous media 	<ol style="list-style-type: none"> (1) Being sensitive to numerical parameters, such as lattice spacing, time step size, and relaxation time (2) Lack of well-established model considering mechanical behaviours of frozen soils
	PD	TH	–	<ol style="list-style-type: none"> (1) Ensuring mathematically consistent formulation and remaining valid in the presence of non-linearities and discontinuities (2) The meshless approach allows for more flexible and efficient modelling for complex geometries (3) Being capable of integrating with other physics models and simulation of multiphysics problems (4) It inherently accounts for long-range interactions and is suitable for simulating long-range forces 	<ol style="list-style-type: none"> (1) Computationally expensive for large-scale problems (2) Limited user-friendly and widely adopted software packages

FEM finite element method, FVM finite volume method, FDM finite difference method, PFM phase-field method, DEM discrete element method, LBM lattice Boltzmann method, PD Peridynamics, TH thermo-hydraulic coupling, THM thermo–hydro-mechanical coupling, THMC thermo–hydro-mechanical–chemical coupling

Table 8 Summary of typical water and mass transfer simulators

Simulators	References	Features	Applications
Simultaneous heat and water (SHAW)	Flerchinger and Saxton [71], Flerchinger [70]	<ol style="list-style-type: none"> (1) Considering the effects of plant cover and snow (2) Involving three processes of solutes, convection, molecular diffusion, and dispersion 	<ol style="list-style-type: none"> (1) For water, heat, and solute transfer simulation (2) Predicting temperature and surface water balance in permafrost regions (3) More suitable for salt and water process and predicting the soil freezing depth and effect of water and solutes
Coupled heat and mass transfer (CoupModel)	Jansson [117]	<ol style="list-style-type: none"> (1) Considering the effects of ice on water migration (2) Only considers convection of solute transport (3) Reducing modelling uncertainty with automated calibration via general likelihood uncertainty estimation or Markov Chain Monte Carlo 	<ol style="list-style-type: none"> (1) Simulating TH process and water–heat–salt interactions (2) Considering the impact of snow and organic content (3) More suitable for TH under the FT process
Hydrus-1D models	Hansson et al. [87]	<ol style="list-style-type: none"> (1) Considering the blocking effect on permeability (2) Not considering frost heave explicitly 	Best choice for the seasonal variability of frozen soils under the FT process
Advanced Terrestrial Simulator (ATS)	https://amanzi.github.io/ats/	<ol style="list-style-type: none"> (1) Using unstructured meshes (2) Employing second-order, mimetic finite difference discretizations (3) Containing a wide range of libraries for both linear and non-linear solvers 	<ol style="list-style-type: none"> (1) For the interaction of vegetation, surface energy balance, snow, and other environmental factors with hydrology (2) Modelling flow in partially frozen variably saturated soils
Cast3M	www.cast3m.cea.fr	<ol style="list-style-type: none"> (1) Initially developed for nuclear reactors using FEM (2) Containing various procedures can be reorganised for more complex problems 	<ol style="list-style-type: none"> (1) Accurate for the flow and transfer of nuclear waste storage (2) Coupling between surface and sub-surface transfer
DarcyTools	Svensson et al. [285], Svensson [284]	<ol style="list-style-type: none"> (1) Initially developed for nuclear reactors (2) Using upscaling techniques for equivalent continuous porous medium representation by FVM 	For thermo-hydraulics, hydro-mechanics, hydrochemistry, and unsaturated flow in porous and/or fractured media
Finite Element subsurface FLOW system (FEFLOW)	Diersch [57], Anbergen et al. [7]	<ol style="list-style-type: none"> (1) Solving the groundwater flow under saturated/unsaturated conditions and mass and heat transport using FEM (2) Considering the effects of fluid density, chemical reaction kinetics 	For the TH process in porous media and fractured media
FlexPDE	www.pdesolutions.com	Solving the PDEs using FEM	For TH and geomechanical coupling issues
GEOAN	Holmén et al. [99]	<ol style="list-style-type: none"> (1) Using FDM and block-centred flow method based on continuum approach (2) Considering the ice creation, density influences, solid deformation, and TM effects (3) Involving parallel computation and tens of millions of nodes 	For 3D simulation of groundwater head, saturated/unsaturated flow, transport (solute concentration and heat)

Table 8 (continued)

Simulators	References	Features	Applications
Ginette	Rivière et al. [249, 250]	Initially developed for the interactions between streams and aquifers using FVM	For TH in saturated porous media
MELT	Frederick and Buffett [72]	(1) Solving the TH based on two-phase Darcy's Law, conservation of mass, and energy conservation using FVM (2) Based on IMPES algorithm (flow: implicit pressure and explicit saturation, and scalar heat and mass transport)	For the modelling process in saturated porous media under FT conditions (particularly for the interaction of submarine permafrost, methane hydrate, and multi-phase pore fluid)
PermaFoam	Orgogozo et al. [234, 235]	(1) A specialised solver based on OpenFOAM using FVM, specifically for cryo-hydrogeology modelling (2) Capable of using parallel computation and to deal with solid coupling and nonlinear issues	Solving TH process in variably saturated and heterogeneous porous media
PFLOTRAN-ICE	Karra et al. [128]	(1) Solving nonlinear PDEs using FEM (2). Being capable of using parallel computation by domain decomposition	For ice–water–vapour flow, THC process, supercritical CO ₂ behaviour, surface flow dynamics, sorption, precipitation and dissolution, reactive transport
HEATFLOW-SMOKER	Molson and Frind [222]	(1) Developed by Université Laval and University of Waterloo (Canada) (2) Solving 1D, 2D, and 3D transport issues within a variety of hydrogeological systems using FEM, e.g., discretely-fractured porous media	For solving density-dependent flow, contaminant transport, groundwater age, and thermal energy transport issues
SUTRA	Voss and Provost [302]	Developed for TH issues using FEM and IFD, and applied for density-driven groundwater flow, e.g., saltwater intrusion and heat convection Modified to address the phase change	For the TH process in permafrost or seasonally freezing ground

FT freeze and thaw, FEM finite element method, FVM finite volume method, PDE partial differential equation, IFD integrated finite difference

4 Conclusions and Future Prospects

The multi-physical field modelling of frozen soil plays a crucial role in the design of structures, oil pipelines, and engineering constructions in cold regions. However, coupling these multi-physical fields presents a complex and interdisciplinary challenge. Further efforts are needed to improve the accuracy of predicting the soil freezing process, understand the coupling mechanisms, refine coupling methods, and develop effective solving techniques. Accordingly, this study provides a comprehensive state-of-the-art review of coupled models for frozen soils.

The advancements in coupled multi-field models and corresponding numerical solvers for frozen soils are extensively summarised. Firstly, studies on coupled multi-physical field models for frozen soils were thoroughly examined and discussed, which provides insights into the various approaches and methodologies used to model frozen soils' coupled behaviours under the freezing and thawing process. Secondly, this review explored existing numerical simulations employed in frozen soil coupling modelling. Each numerical method's key advantages and disadvantages are also listed to provide guidelines for choosing appropriate solvers for coupled models of frozen soils. However, due to the complexity of the interaction process occurring in frozen soils, some critical issues in coupled multi-physics field modelling and numerical methods require further research. Based on the critical discussion in this review, the primary conclusion and challenges in simulating the multi-field coupling process on frozen soils are summarised as follows.

(1) The coupled models of frozen soils can be categorised into six types, i.e., TH models, TM models, HM models, THM models, THC models, and THMC models. In general, the TH and THM models have been extensively investigated, while the other coupled models, especially models incorporating chemical effects, are worthy of further development. TH models primarily concentrated on the interaction mechanisms of frozen soils and external environments (e.g., climate change) and their influences on the environment and engineering. In contrast, THM models addressing the mechanical effect have been developed to analyse the freeze–thaw action of frozen soils, which sheds light on the frost and settlement mechanisms of interaction processes in frozen soils.

(2) Further establishment of 3D models and numerical simulators for coupled multi-physics fields with different scales is essential. It is crucial to comprehensively consider the realistic conditions of frozen soils at various scales when modelling complex multi-field interactions. By simulating the physical environment of frozen soils across different scales, the coupling mechanisms of multi-physics can be investigated from micro, meso, and macro/multi-scales. This

approach provides valuable insights for solving practical engineering problems in various domains.

(3) It is essential to conduct large-scale and long-term in situ tests to investigate multi-physics coupling in frozen soils. To establish accurate multi-physics coupling models, it is crucial to understand the interactions among hydraulic, mechanical, thermal, solute transport, and other fields in frozen soils. However, current coupling models often rely on small-scale laboratory tests at the centimetre or meter level. These tests simplify the actual conditions using similarity criteria and neglect secondary factors. To overcome these limitations, it is necessary to minimise the size effect in testing by conducting large-scale in situ tests that encompass multi-physics coupling and long-term monitoring.

(4) A more comprehensive, fully coupled model for frozen soils needs to be developed by incorporating additional factors to simulate multi-physics field interactions more accurately. The prediction errors in existing models might be attributed to the oversimplification of complex boundary conditions (e.g., groundwater exchange, change in soil surface albedo, and salt expulsion) and neglecting critical behaviours of frozen soils (e.g., time/temperature dependence, pressure melting, freezing point depression, hysteresis of the freeze–thaw cycle, and vapour effects). Furthermore, the heterogeneity of structures (e.g., ice lenses) in frozen soils will be of interest in subsequent work to derive more general coupled models.

(5) Concerning the numerical simulations of multi-physics field processes in frozen soils, a balance needs to be struck between simulation accuracy, simulation efficiency, calculation complexity, and ease of implementation. Several challenges exist in the numerical implementation of coupled models for frozen soils. (i) Efficient and unified software systems for large-scale and long-term computations with coupled multi-field processes should be further developed. (ii) Numerical simulators should contain core moduli, such as user-defined material modes, adaptive inputs for boundary conditions, engineering/environmental procedures (e.g., AGF), and functions that evaluate model uncertainty/sensibility. (iii) Special attention can be given to techniques that can enhance calculation efficiency (e.g., parallel computing), interface with visualisation techniques (e.g., BIM or digital twin), artificial intelligence, and other emerging technologies. Advancements in these areas will strengthen the foundation of simulation models and contribute to a comprehensive and holistic simulation platform for frozen soils subjected to freezing/thawing actions.

Acknowledgements This research was financially supported by the Research Grants Council (RGC) of Hong Kong Special Administrative Region Government (HKSARG) of China (NSFC/RGC Joint Research Scheme, Grant No. N_PolyU534/20; General Research Fund, Grant No. 15220221, 15229223).

Author Contributions Kai-Qi Li: Conceptualization; Methodology; Software; Validation; Formal Analysis; Investigation; Data Curation; Writing—Original Draft; Writing—Review & Editing. Zhen-Yu Yin: Writing—Review & Editing; Supervision; Project Administration; Funding Acquisition.

Funding Open access funding provided by The Hong Kong Polytechnic University.

Data Availability All data that support the findings of this study are available from the corresponding author upon reasonable request.

Declarations

Conflict of interest The authors declare there are no competing interests.

Open Access This article is licensed under a Creative Commons Attribution 4.0 International License, which permits use, sharing, adaptation, distribution and reproduction in any medium or format, as long as you give appropriate credit to the original author(s) and the source, provide a link to the Creative Commons licence, and indicate if changes were made. The images or other third party material in this article are included in the article's Creative Commons licence, unless indicated otherwise in a credit line to the material. If material is not included in the article's Creative Commons licence and your intended use is not permitted by statutory regulation or exceeds the permitted use, you will need to obtain permission directly from the copyright holder. To view a copy of this licence, visit <http://creativecommons.org/licenses/by/4.0/>.

References

- Aboustit BL, Advani SH, Lee JK, Sandhu RS (1982) Finite element evaluations of thermo-elastic consolidation. In: ARMA US rock mechanics/geomechanics symposium, 1982. ARMA, p ARMA-82
- Agwai A, Guven I, Madenci E (2011) Predicting crack propagation with peridynamics: a comparative study. *Int J Fract* 171:65–78
- Alexeev VA, Nicolsky DJ, Romanovsky VE, Lawrence DM (2007) An evaluation of deep soil configurations in the CLM3 for improved representation of permafrost. *Geophys Res Lett*. <https://doi.org/10.1029/2007GL029536>
- Alonso EE, Gens A, Josa A (1990) A constitutive model for partially saturated soils. *Géotechnique* 40(3):405–430
- Amiri EA, Craig JR, Kurylyk BL (2018) A theoretical extension of the soil freezing curve paradigm. *Adv Water Resour* 111:319–328
- An M, Zhang F, Min KB, Elsworth D, He C, Zhao L (2022) Frictional stability of metamorphic epidote in granitoid faults under hydrothermal conditions and implications for injection-induced seismicity. *J Geophys Res Solid Earth* 127(3):e2021JB023136
- Anbergen H, Rühaak W, Frank J, Sass I (2015) Numerical simulation of a freeze–thaw testing procedure for borehole heat exchanger grouts. *Can Geotech J* 52(8):1087–1100
- Andersland OB, Ladanyi B (2004) *Frozen ground engineering*. Wiley, Hoboken
- Arzanfudi MM, Al-Khoury R (2018) Freezing–thawing of porous media: an extended finite element approach for soil freezing and thawing. *Adv Water Resour* 119:210–226
- Askes H, Metrikine AV (2005) Higher-order continua derived from discrete media: continualisation aspects and boundary conditions. *Int J Solids Struct* 42(1):187–202
- Aukenthaler M (2016) The frozen and unfrozen Barcelona Basic Model. Master's Thesis, Delft University of Technology
- Bai R, Lai Y, You Z, Ren J (2020) Simulation of heat–water–mechanics process in a freezing soil under stepwise freezing. *Permafrost Periglacial Process* 31(1):200–212
- Baker GC, Osterkamp TE (1989) Salt redistribution during freezing of saline sand columns at constant rates. *Water Resour Res* 25(8):1825–1831
- Baniasadi M, Baniasadi M, Peters B (2018) Coupled CFD–DEM with heat and mass transfer to investigate the melting of a granular packed bed. *Chem Eng Sci* 178:136–145
- Bao H, Koike T, Yang K, Wang L, Shrestha M, Lawford P (2016) Development of an enthalpy-based frozen soil model and its validation in a cold region in China. *J Geophys Res Atmos* 121(10):5259–5280
- Beaudoin JJ, MacInnis C (1974) The mechanism of frost damage in hardened cement paste. *Cem Concr Res* 4(2):139–147
- Bekele YW, Kyokawa H, Kvarving AM, Kvamsdal T, Nordal S (2017) Isogeometric analysis of THM coupled processes in ground freezing. *Comput Geotech* 88:129–145
- Bigl SR, Shoop SA (1994) Soil moisture prediction during freeze and thaw using a coupled heat and moisture flow model. Technical Report
- Bing H, Ma W (2011) Laboratory investigation of the freezing point of saline soil. *Cold Reg Sci Technol* 67(1–2):79–88
- Biot MA (1941) General theory of three-dimensional consolidation. *J Appl Phys* 12(2):155–164
- Biot MA (1956) Theory of propagation of elastic waves in a fluid-saturated porous solid. II. Higher frequency range. *J Acoust Soc Am* 28(2):179–191
- Bittelli M, Flury M, Campbell GS (2003) A thermodielectric analyzer to measure the freezing and moisture characteristic of porous media. *Water Resour Res*. <https://doi.org/10.1029/2001WR000930>
- Black PB, Hardenberg MJ (1991) Historical perspectives in frost heave research: the early works of S. Taber and G. Beskow. CRREL, Hanover, p 37
- Bluhm J, Bloßfeld WM, Ricken T (2014) Energetic effects during phase transition under freezing–thawing load in porous media—a continuum multiphase description and FE-simulation. *J Appl Math Mech/Z Angew Math Mech* 94(7–8):586–608
- Bobaru F, Duangpanya M (2010) The peridynamic formulation for transient heat conduction. *Int J Heat Mass Transf* 53(19–20):4047–4059
- Bobaru F, Duangpanya M (2012) A peridynamic formulation for transient heat conduction in bodies with evolving discontinuities. *J Comput Phys* 231(7):2764–2785
- Bonacina C, Comini G, Fasano A, Primicerio M (1973) Numerical solution of phase-change problems. *Int J Heat Mass Transf* 16(10):1825–1832
- Bonan GB (1996) Land surface model (LSM version 1.0) for ecological, hydrological, and atmospheric studies: technical description and users guide. Technical note (No. PB-97-131494/XAB; NCAR/TN-417-STR). National Center for Atmospheric Research, Climate and Global Dynamics Division, Boulder
- Bowen RM (1982) Compressible porous media models by use of the theory of mixtures. *Int J Eng Sci* 20(6):697–735
- Bowen RM (1960) Theory of mixtures in engineering. In: *Continuum physics, vol III*. Academic, New York, p 19
- Brooks RH (1965) *Hydraulic properties of porous media*. Colorado State University, Fort Collins

32. Cahn JW, Hilliard JE (1958) Free energy of a nonuniform system. I. Interfacial free energy. *J Chem Phys* 28(2):258–267
33. Cai H, Hong R, Xu L, Wang C, Rong C (2022) Frost heave and thawing settlement of the ground after using a freeze-sealing pipe-roof method in the construction of the Gongbei Tunnel. *Tunn Undergr Space Technol* 125:104503
34. Carslaw HS, Jaeger JC (1959) *Conduction of heat in solids*, 2nd edn. Oxford University Press, New York
35. Casini F, Gens A, Olivella S, Viggiani GM (2016) Artificial ground freezing of a volcanic ash: laboratory tests and modelling. *Environ Geotech* 3(3):141–154
36. Chang J, Deng S, Li X, Li Y, Chen J, Duan C (2022) Effective treatment of acid mine drainage by constructed wetland column: coupling walnut shell and its biochar product as the substrates. *J Water Process Eng* 49:103116
37. Chang Y, Qihao Y, Yanhui Y, Lei G (2018) Formation mechanism of longitudinal cracks in expressway embankments with inclined thermosyphons in warm and ice-rich permafrost regions. *Appl Therm Eng* 133:21–32
38. Chen Z, Bobaru F (2015) Selecting the kernel in a peridynamic formulation: a study for transient heat diffusion. *Comput Phys Commun* 197:51–60
39. Chen H, Gao X, Wang Q (2023) Research progress and prospect of frozen soil engineering disasters. *Cold Reg Sci Technol* 212:103901
40. Chen QM, Ghimire B, Su LB, Liu Y (2024) Micro-scale investigations on the mechanical properties of expansive soil subjected to freeze–thaw cycles. *Cold Reg Sci Technol* 219:104128
41. Chen Y, Lai Y, Li H, Pei W (2022) Finite element analysis of heat and mass transfer in unsaturated freezing soils: formulation and verification. *Comput Geotech* 149:104848
42. Chen A, Liang X, Bian L, Liu Y (2016) Analysis on MODIS albedo retrieval quality over the Qinghai-Tibet Plateau. *Plateau Meteorol* 35:277–284
43. Chen, F. X. (2001). The fully coupled modelling of the thermal-moisture-deformation behaviour for the saturated freezing soils. Xi'an University of Technology, Xi'an.
44. Cheng P, Liu Y, Li YP, Yi JT (2022) A large deformation finite element analysis of uplift behaviour for helical anchor in spatially variable clay. *Comput Geotech* 141:104542
45. Collins JB, Levine H (1985) Diffuse interface model of diffusion-limited crystal growth. *Phys Rev B* 31(9):6119
46. Côté J, Konrad JM (2005) Thermal conductivity of base-course materials. *Can Geotech J* 42(1):61–78
47. Coussy O (2005) Poromechanics of freezing materials. *J Mech Phys Solids* 53(8):1689–1718
48. Cox PM, Betts RA, Bunton CB, Essery RLH, Rowntree PR, Smith J (1999) The impact of new land surface physics on the GCM simulation of climate and climate sensitivity. *Clim Dyn* 15:183–203
49. Cui HH, Liu JK, Zhang LQ, Tian TH (2015) A constitutive model of subgrade in a seasonally frozen area with considering freeze–thaw cycles. *Rock Soil Mech* 36(8):2228–2236
50. Dai Y, Zeng X, Dickinson RE et al (2003) The common land model. *Bull Am Meteorol Soc* 84(8):1013–1024
51. Dall'Amico M, Endrizzi S, Gruber S, Rigon RJTC (2011) A robust and energy-conserving model of freezing variably-saturated soil. *Cryosphere* 5(2):469–484
52. Dallimore SR, Williams PJ (eds) (1984) *Pipelines and frost heave: a seminar*. Carleton University, Ottawa, p 75
53. Dallimore SR (1985) Observations and predictions of frost heave around a chilled pipeline. MA Thesis, Carleton University
54. Dayarathne R, Hawlader B, Phillips R, Robert D (2023) Two-dimensional finite element modelling of long-term frost heave beneath chilled gas pipelines. *Cold Reg Sci Technol* 208:103781
55. Demirdžić I, Muzaferija S (1995) Numerical method for coupled fluid flow, heat transfer and stress analysis using unstructured moving meshes with cells of arbitrary topology. *Comput Methods Appl Mech Eng* 125(1–4):235–255
56. Deng X, Pan S, Wang Z, Ke K, Zhang J (2019) Application of the Darcy-Stefan model to investigate the thawing subsidence around the wellbore in the permafrost region. *Appl Therm Eng* 156:392–401
57. Diersch HJG (2013) *FEFLOW: finite element modelling of flow, mass and heat transport in porous and fractured media*. Springer, Berlin
58. Dirksen C, Miller RD (1966) Closed-system freezing of unsaturated soil. *Soil Sci Soc Am J* 30(2):168–173
59. Dobinski W (2011) Permafrost. *Earth Sci Rev* 108(3–4):158–169
60. Dong S, Jiang Y, Yu X (2021) Analyses of the impacts of climate change and forest fire on cold region slopes stability by random finite element method. *Landslides* 18:2531–2545
61. Dong S, Yu X (2019) Analysis of the stability of thawing slopes by random finite element method. *Transp Res Rec* 2673(10):465–476
62. Dong S, Yu X (2020) Microstructure-based random finite element method model for freezing effects in soils and cold region retaining walls. *Transp Res Rec* 2674(11):708–719
63. Dong S, Yu X (2017) Microstructure-based random finite element simulation of thermal and hydraulic conduction processes in unsaturated frozen soils. In: *Geotechnical frontiers 2017*. American Society of Civil Engineers, Reston, pp 781–790
64. Dumais S, Konrad JM (2018) One-dimensional large-strain thaw consolidation using nonlinear effective stress–void ratio–hydraulic conductivity relationships. *Can Geotech J* 55(3):414–426
65. Eugster W, Rouse WR, Pielke RA Sr, Mcfadden JP, Baldocchi DD, Kittel TGF et al (2000) Land–atmosphere energy exchange in Arctic tundra and boreal forest: available data and feedbacks to climate. *Glob Change Biol* 6(S1):84–115
66. Fallah NA, Bailey C, Cross M, Taylor GA (2000) Comparison of finite element and finite volume methods application in geometrically nonlinear stress analysis. *Appl Math Model* 24(7):439–455
67. Fang PP, Liu Y, Shields MD (2022) Direct simulation methods for a class of normal and lognormal random fields with applications in modelling material properties. *J Eng Mech* 148(2):04021146
68. Feng S, Zhang Y, Shi M, Wen T, Lu TJ (2015) Unidirectional freezing of phase change materials saturated in open-cell metal foams. *Appl Therm Eng* 88:315–321
69. Fierz C, Lehning M (2001) Assessment of the microstructure-based snow-cover model SNOWPACK: thermal and mechanical properties. *Cold Reg Sci Technol* 33(2–3):123–131
70. Flerchinger GN (2000) *The simultaneous heat and water (SHAW) model: technical documentation*. Northwest Watershed Research Center, USDA Agricultural Research Service, Boise
71. Flerchinger GN, Saxton KE (1989) Simultaneous heat and water model of a freezing snow–residue–soil system I. Theory and development. *Trans ASAE* 32(2):565–571
72. Frederick JM, Buffett BA (2014) Taliks in relict submarine permafrost and methane hydrate deposits: pathways for gas escape under present and future conditions. *J Geophys Res Earth Surf* 119(2):106–122
73. Fredlund DG, Xing A (1994) Equations for the soil–water characteristic curve. *Can Geotech J* 31(4):521–532
74. Fukuda M, Kim HS, Kim YC (1997) Preliminary results of frost heave experiments using standard test sample provided by TC8. In: *Ground freezing 97: frost action in soils*. CRC Press, Boca Raton, pp 25–30

75. Gan Y, Kamlah M (2010) Discrete element modelling of pebble beds: with application to uniaxial compression tests of ceramic breeder pebble beds. *J Mech Phys Solids* 58(2):129–144
76. Gao H, Ghoreishian Amiri SA, Kjelstrup S, Grimstad G, Loranger B, Scibilia E (2023) Formation and growth of multiple, distinct ice lenses in frost heave. *Int J Numer Anal Methods Geomech* 47(1):82–105
77. Gao Y, Yu Y, Yang L, Qin S, Hou G (2021) Development of a coupled simplified lattice Boltzmann method for thermal flows. *Comput Fluids* 229:105042
78. Gerstle W, Silling S, Read D, Tewary V, Lehoucq R (2008) Peridynamic simulation of electromigration. *Comput Mater Contin* 8(2):75–92
79. Giakoumakis SG (1994) A model for predicting coupled heat and mass transfers in unsaturated partially frozen soil. *Int J Heat Fluid Flow* 15(2):163–171
80. Gilpin R (1980) A model for the prediction of ice lensing and frost heave in soils. *Water Resour Res* 16(5):918–930
81. Gosink JP, Kawasaki K, Osterkamp TE, Holty J (1988) Heat and moisture transport during annual freezing and thawing. In: *Proceedings of the fifth international conference on permafrost, 1988*, pp 355–360
82. Grenier C, Anbergen H, Bense V et al (2018) Groundwater flow and heat transport for systems undergoing freeze–thaw: intercomparison of numerical simulators for 2D test cases. *Adv Water Resour* 114:196–218
83. Grenier C, Régnier D, Mouche E, Benabderrahmane H, Costard F, Davy P (2013) Impact of permafrost development on groundwater flow patterns: a numerical study considering freezing cycles on a two-dimensional vertical cut through a generic river–plain system. *Hydrogeol J* 21(1):257
84. Groenevelt PH, Kay BD (1974) On the interaction of water and heat transport in frozen and unfrozen soils: II. The liquid phase. *Soil Sci Soc Am J* 38(3):400–404
85. Guo L, Li T, Niu Z (2012) Finite element simulation of the coupled heat–fluid transfer problem with phase change in frozen soil. In: *Earth and space 2012: engineering, science, construction, and operations in challenging environments*. ASCE, Reston, pp 867–877
86. Gupta S, Deusner C, Haeckel M, Helmig R, Wohlmuth B (2017) Testing a thermo–chemo–hydro–geomechanical model for gas hydrate-bearing sediments using triaxial compression laboratory experiments. *Geochem Geophys Geosyst* 18(9):3419–3437
87. Hansson K, Simunek J, Mizoguchi M, Lundin LC, Van Genuchten MT (2004) Water flow and heat transport in frozen soil: numerical solution and freeze–thaw applications. *Vadose Zone J* 3(2):693–704
88. Hardy J, Pomeau Y, De Pazzis O (1973) Time evolution of a two-dimensional classical lattice system. *Phys Rev Lett* 31(5):276
89. Harlan RL (1973) Analysis of coupled heat–fluid transport in partially frozen soil. *Water Resour Res* 9(5):1314–1323
90. Harris C, Arenson LU, Christiansen HH et al (2009) Permafrost and climate in Europe: monitoring and modelling thermal, geomorphological and geotechnical responses. *Earth Sci Rev* 92(3–4):117–171
91. Hassan AE, Mohamed MM (2003) On using particle tracking methods to simulate transport in single-continuum and dual continua porous media. *J Hydrol* 275(3–4):242–260
92. Hassanizadeh SM, Leijnse T (1988) On the modelling of brine transport in porous media. *Water Resour Res* 24(3):321–330
93. Hazirbaba K (2019) Effects of freeze–thaw on settlement of fine grained soil subjected to cyclic loading. *Cold Reg Sci Technol* 160:222–229
94. He M, Feng X, Li N (2018) Modelling of coupled heat–moisture transfer and deformation behaviour of frozen soil. *Soil Mech Found Eng* 55:153–161
95. He H, Flerchinger GN, Kojima Y, Dyck M, Lv J (2021) A review and evaluation of 39 thermal conductivity models for frozen soils. *Geoderma* 382:114694
96. Heinze T (2021) A multi-phase heat transfer model for water infiltration into frozen soil. *Water Resour Res* 57(10):e2021WR030067
97. Henry KS (2000) A review of the thermodynamics of frost heave. Technical Report ERDC/CRREL TR-00-16. US Army Corps of Engineers
98. Hjort J, Streletskiy D, Doré G, Wu Q, Bjella K, Luoto M (2022) Impacts of permafrost degradation on infrastructure. *Nat Rev Earth Environ* 3(1):24–38
99. Holmén J, Benabderrahmane H, Buoro A, Brulhet J (2011) Modelling of permafrost freezing and melting and the impact of a climatic cycle on groundwater flow at the Meuse/Haute-Marne site. *Phys Chem Earth A/B/C* 36(17–18):1531–1538
100. Hong W, Wang X (2013) A phase-field model for systems with coupled large deformation and mass transport. *J Mech Phys Solids* 61(6):1281–1294
101. Hornum MT, Bense V, van der Ploeg M, Kroon A, Sjöberg Y (2023) Arctic spring systems driven by permafrost aggradation. *Geophys Res Lett* 50(17):e2023GL104719
102. Hu J, Che T, Sun H, Yang X (2022) Numerical modelling and simulation of thermo–hydrologic processes in frozen soils on the Qinghai–Tibet Plateau. *J Hydrol Reg Stud* 40:101050
103. Hu K (2011) Development of separated ice model coupled heat and moisture transfer in freezing soils. Unpublished PhD Dissertation, China University of Mining and Technology, Xuzhou (in Chinese)
104. Huang S, Guo Y, Liu Y, Ke L, Liu G (2018) Study on the influence of water flow on temperature around freeze pipes and its distribution optimization during artificial ground freezing. *Appl Therm Eng* 135:435–445
105. Huang X, Rudolph DL (2021) Coupled model for water, vapour, heat, stress and strain fields in variably saturated freezing soils. *Adv Water Resour* 154:103945
106. Huang X, Rudolph DL (2023) Numerical study of coupled water and vapour flow, heat transfer, and solute transport in variably-saturated deformable soil during freeze–thaw cycles. *Water Resour Res* 59(10):e2022WR032146
107. Huang X, Rudolph DL, Glass B (2022) A coupled thermal–hydraulic–mechanical approach to modelling the impact of roadbed frost loading on water main failure. *Water Resour Res* 58(3):e2021WR030933
108. Huang XW, Wang ZZ, Jiang PM, Li KQ, Tang CX (2024) Mesoscale investigation of the effects of groundwater seepage on the thermal performance of borehole heat exchangers. *Appl Therm Eng* 236:121809
109. Huang R, Wu H, Adams NA (2021) Mesoscopic lattice Boltzmann modelling of the liquid–vapour phase transition. *Phys Rev Lett* 126(24):244501
110. Huang R, Wu H, Adams NA (2021) Mesoscopic lattice Boltzmann modeling of the liquid–vapor phase transition. *Phys Rev Lett* 126(24):244501
111. Hughes TJ (2012) *The finite element method: linear static and dynamic finite element analysis*. Courier Corporation, Chelmsford
112. Ishikawa T, Tokoro T, Akagawa S (2015) Frost heave behaviour of unsaturated soils under low overburden pressure and its estimation. In: *Proceedings of GEO Quebec, 2015*
113. Jabakhanji R, Mohtar RH (2015) A peridynamic model of flow in porous media. *Adv Water Resour* 78:22–35
114. Jame YW, Norum DI (1972) Phase composition of a partially frozen soil. Division of Hydrology, College of Engineering, University of Saskatchewan, Saskatoon

115. Jame YW, Norum DI (1980) Heat and mass transfer in a freezing unsaturated porous medium. *Water Resour Res* 16(4):811–819
116. Jame YW (1977) Heat and mass transfer in freezing unsaturated soil. PhD Thesis, Agricultural Engineering Department, University of Saskatchewan, Saskatoon
117. Jansson PE (2012) CoupModel: model use, calibration, and validation. *Trans ASABE* 55(4):1337–1344
118. Ji Y, Zhou G, Hall MR, Vandeginste V, Zhao X (2022) Thermal–hydraulic–mechanical coupling research on overburden pressure mitigated ice lens growth in the freezing soil. *KSCE J Civ Eng* 26(4):1606–1617
119. Ji Y, Zhou G, Vandeginste V, Zhou Y (2021) Thermal–hydraulic–mechanical coupling behaviour and frost heave mitigation in freezing soil. *Bull Eng Geol Environ* 80:2701–2713
120. Ji Y, Zhou G, Zhou Y, Hall MR, Zhao X, Mo PQ (2018) A separate-ice based solution for frost heaving-induced pressure during coupled thermal-hydro-mechanical processes in freezing soils. *Cold Reg Sci Technol* 147:22–33
121. Jiao C, Wang Y, Shan Y, He P, He J (2023) Quantifying the effect of a retrogressive thaw slump on soil freeze–thaw erosion in permafrost regions on the Qinghai-Tibet Plateau, China. *Land Degrad Dev*. <https://doi.org/10.1002/ldr.4631>
122. Jin YF, Yin ZY, Yuan WH (2020) Simulating retrogressive slope failure using two different smoothed particle finite element methods: a comparative study. *Eng Geol* 279:105870
123. Johansen O (1977) Thermal conductivity of soils. Cold Regions Research and Engineering Lab, Hanover
124. Jumikis AR (1966) Thermal soil mechanics. Rutgers University Press, New Brunswick
125. Kang Q, Li KQ, Fu JL, Liu Y (2024) Hybrid LBM and machine learning algorithms for permeability prediction of porous media: a comparative study. *Comput Geotech* 168:106163
126. Karma A, Kessler DA, Levine H (2001) Phase-field model of mode III dynamic fracture. *Phys Rev Lett* 87(4):045501
127. Karma A, Rappel WJ (1996) Phase-field method for computationally efficient modelling of solidification with arbitrary interface kinetics. *Phys Rev E* 53(4):R3017
128. Karra S, Painter SL, Lichtner PC (2014) Three-phase numerical model for subsurface hydrology in permafrost-affected regions (PFLOTTRAN-ICE v1.0). *Cryosphere* 8(5):1935–1950
129. Katiyar A, Foster JT, Ouchi H, Sharma MM (2014) A peridynamic formulation of pressure driven convective fluid transport in porous media. *J Comput Phys* 261:209–229
130. Kaviany M (2012) Principles of heat transfer in porous media. Springer, New York
131. Kebria MM, Na S, Yu F (2022) An algorithmic framework for computational estimation of soil freezing characteristic curves. *Int J Numer Anal Methods Geomech* 46(8):1544–1565
132. Kelleners TJ (2013) Coupled water flow and heat transport in seasonally frozen soils with snow accumulation. *Vadose Zone J*. <https://doi.org/10.2136/vzj2012.0162>
133. Kern-Luetsch M, Harris C, Cleall P, Li Y, Thomas H (2008) Scaled centrifuge modelling of solifluction in permafrost and seasonally frozen soils. In: Proceedings of the ninth international conference on permafrost, June 2008, pp 919–924
134. Khoei AR (2014) Extended finite element method: theory and applications. Wiley, Hoboken
135. Kim HC, Bishnoi PR, Heidemann RA, Rizvi SS (1987) Kinetics of methane hydrate decomposition. *Chem Eng Sci* 42(7):1645–1653
136. Kimiaghali N, Goharrokhi M, Clark SP, Ahmari H (2015) A comprehensive fluvial geomorphology study of riverbank erosion on the Red River in Winnipeg, Manitoba, Canada. *J Hydrol* 529:1488–1498
137. Kimoto S, Oka F, Fushita T (2010) A chemo–thermo-mechanically coupled analysis of ground deformation induced by gas hydrate dissociation. *Int J Mech Sci* 52(2):365–376
138. Kimoto S, Oka F, Fushita T, Fujiwaki M (2007) A chemo–thermo-mechanically coupled numerical simulation of the subsurface ground deformations due to methane hydrate dissociation. *Comput Geotech* 34(4):216–228
139. Kjelstrup S, Ghoreishian Amiri SA, Loranger B, Gao H, Grimstad G (2021) Transport coefficients and pressure conditions for growth of ice lens in frozen soil. *Acta Geotech* 16:2231–2239
140. Kolditz O, Bauer S, Bilke L et al (2012) OpenGeoSys: an open-source initiative for numerical simulation of thermo–hydro-mechanical/chemical (THM/C) processes in porous media. *Environ Earth Sci* 67(2):589–599
141. Koniorczyk M (2012) Salt transport and crystallization in non-isothermal, partially saturated porous materials considering ions interaction model. *Int J Heat Mass Transf* 55(4):665–679
142. Konrad JM, Duquenois C (1993) A model for water transport and ice lensing in freezing soils. *Water Resour Res* 29(9):3109–3124
143. Konrad JM, Morgenstern NR (1981) The segregation potential of a freezing soil. *Can Geotech J* 18(4):482–491
144. Konrad JM, Morgenstern NR (1984) Frost heave prediction of chilled pipelines buried in unfrozen soils. *Can Geotech J* 21(1):100–115
145. Konrad JM (1980) Frost heave mechanics. PhD Dissertation, Department of Civil Engineering, The University of Alberta
146. Koop T, Luo B, Tsias A, Peter T (2000) Water activity as the determinant for homogeneous ice nucleation in aqueous solutions. *Nature* 406(6796):611–614
147. Koopmans RWR, Miller RD (1966) Soil freezing and soil water characteristic curves. *Soil Sci Soc Am J* 30(6):680–685
148. Korshunov AA, Doroshenko SP, Nevzorov AL (2016) The impact of freezing–thawing process on slope stability of earth structure in cold climate. *Procedia Eng* 143:682–688
149. Kozłowski T, Nartowska E (2013) Unfrozen water content in representative bentonites of different origin subjected to cyclic freezing and thawing. *Vadose Zone J* 12(1):vzj2012-0057
150. Lackner R, Amon A, Lager H (2005) Artificial ground freezing of fully saturated soil: thermal problem. *J Eng Mech* 131(2):211–220
151. Lai Y, Pei W, Zhang M, Zhou J (2014) Study on theory model of hydro-thermal–mechanical interaction process in saturated freezing silty soil. *Int J Heat Mass Transf* 78:805–819
152. Lai YM, Wu ZW, Liu SY, Den XJ (2001) Nonlinear analyses for the semicoupled problem of temperature, seepage, and stress fields in cold region retaining walls. *J Therm Stress* 24(12):1199–1216
153. Lai YM, Wu ZW, Zhu YL, Zhu LN (1998) Nonlinear analysis for the coupled problem of temperature, seepage and stress fields in cold-region tunnels. *Tunn Undergr Space Technol* 13(4):435–440
154. Lai Y, You Z, Zhang J (2021) Constitutive models and salt migration mechanisms of saline frozen soil and the-state-of-the-practice countermeasures in cold regions. *Sci Cold Arid Reg* 13(1):1–17
155. Lai YM, Zhang XF, Xiao JZ, Zhang SJ, Liu ZQ (2005) Nonlinear analysis for frost-heaving force of land bridges on Qing-Tibet Railway in cold regions. *J Therm Stress* 28(3):317–331
156. Lam L, Fredlund DG, Barbour SL (1987) Transient seepage model for saturated–unsaturated soil systems: a geotechnical engineering approach. *Can Geotech J* 24(4):565–580
157. Lan T, Luo X, Ma Q, Jiang W, Xia H (2023) Desertification caused by embankment construction in permafrost environment on the Qinghai-Tibetan Plateau. *Arab J Sci Eng* 48(1):583–599
158. Lei D, Yang Y, Cai C, Chen Y, Wang S (2020) The modelling of freezing process in saturated soil based on the

- thermal-hydro-mechanical multi-physics field coupling theory. *Water* 12(10):2684
159. LeVeque RJ (2002) *Finite volume methods for hyperbolic problems*, vol 31. Cambridge University Press, Cambridge
 160. Li KQ, Chen QM, Chen G (2024) Scale dependency of anisotropic thermal conductivity of heterogeneous geomaterials. *Bull Eng Geol Environ* 83:73
 161. Li N, Chen B, Chen F, Xu X (2000) The coupled heat–moisture–mechanic model of the frozen soil. *Cold Reg Sci Technol* 31(3):199–205
 162. Li KQ, Chen G, Liu Y, Yin ZY (2023) Scale effect on the apparent anisotropic hydraulic conductivity of geomaterials. *ASCE-ASME J Risk Uncertain Eng Syst A* 9(3):04023020
 163. Li N, Chen F, Su B, Cheng G (2002) Theoretical frame of the saturated freezing soil. *Cold Reg Sci Technol* 35(2):73–80
 164. Li Z, Chen J, Tang A, Sugimoto M (2021) A novel model of heat–water–air–stress coupling in unsaturated frozen soil. *Int J Heat Mass Transf* 175:121375
 165. Li DQ, Ding YN, Tang XS, Liu Y (2021) Probabilistic risk assessment of landslide-induced surges considering the spatial variability of soils. *Eng Geol* 283:105976
 166. Li K, Horton R, He H (2023) Application of machine learning algorithms to model soil thermal diffusivity. *Int Commun Heat Mass Transf* 149:107092
 167. Li KQ, Kang Q, Nie JY, Huang XW (2022) Artificial neural network for predicting the thermal conductivity of soils based on a systematic database. *Geothermics* 103:102416
 168. Li H, Lai Y, Li L (2020) Impact of hydro-thermal behaviour around a buried pipeline in cold regions. *Cold Reg Sci Technol* 171:102961
 169. Li H, Lai Y, Wang L et al (2019) Review of the state of the art: interactions between a buried pipeline and frozen soil. *Cold Reg Sci Technol* 157:171–186
 170. Li X, Li X (2023) A soil freezing–thawing model based on thermodynamics. *Cold Reg Sci Technol* 211:103867
 171. Li KQ, Li DQ, Chen DH, Gu SX, Liu Y (2021) A generalized model for effective thermal conductivity of soils considering porosity and mineral composition. *Acta Geotech* 16(11):3455–3466
 172. Li KQ, Li DQ, Li PT, Liu Y (2019) Meso-mechanical investigations on the overall elastic properties of multi-phase construction materials using finite element method. *Constr Build Mater* 228:116727
 173. Li KQ, Li DQ, Liu Y (2020) Meso-scale investigations on the effective thermal conductivity of multi-phase materials using the finite element method. *Int J Heat Mass Transf* 151:119383
 174. Li X, Li X, Liu J (2023) A dynamic soil freezing characteristic curve model for frozen soil. *J Rock Mech Geotech Eng*. <https://doi.org/10.1016/j.jrmge.2023.09.008>
 175. Li XK, Li X, Liu S, Qi JL (2023) Thermal-seepage coupled numerical simulation methodology for the artificial ground freezing process. *Comput Geotech* 156:105246
 176. Li Z, Liu S, Feng Y, Liu K, Zhang C (2013) Numerical study on the effect of frost heave prevention with different canal lining structures in seasonally frozen ground regions. *Cold Reg Sci Technol* 85:242–249
 177. Li KQ, Liu Y, Kang Q (2022) Estimating the thermal conductivity of soils using six machine learning algorithms. *Int Commun Heat Mass Transf* 136:106139
 178. Li N, Liu ZQ, Niu GD, Zhang J, Li JP, Zhang F (2021) Numerical simulation considering the effect of uneven frost heave on tunnel structure in cold regions. *Therm Sci* 25(6 Part B):4545–4552
 179. Li X, Liu Y, Wong H, Pardo B, Fabbri A, McGregor F, Liu E (2022) Analytical and numerical studies on the behavior of a freezing soil layer. *Cold Reg Sci Technol* 198:103538
 180. Li KQ, Liu Y, Yin ZY (2023) An improved 3D microstructure reconstruction approach for porous media. *Acta Mater* 242:118472
 181. Li KQ, Miao Z, Li DQ, Liu Y (2022) Effect of mesoscale internal structure on effective thermal conductivity of anisotropic geomaterials. *Acta Geotech* 17:3553–3566
 182. Li H, Wang F, Wang Y, Yuan Y, Feng G, Tian H, Xu T (2023) Phase-field modelling of coupled reactive transport and pore structure evolution due to mineral dissolution in porous media. *J Hydrol* 619:129363
 183. Li KQ, Yin ZY, Liu Y (2023) A hybrid SVR-BO model for predicting the soil thermal conductivity with uncertainty. *Can Geotech J* 61(2):258–274
 184. Li KQ, Yin ZY, Liu Y (2023) Influences of spatial variability of hydrothermal properties on the freezing process in artificial ground freezing technique. *Comput Geotech* 159:105448
 185. Li KQ, Yin ZY, Qi JL, Liu Y (2024) State-of-the-art constitutive modelling of frozen soils. *Arch Comput Methods Eng*. <https://doi.org/10.1007/s11831-024-10102-w>
 186. Li KQ, Yin ZY, Zhang N, Li J (2024) A PINN-based modelling approach for hydromechanical behaviour of unsaturated expansive soils. *Comput Geotech* 169:106174
 187. Li G, Yin BB, Zhang LW, Liew KM (2020) Modelling microfracture evolution in heterogeneous composites: a coupled cohesive phase-field model. *J Mech Phys Solids* 142:103968
 188. Li KQ, Yin ZY, Zhang N, Liu Y (2023) A data-driven method to model stress–strain behaviour of frozen soil considering uncertainty. *Cold Reg Sci Technol* 213:103906
 189. Li S, Zhang M, Pei W, Lai Y (2018) Experimental and numerical simulations on heat–water–mechanics interaction mechanism in a freezing soil. *Appl Therm Eng* 132:209–220
 190. Li R, Zhao L, Wu T, Wang Q, Ding Y, Yao J et al (2019) Soil thermal conductivity and its influencing factors at the Tanggula permafrost region on the Qinghai-Tibet Plateau. *Agric For Meteorol* 264:235–246
 191. Ling XZ, Yu Y, Tang L, Geng L, Han X (2022) The lining responses for shallow mountain tunnels subjected to frost heaving. *J Mt Sci* 19(2):529–546
 192. Liu Q, Cai G, Zhou C, Yang R, Li J (2024) Thermo–hydro-mechanical coupled model of unsaturated frozen soil considering frost heave and thaw settlement. *Cold Reg Sci Technol* 217:104026
 193. Liu S, Fang G, Liang J, Fu M, Wang B (2020) A new type of peridynamics: element-based peridynamics. *Comput Methods Appl Mech Eng* 366:113098
 194. Liu S, Huang Q, Zhang W, Ren D, Huang G (2023) Improving soil hydrological simulation under freeze–thaw conditions by considering soil deformation and its impact on soil hydrothermal properties. *J Hydrol* 619:129336
 195. Liu E, Lai Y, Wong H, Feng J (2018) An elastoplastic model for saturated freezing soils based on thermo-poromechanics. *Int J Plast* 107:246–285
 196. Liu Y, Li KQ, Li DQ, Tang XS, Gu SX (2022) Coupled thermal–hydraulic modelling of artificial ground freezing with uncertainties in pipe inclination and thermal conductivity. *Acta Geotech* 17(1):257–274
 197. Liu XQ, Liu JK, Tian YH, Shen YP, Wang QZ (2021) Effect of dynamic load and cooling path on the frost characteristics of saturated lean clay. *Transp Geotech* 31:100645
 198. Liu X, Shen Y, Zhang Z, Liu Z, Wang B, Tang T, Liu C (2022) Field measurement and numerical investigation of artificial ground freezing for the construction of a subway cross passage under groundwater flow. *Transp Geotech* 37:100869
 199. Liu J, Yang P, Wang J, Wang S, Jiang H (2023) Freezing front evolution in chloride soils under unidirectional freezing

- conditions and the characterization via electrical conductivity. *Cold Reg Sci Technol* 213:103913
200. Liu Z, Yu X (2011) Coupled thermo–hydro–mechanical model for porous materials under frost action: theory and implementation. *Acta Geotech* 6:51–65
 201. Liu Z, Yu X (2014) Coupled thermo–hydraulic modelling of pavement under frost. *Int J Pavement Eng* 15(5):427–437
 202. Liu J, Zhang W, Cui J, Ren Z, Wang E, Li X et al (2023) Extreme low-temperature freezing process and characteristic curve of icy lunar regolith simulant. *Acta Astronaut* 202:485–496
 203. Liu Y, Li KQ, Li PT, Hu J (2019) Artificial ground freezing technique in tunnel construction considering uncertain drilling inaccuracy of freeze pipes. In: *Proceedings of the 29th European safety and reliability conference*, Hannover, Germany, 2019
 204. Loch JPG (1978) Thermodynamic equilibrium between ice and water in porous media. *Soil Sci* 126(2):77–80
 205. Loli M, Tsatsis A, Kourkoulis R, Anastasopoulos I (2020) A simplified numerical method to simulate the thawing of frozen soil. *Proc Inst Civ Eng Geotech Eng* 173(5):408–427
 206. Lunardini VJ (1981) Heat transfer in cold climates. Van Nostrand Reinhold, New York
 207. Luo B, Ishikawa T, Tokoro T, Lai H (2017) Coupled thermo–hydro–mechanical analysis of freeze–thaw behaviour of pavement structure over a box culvert. *Transp Res Rec* 2656(1):12–22
 208. Ma QG, Luo XX, Gao JQ, Lan TL (2023) Evaluation of the application effect of the inclined TPCTs on an embankment with the shady–sunny slope effect in permafrost regions. *Cold Reg Sci Technol* 213:103936
 209. Ma W, Zhang L, Yang C (2015) Discussion of the applicability of the generalized Clausius–Clapeyron equation and the frozen fringe process. *Earth Sci Rev* 142:47–59
 210. Madenci E, Barut A, Futch M (2016) Peridynamic differential operator and its applications. *Comput Methods Appl Mech Eng* 304:408–451
 211. Madenci E, Dorduncu M, Barut A, Futch M (2017) Numerical solution of linear and nonlinear partial differential equations using the peridynamic differential operator. *Numer Methods Partial Differ Equ* 33(5):1726–1753
 212. Madenci E, Oterkus E (2013) Peridynamic theory. In: *Peridynamic theory and its applications*. Springer, New York, pp 19–43
 213. Marwan A, Zhou MM, Abdelrehim MZ, Meschke G (2016) Optimization of artificial ground freezing in tunneling in the presence of seepage flow. *Comput Geotech* 75:112–125
 214. Masuda Y (1999) Modelling and experimental studies on dissociation of methane gas hydrates in Berea sandstone cores. In: *Proceedings of the third international gas hydrate conference*, 1999
 215. Matthies H, Strang G (1979) The solution of nonlinear finite element equations. *Int J Numer Methods Eng* 14(11):1613–1626
 216. McKenzie JM, Voss CI, Siegel DI (2007) Groundwater flow with energy transport and water–ice phase change: numerical simulations, benchmarks, and application to freezing in peat bogs. *Adv Water Resour* 30(4):966–983
 217. Mendoza PA, Clark MP, Barlage M, Rajagopalan B, Samaniego L, Abramowitz G, Gupta H (2015) Are we unnecessarily constraining the agility of complex process-based models? *Water Resour Res* 51(1):716–728
 218. Miller RD (1978) Frost heaving in non-colloidal soils. In: *Proceedings, 3rd international conference on permafrost*, 1978, pp 708–713
 219. Ming F, Li D (2014) Modelling and experimental investigation of one dimension coupled moisture and heat in unsaturated freezing soil. *J Cent South Univ (Sci Technol)* 25(3):889–894
 220. Mino Y, Tanaka H, Nakaso K, Gotoh K, Shinto H (2022) Lattice Boltzmann model for capillary interactions between particles at a liquid–vapour interface under gravity. *Phys Rev E* 105(4):045316
 221. Mizoguchi M (1990) Water, heat and salt transport in freezing soil. University of Tokyo, Tokyo
 222. Molson JW, Frind EO (2015) HEATFLOW-SMOKER: density-dependent flow and advective–dispersive transport of thermal energy, mass or residence time. University of Laval, Quebec, and University of Waterloo, Waterloo, p 116
 223. Morgenstern NT, Nixon JF (1971) One-dimensional consolidation of thawing soils. *Can Geotech J* 8(4):558–565
 224. Mosavat N, Hasanidarabadi B, Pourafshary P (2019) Gaseous slip flow simulation in a micro/nano pore-throat structure using the lattice Boltzmann model. *J Pet Sci Eng* 177:93–103
 225. Mu S, Ladanyi B (1987) Modelling of coupled heat, moisture and stress field in freezing soil. *Cold Reg Sci Technol* 14(3):237–246
 226. Na S, Sun W (2017) Computational thermo–hydro–mechanics for multiphase freezing and thawing porous media in the finite deformation range. *Comput Methods Appl Mech Eng* 318:667–700
 227. Na S, Malekzade Kebria M, Roy K (2020) A coupled thermo–hydro–mechanical model for capturing frost heave under chilled gas pipelines. In: *International pipeline conference*, 2020, vol 84454. American Society of Mechanical Engineers, p V002T08A005
 228. Newman GP, Wilson GW (1997) Heat and mass transfer in unsaturated soils during freezing. *Can Geotech J* 34(1):63–70
 229. Nikolaev P, Sedighi M, Jivkov AP, Margetts L (2022) Analysis of heat transfer and water flow with phase change in saturated porous media by bond-based peridynamics. *Int J Heat Mass Transf* 185:122327
 230. Nishimura S, Gens A, Olivella S, Jardine RJ (2009) THM-coupled finite element analysis of frozen soil: formulation and application. *Géotechnique* 59(3):159–171
 231. Niu GY, Yang ZL (2006) Effects of frozen soil on snowmelt runoff and soil water storage at a continental scale. *J Hydrometeorol* 7(5):937–952
 232. Okkonen J, Ala-Aho P, Hänninen P, Hayashi M, Sutinen R, Liwata P (2017) Multi-year simulation and model calibration of soil moisture and temperature profiles in till soil. *Eur J Soil Sci* 68(6):829–839
 233. O’Neill K, Miller RD (1985) Exploration of a rigid ice model of frost heave. *Water Resour Res* 21(3):281–296
 234. Orgogozo L, Xavier T, Oulbani H, Grenier C (2023) Permafrost modelling with OpenFOAM®: new advancements of the permaFoam solver. *Comput Phys Commun* 282:108541
 235. Orgogozo L, Grenier C, Quintard M et al (2017) Coupled water and energy transfers in porous media with freeze/thaw: permaFoam, a massively parallel OpenFOAM® solver. In: *9th International conference on porous media*, Rotterdam, Netherlands, 2017
 236. Padilla F, Villeneuve JP (1992) Modelling and experimental studies of frost heave including solute effects. *Cold Reg Sci Technol* 20(2):183–194
 237. Parameswaran VR (1980) Deformation behaviour and strength of frozen sand. *Can Geotech J* 17(1):74–88
 238. Parameswaran VR, Jones SJ (1981) Triaxial testing of frozen sand. *J Glaciol* 27(95):147–155
 239. Park DS, Shin MB, Park WJ, Seo YK (2023) Slope stability analysis model for the frost-susceptible soil based on thermal–hydro–mechanical coupling. *Comput Geotech* 163:105715
 240. Parker KH, Mehta RV, Caro CG (1987) Steady flow in porous, elastically deformable materials. *J Appl Mech Trans ASME* 54:794–800
 241. Peiró J, Sherwin S (2005) Finite difference, finite element and finite volume methods for partial differential equations. In:

- Handbook of materials modelling: methods. Springer, Dordrecht, pp 2415–2446
242. Penner E (1986) Aspects of ice lens growth in soils. *Cold Reg Sci Technol* 13(1):91–100
 243. Pimentel E, Sres A, Anagnostou G (2012) Large-scale laboratory tests on artificial ground freezing under seepage-flow conditions. *Geotechnique* 62(3):227–241
 244. Pomeroy JW, Brown T, Fang X, Shook KR, Pradhananga D, Armstrong R et al (2022) The Cold Regions Hydrological Modelling Platform for hydrological diagnosis and prediction based on process understanding. *J Hydrol* 615:128711
 245. Qi J, Cui W, Wang D (2024) Applicability of the principle of effective stress in cold regions geotechnical engineering. *Cold Reg Sci Technol* 219:104129
 246. Qin Z, Lai Y, Tian Y, Zhang M (2021) Stability behaviour of a reservoir soil bank slope under freeze–thaw cycles in cold regions. *Cold Reg Sci Technol* 181:103181
 247. Qin Y, Pan Z, Liu Z, Shang L, Zhou L (2021) Influence of the particle size of porous media on the formation of natural gas hydrate: a review. *Energy Fuels* 35(15):11640–11664
 248. Ran HW, Fan JH, Huang J (2019) Review of the coupling of water and heat in the freeze–thaw process and its model of frozen soil. *Pratacult Sci* 36(04):991–999
 249. Rivière A, Goncalves J, Jost A, Font M (2014) Experimental and numerical assessment of transient stream–aquifer exchange during disconnection. *J Hydrol* 517:574–583
 250. Rivière A, Jost A, Gonçalves J, Font M (2019) Pore water pressure evolution below a freezing front under saturated conditions: large-scale laboratory experiment and numerical investigation. *Cold Reg Sci Technol* 158:76–94
 251. Roth K, Boike J (2001) Quantifying the thermal dynamics of a permafrost site near Ny-Ålesund, Svalbard. *Water Resour Res* 37(12):2901–2914
 252. Ruffine L, Tang AM, O’Neill N et al (2023) Environmental challenges related to methane hydrate decomposition from climate change scenario and anthropic activities: state of the art, potential consequences and monitoring solutions. *Earth Sci Rev* 246:104578
 253. Sakai M, Toride N, Šimůnek J (2009) Water and vapour movement with condensation and evaporation in a sandy column. *Soil Sci Soc Am J* 73(3):707–717
 254. Sapriza-Azuri G, Gamazo P, Razavi S, Wheeler HS (2018) On the appropriate definition of soil profile configuration and initial conditions for land surface–hydrology models in cold regions. *Hydrol Earth Syst Sci* 22(6):3295–3309
 255. Scaringi G, Loche M (2022) A thermo–hydro–mechanical approach to soil slope stability under climate change. *Geomorphology* 401:108108
 256. Schofield RK (1935) The pF of the water in soil. In: International congress of soil science. 2, Plenary Session papers, Oxford, UK, 30 July–7 August 1935, pp 37–48
 257. Selvadurai APS, Hu J, Konuk I (1999) Computational modelling of frost heave induced soil–pipeline interaction: I. Modelling of frost heave. *Cold Reg Sci Technol* 29(3):215–228
 258. Selvadurai APS, Hu J, Konuk I (1999) Computational modelling of frost heave induced soil–pipeline interaction: II. Modelling of experiments at the Caen test facility. *Cold Reg Sci Technol* 29(3):229–257
 259. Shan W, Yang T, Guo Y, Zhang C (2022) Study on stress–temperature coupled damage model of warm frozen soil. *Authorea Preprints*
 260. Shao L, Guo X, Liu S, Zheng G (2017) Effective stress and equilibrium equation for soil mechanics. CRC Press, Boca Raton
 261. Shastri A, Sánchez M, Gai X, Lee MY, Dewers T (2021) Mechanical behaviour of frozen soils: experimental investigation and numerical modelling. *Comput Geotech* 138:104361
 262. Shastri A, Sanchez M (2012) Mechanical modelling of frozen soils incorporating the effect of cryogenic suction and temperature. In: *GeoCongress 2012: state of the art and practice in geotechnical engineering, 2012*, pp 2492–2501
 263. She Y, Kemp J, Richards L, Loewen M (2016) Investigation into freezing point depression in stormwater ponds caused by road salt. *Cold Reg Sci Technol* 131:53–64
 264. Shen T, Jiang P, Ju Q, Chen X, Lin H, Zhao J et al (2023) Frozen carbon is gradually thawing: assessing interannual dynamics of thawed soil organic carbon stocks in the Tibetan Plateau permafrost area from 1901–2020. *Agric For Meteorol* 343:109793
 265. Shi L, Li S, Wang C, Yang J, Zhao Y (2023) Heat–moisture–deformation coupled processes of a canal with a berm in seasonally frozen regions. *Cold Reg Sci Technol* 207:103773
 266. Silling SA (2000) Reformulation of elasticity theory for discontinuities and long-range forces. *J Mech Phys Solids* 48(1):175–209
 267. Silling SA, Epton M, Weckner O, Xu J, Askari E (2007) Peridynamic states and constitutive modelling. *J Elast* 88:151–184
 268. Siva Subramanian S, Fan X, Yunus AP, Van Asch T, Scaringi G, Xu Q et al (2020) A sequentially coupled catchment-scale numerical model for snowmelt-induced soil slope instabilities. *J Geophys Res Earth Surf* 125(5):e2019JF005468
 269. Slusarchuk WA, Clark JI, Nixon JF, Morgenstern NR, Gaskin PN (1978) Field test results of a chilled pipeline buried in unfrozen ground. In: *Proceedings of the 3rd international conference on permafrost, Edmonton, 1978, vol 1*, pp 878–883
 270. Smerdon BD, Mendoza CA, Devito KJ (2007) Simulations of fully coupled lake–groundwater exchange in a subhumid climate with an integrated hydrologic model. *Water Resour Res* 43(1):W01416
 271. Smith MW, Patterson DE (1989) Detailed observations on the nature of frost heaving at a field scale. *Can Geotech J* 26(2):306–312
 272. Sokolova I, Bastisya MG, Hajibeygi H (2019) Multiscale finite volume method for finite-volume-based simulation of poroelasticity. *J Comput Phys* 379:309–324
 273. Soltanpour S, Foriero A (2023) Numerical simulations of frost heave using COMSOL multiphysics software in unsaturated freezing soils. *Int J Geotech Geol Eng* 17(8):111–118
 274. Sousani M, Hobbs AM, Anderson A, Wood R (2019) Accelerated heat transfer simulations using coupled DEM and CFD. *Powder Technol* 357:367–376
 275. Spaans EJ, Baker JM (1996) The soil freezing characteristic: its measurement and similarity to the soil moisture characteristic. *Soil Sci Soc Am J* 60(1):13–19
 276. Stähli M, Jansson PE, Lundin LC (1999) Soil moisture redistribution and infiltration in frozen sandy soils. *Water Resour Res* 35(1):95–103
 277. Stein E (2014) History of the finite element method—mathematics meets mechanics—Part I: engineering developments. In: *The history of theoretical, material and computational mechanics—mathematics meets mechanics and engineering*. Springer, Berlin, pp 399–442
 278. Steinbach I (2009) Phase-field models in materials science. *Model Simul Mater Sci Eng* 17(7):073001
 279. Strang G, Fix GJ (1973) *An analysis of the Finite Element Method*. Prentice-Hall, Englewood Cliffs
 280. Suh HS, Sun W (2022) Multi-phase-field microporomechanics model for simulating ice-lens growth in frozen soil. *Int J Numer Anal Methods Geomech* 46(12):2307–2336

281. Sun R, Liu R, Zhang H, Zhang R, Jiang Y, Yin R (2023) A DEM-based approach for modelling the thermal–mechanical behaviour of frozen soil. *Eur J Environ Civ Eng* 28(4):1–26
282. Sun X, Luo H, Soga K (2018) A coupled thermal–hydraulic–mechanical–chemical (THMC) model for methane hydrate bearing sediments using COMSOL Multiphysics. *J Zhejiang Univ Sci A* 19(8):600–623
283. Sun Z, Zhao L, Hu G, Qiao Y, Du E, Zou D, Xie C (2021) Influence of lower boundary conditions on the numerical simulation of permafrost temperature field change. *J Glaciol Geocryol* 43:357–369
284. Svensson U (2014) DarcyTools: a computer code for hydrogeological analysis of nuclear waste repositories in fractured rock. *J Appl Math Phys* 2(06):365
285. Svensson U, Kuylenstierna HO, Ferry M (2010) DarcyTools version 3.4—concepts, methods and equations. SKB R-10-70. Svensk Kärnbränslehantering AB
286. Sweidan AH, Heider Y, Markert B (2020) A unified water/ice kinematics approach for phase-field thermo–hydro-mechanical modelling of frost action in porous media. *Comput Methods Appl Mech Eng* 372:113358
287. Sweidan AH, Niggemann K, Heider Y, Ziegler M, Markert B (2022) Experimental study and numerical modelling of the thermo–hydro-mechanical processes in soil freezing with different frost penetration directions. *Acta Geotech* 17(1):231–255
288. Tananaev N, Lotsari E (2022) Defrosting northern catchments: fluvial effects of permafrost degradation. *Earth Sci Rev* 228:103996
289. Tang T, Shen Y, Liu X, Zhang Z, Xu J, Zhang Z (2021) The effect of horizontal freezing on the characteristics of water migration and matrix suction in unsaturated silt. *Eng Geol* 288:106166
290. Tang CX, Zhu ZY, Luo F, He ZH, Zou ZY, Guo ZH (2021) Deformation behaviour and influence mechanism of thaw consolidation of embankments on the Qinghai-Tibet Railway in permafrost regions. *Transp Geotech* 28:100513
291. Taylor GS, Luthin JN (1978) A model for coupled heat and moisture transfer during soil freezing. *Can Geotech J* 15(4):548–555
292. Terzaghi K (1925) *Erdbaumechanik auf bodenphysikalischer Grundlage*. F. Deuticke, Leipzig
293. Thomas HR, Cleall P, Li YC, Harris C, Kern-Luetschg M (2009) Modelling of cryogenic processes in permafrost and seasonally frozen soils. *Geotechnique* 59(3):173–184
294. Tian Y, Yang ZJ, Tai B, Li Y, Shen Y (2019) Damage and mitigation of railway embankment drainage trench in warm permafrost: a case study. *Eng Geol* 261:105276
295. Tokoro T, Ishikawa T, Akagawa S (2016) Temperature dependency of permeability coefficient of frozen soil. In: *Proceedings of the 69th annual Canadian geotechnical conference*, Vancouver, BC, Canada, 2016, pp 2–5
296. Tounsi H, Rouabhi A, Jahangir E (2020) Thermo–hydro-mechanical modelling of artificial ground freezing taking into account the salinity of the saturating fluid. *Comput Geotech* 119:103382
297. Truesdell C (1957) Sulle basi della termomeccanica. *Rend Lincei* 22(8):33–38
298. Van Genuchten MT (1980) A closed-form equation for predicting the hydraulic conductivity of unsaturated soils. *Soil Sci Soc Am J* 44(5):892–898
299. Van der Waals JD (1894) *Z. Phys. Chem.* 13, 657. (Translated by Rowlinson, J.S. and published in English at: van der Waals, J.D. 1979. The thermodynamic theory of capillarity under the hypothesis of a continuous variation of density. *J Stat Phys* 20:200–244
300. Vitel M, Rouabhi A, Tijani M, Guérin F (2016) Thermo-hydraulic modelling of artificial ground freezing: application to an underground mine in fractured sandstone. *Comput Geotech* 75:80–92
301. Vogel T, Van Genuchten MT, Cislerova M (2000) Effect of the shape of the soil hydraulic functions near saturation on variably-saturated flow predictions. *Adv Water Resour* 24(2):133–144
302. Voss CI, Provost AM (2002) SUTRA—a model for saturated–unsaturated variable-density ground-water flow with solute or energy transport. US Geological Survey Open-File Report 02-4231. USGS, Reston, p 250
303. Wan H, Bian J, Zhang H, Li Y (2021) Assessment of future climate change impacts on water–heat–salt migration in unsaturated frozen soil using CoupModel. *Front Environ Sci Eng* 15:1–17
304. Wan Y, Wu N, Chen Q, Li W, Hu G, Huang L, Ouyang W (2022) Coupled thermal–hydrodynamic–mechanical–chemical numerical simulation for gas production from hydrate-bearing sediments based on hybrid finite volume and finite element method. *Comput Geotech* 145:104692
305. Wang RH (2005) Research on hydro-thermal–mechanical coupling of artificial multi-loop tube frozen ground and calculation of frozen wall. University of Science and Technology of China, Hefei
306. Wang X, Chang D, Liu J (2022) Numerical simulation of frost jacking response of a single pile considering hydro–thermo-mechanical coupling. *Res Cold Arid Reg* 14(5):307–316
307. Wang Z, Feyen J, Nielsen DR, van Genuchten MT (1997) Two-phase flow infiltration equations accounting for air entrapment effects. *Water Resour Res* 33(12):2759–2767
308. Wang Z, Fu Q, Jiang Q, Li T (2011) Numerical simulation of water–heat coupled movements in seasonal frozen soil. *Math Comput Model* 54(3–4):970–975
309. Wang T, Huang H, Zhang F, Han Y (2020) DEM-continuum mechanics coupled modelling of slot-shaped breakout in high-porosity sandstone. *Tunn Undergr Space Technol* 98:103348
310. Wang M, Li X, Liu Z, Liu J, Chang D (2020) Application of PIV technique in model test of frost heave of unsaturated soil. *J Cold Reg Eng* 34(3):04020014
311. Wang T, Liu J, Tai B, Zang C, Zhang Z (2017) Frost jacking characteristics of screw piles in seasonally frozen regions based on thermo–mechanical simulations. *Comput Geotech* 91:27–38
312. Wang C, Ma Z (2021) Mathematical model and numerical simulation of hydrothermal coupling for unsaturated soil subgrade in the seasonal frozen zone. *IOP Conf Ser Earth Environ Sci* 719(3):032042
313. Wang J, Nishimura S, Tokoro T (2017) Laboratory study and interpretation of mechanical behaviour of frozen clay through state concept. *Soils Found* 57(2):194–210
314. Wang W, Wang L, Yu F, Wang Q (2016) One dimensional thaw consolidation behaviours with periodical thermal boundaries. *KSCE J Civ Eng* 20:1250–1258
315. Wang K, Wu M, Zhang R (2016) Water and solute fluxes in soils undergoing freezing and thawing. *Soil Sci* 181(5):193–201
316. Wang Z, Xie K, Zhang Y, Hou X, Zhao W, Li B (2023) A multiphase model developed for mesoscopic heat and mass transfer in thawing frozen soil based on lattice Boltzmann method. *Appl Therm Eng* 229:120580
317. Wang P, Yin ZY, Hicher PY, Cui YJ (2023) Micro-mechanical analysis of one-dimensional compression of clay with DEM. *Int J Numer Anal Methods Geomech* 47(15):2706–2724
318. Wang T, Zhang F, Furtney J, Damjanac B (2022) A review of methods, applications and limitations for incorporating fluid flow in the discrete element method. *J Rock Mech Geotech Eng* 14(3):1005–1024

319. Wang K, Zhang Z, Leo CJ, Xie K (2008) Dynamic torsional response of an end bearing pile in saturated poroelastic medium. *Comput Geotech* 35(3):450–458
320. Wang YT (2016) Experimental study of frost heaving process and its mechanism by using digital image processing. PhD Thesis, University of Chinese Academy of Sciences
321. Watanabe K, Kito T, Wake T, Sakai M (2011) Freezing experiments on unsaturated sand, loam and silt loam. *Ann Glaciol* 52(58):37–43
322. Watanabe K, Kugisaki Y (2017) Effect of macropores on soil freezing and thawing with infiltration. *Hydrol Process* 31(2):270–278
323. Watanabe K, Osada Y (2016) Comparison of hydraulic conductivity in frozen saturated and unfrozen unsaturated soils. *Vadose Zone J* 15(5):vzj2015-11
324. Weng X, Sun Y, Yang Z, Wang D, Yu H (2020) A thermal–hydromechanical coupled model for poro-viscoplastic saturated freezing soil. *Eur J Environ Civ Eng* 26(9):4220–4236
325. Wettlaufer JS, Worster MG (2006) Premelting dynamics. *Annu Rev Fluid Mech* 38:427–452
326. Wu Y, Ishikawa T (2022) Thermal-Hydro-Mechanical coupled analysis of unsaturated frost susceptible soils. *Res Cold Arid Reg* 14(4):223–234
327. Wu M, Jansson PE, Tan X, Wu J, Huang J (2016) Constraining parameter uncertainty in simulations of water and heat dynamics in seasonally frozen soil using limited observed data. *Water* 8(2):64
328. Wu D, Lai Y, Zhang M (2017) Thermo–hydro–salt–mechanical coupled model for saturated porous media based on crystallization kinetics. *Cold Reg Sci Technol* 133:94–107
329. Wu M, Tan X, Huang J, Wu J, Jansson PE (2015) Solute and water effects on soil freezing characteristics based on laboratory experiments. *Cold Reg Sci Technol* 115:22–29
330. Wu M, Wu J, Tan X, Huang J, Jansson PE, Zhang W (2019) Simulation of dynamical interactions between soil freezing/thawing and salinization for improving water management in cold/arid agricultural region. *Geoderma* 338:325–342
331. Wu Y, Zhai E, Zhang X, Wang G, Lu Y (2021) A study on frost heave and thaw settlement of soil subjected to cyclic freeze–thaw conditions based on hydro–thermal–mechanical coupling analysis. *Cold Reg Sci Technol* 188:103296
332. Wu W, Zhang S, Wang S (2017) A novel lattice Boltzmann model for the solid–liquid phase change with the convection heat transfer in the porous media. *Int J Heat Mass Transf* 104:675–687
333. Wu J, Zheng B, Shi Y (2015) Analysis of causes of side wall cracking of tunnel located in highly weathered sandstone and mudstone in seasonal frozen soil area and its treatment measures. *Railw Eng* 6:67–71
334. Xiao W, Liu E, Yin X, Zhang G, Zhang C, Yu Q (2022) Numerical simulation of coupled liquid water, stress and heat for frozen soil in the thawing process. *Eng Comput* 39(4):1492–1510
335. Yan K, Zhao T, Liu Y (2022) Numerical investigation into the plane breach process of cohesionless dikes induced by overtopping. *Int J Geomech* 22(11):04022204
336. Yang JY, Dai XY, Xu QH, Liu ZY, Shi L, Long W (2021) Lattice Boltzmann modelling of interfacial mass transfer in a multiphase system. *Phys Rev E* 104(1):015307
337. Yang Q, Dan L, Wu J et al (2018) The improved freeze–thaw process of a climate–vegetation model: calibration and validation tests in the source region of the Yellow River. *J Geophys Res Atmos* 123(23):13–346
338. Yang P, Ke JM, Wang JG, Chow YK, Zhu FB (2006) Numerical simulation of frost heave with coupled water freezing, temperature and stress fields in tunnel excavation. *Comput Geotech* 33(6–7):330–340
339. Yang Y, Lei D, Chen Y, Cai C, Hou S (2022) Coupled thermal–hydro–mechanical model of deep artificial freezing clay. *Cold Reg Sci Technol* 198:103534
340. Yang K, Yang J, Zhaoye P, Zhang F, Zhang G, Wang C (2023) Optimization and validation of soil frozen–thawing parameterizations in Noah-MP. *J Geophys Res Atmos* 128(23):e2022JD038217
341. Yao X, Qi J, Liu M, Yu F (2017) Pore water pressure distribution and dissipation during thaw consolidation. *Transp Porous Media* 116:435–451
342. Yao X, Qi J, Wu W (2012) Three dimensional analysis of large strain thaw consolidation in permafrost. *Acta Geotech* 7:193–202
343. Yao XL (2010) Theoretical and application study on thaw settlement of frozen soils. Dissertation for PhD, Graduate University of the Chinese Academy of Sciences, Beijing, pp 29–37
344. Yin X, Liu E, Song B, Zhang D (2018) Numerical analysis of coupled liquid water, vapour, stress and heat transport in unsaturated freezing soil. *Cold Reg Sci Technol* 155:20–28
345. Yu F, Guo P, Lai Y, Stolle D (2020) Frost heave and thaw consolidation modelling. Part 2: one-dimensional thermohydromechanical (THM) framework. *Can Geotech J* 57(10):1595–1610
346. Yu Y, Ling X, Tang L, Han X, Geng L, Wei S (2021) Preliminary identification of the failure mode of shallow tunnels in soil subjected to frost heave: model test and numerical simulation. *Transp Geotech* 29:100555
347. Yu WB, Yi X, Niu YZ et al (2016) Dynamic thermal regime of permafrost beneath embankment of Qinghai-Tibet Highway under the scenarios of changing structure and climate warming. *Cold Reg Sci Technol* 126:76–81
348. Zhan Y, Lu Z, Yao H, Xian S (2018) A coupled thermo–hydromechanical model of soil slope in seasonally frozen regions under freeze–thaw action. *Adv Civ Eng* 2018:1–10. <https://doi.org/10.1155/2018/7219826>
349. Zhan Y, Zhao M, Lu Z, Yao H (2023) Analysis of the water–vapour–heat coupling migration of unsaturated soil slope in seasonal frozen regions. Available at SSRN 4386862
350. Zhang Y, Bei J, Li P, Liang X (2020) Numerical simulation of the thermal–hydro–mechanical characteristics of high-speed railway roadbeds in seasonally frozen regions. *Adv Civ Eng* 2020:1–14
351. Zhang Q, Borja RI (2021) Poroelastic coefficients for anisotropic single and double porosity media. *Acta Geotech* 16(10):3013–3025
352. Zhang J, Lai Y, Li J, Zhao Y (2020) Study on the influence of hydro–thermal–salt–mechanical interaction in saturated frozen sulfate saline soil based on crystallization kinetics. *Int J Heat Mass Transf* 146:118868
353. Zhang Y, Michalowski RL (2015) Thermal–hydro–mechanical analysis of frost heave and thaw settlement. *J Geotech Geoenviron Eng* 141(7):04015027
354. Zhang M, Pei W, Li S, Lu J, Jin L (2017) Experimental and numerical analyses of the thermo–mechanical stability of an embankment with shady and sunny slopes in a permafrost region. *Appl Therm Eng* 127:1478–1487
355. Zhang J, Qu G, Jin H (2010) Estimates on thermal effects of the China–Russia crude oil pipeline in permafrost regions. *Cold Reg Sci Technol* 64(3):243–247
356. Zhang X, Wang Q, Yu T, Wang G, Wang W (2018) Numerical study on the multifield mathematical coupled model of hydraulic–thermal–salt–mechanical in saturated freezing saline soil. *Int J Geomech* 18(7):04018064
357. Zhang X, Wu Y, Zhai E, Ye P (2021) Coupling analysis of the heat–water dynamics and frozen depth in a seasonally frozen zone. *J Hydrol* 593:125603

358. Zhang L, Wu B, Zhang H (2023) A fully coupled THMC model for simulating hydrate dissociation by using finite element method. *Eng Comput* 40(6):1442–1453
359. Zhang X, Zhai E, Wu Y, Sun DA, Lu Y (2021) Theoretical and numerical analyses on hydro-thermal–salt–mechanical interaction of unsaturated salinized soil subjected to typical unidirectional freezing process. *Int J Geomech* 21(7):04021104
360. Zhang RH, Zhang LH, Luo JX, Yang ZD, Xu MY (2016) Numerical simulation of water flooding in natural fractured reservoirs based on control volume finite element method. *J Pet Sci Eng* 146:1211–1225
361. Zhang H, Zhang J, Zhang Z, Chen J, You Y (2016) A consolidation model for estimating the settlement of warm permafrost. *Comput Geotech* 76:43–50
362. Zhang LL, Zhao L, Li R, Gao LM, Xiao Y, Qiao YP, Shi JZ (2016) Investigating the influence of soil moisture on albedo and soil thermodynamic parameters during the warm season in Tanggula Range, Tibetan Plateau. *J Glaciol Geocryol* 38(2):351–358
363. Zhang Y, Michalowski RL (2014) Thermal-hydro-mechanical modelling of frost action in frost-susceptible soils. In: *Soil behaviour and geomechanics*. Auris Reference, Nottingham, pp 735–744
364. Zhang T, Armstrong RL, Smith J (2003) Investigation of the near-surface soil freeze–thaw cycle in the contiguous United States: algorithm development and validation. *J Geophys Res Atmos* 108(D22)
365. Zhao Y, Borja RI (2020) A continuum framework for coupled solid deformation–fluid flow through anisotropic elastoplastic porous media. *Comput Methods Appl Mech Eng* 369:113225
366. Zhao Y, Yu B, Yu G, Li W (2014) Study on the water-heat coupled phenomena in thawing frozen soil around a buried oil pipeline. *Appl Therm Eng* 73(2):1477–1488
367. Zhao Y, Peth S, Horn R, Šimůnek J, Kodešová R (2008) Modelling of coupled water and heat fluxes in both unfrozen and frozen soils. In: *Proceedings of HYDRUS workshop, 2008*. Czech University of Life Sciences, Prague, pp 55–60
368. Zhelnin M, Kostina A, Plekhov O (2021) Numerical simulation of artificial freezing of soils accounting for thermo–hydro-mechanical effects. *Procedia Struct Integr* 32:238–245
369. Zhelnin M, Kostina A, Prokhorov A, Plekhov O, Semin M, Levin L (2022) Coupled thermo–hydro-mechanical modelling of frost heave and water migration during artificial freezing of soils for mineshaft sinking. *J Rock Mech Geotech Eng* 14(2):537–559
370. Zheng H, Kanie S (2015) Combined thermal–hydraulic–mechanical frost heave model based on Takashi’s equation. *J Cold Reg Eng* 29(4):04014019
371. Zheng T, Miao XY, Naumov D, Shao H, Kolditz O, Nagel T (2022) A thermo–hydro-mechanical finite-element model with freezing processes in saturated soils. *Environ Geotech* 9(8):502–514
372. Zhou J, Li D (2012) Numerical analysis of coupled water, heat and stress in saturated freezing soil. *Cold Reg Sci Technol* 72:43–49
373. Zhou J, Liang Z, Zhang L, Zheng T, Zheng J (2022) Thermal and mechanical analysis of the China-Russia Crude Oil Pipeline suffering settlement disaster in permafrost regions. *Int J Press Vessels Pip* 199:104729
374. Zhou MM, Meschke G (2013) A three-phase thermo–hydro-mechanical finite element model for freezing soils. *Int J Numer Anal Methods Geomech* 37(18):3173–3193
375. Zhou Y, Zhou G (2012) Intermittent freezing mode to reduce frost heave in freezing soils—experiments and mechanism analysis. *Can Geotech J* 49(6):686–693
376. Zhou GQ, Zhou Y, Hu K, Wang YJ, Shang XY (2018) Separate-ice frost heave model for one-dimensional soil freezing process. *Acta Geotech* 13:207–217
377. Zhou X, Zhou J, Kinzelbach W, Stauffer F (2014) Simultaneous measurement of unfrozen water content and ice content in frozen soil using gamma ray attenuation and TDR. *Water Resour Res* 50(12):9630–9655
378. Zhou M, Meschke G (2011) A three-phase finite element model of water-infiltrated porous materials subjected to freezing. In: *COUPLED IV: proceedings of the IV international conference on computational methods for coupled problems in science and engineering, 2011*. CIMNE, pp 1083–1094
379. Zhu H, Tang X, Liu Q, Li K, Xiao J, Jiang S, McLennan JD (2018) 4D multi-physical stress modelling during shale gas production: a case study of Sichuan Basin Shale Gas Reservoir, China. *J Pet Sci Eng* 167:929–943
380. Zienkiewicz OC (1971) *The finite element method in structural and continuum mechanics*. McGraw-Hill, London

Publisher's Note Springer Nature remains neutral with regard to jurisdictional claims in published maps and institutional affiliations.